Supporting Information

Group 14 Metallocene Catalysts for Carbonyl Hydroboration and Cyanosilylation

Haley J. Robertson, Mallory N. Fujiwara, Allegra L. Liberman-Martin*

Chemistry and Biochemistry Program, Schmid College of Science and Technology, Chapman University, One University Drive, Orange, CA 92866, USA

Email: libermanmartin@chapman.edu

Table of Contents

General Considerations

All experiments were conducted using standard Schlenk techniques or in a nitrogen atmosphere glovebox. Solvents were dried by passage through solvent purification columns and stored over activated 3Å molecular sieves. Deuterated solvents were purchased from Cambridge Isotope Laboratory and were degassed and stored over activated 3Å molecular sieves.

Lithium pentamethylcyclopentadienide (Cp*Li), germanium(II) chloride dioxane complex (Gelest), tin(II) chloride (Acros), lead(II) chloride (TCI America), triethylphosphine oxide (Aldrich), and solid aldehyde and ketone substrates (Aldrich, TCI America, or Combi-Blocks) were used as received. Liquid aldehydes, ketones, and amides (Aldrich, TCI America, or Combi-Blocks) were degassed and stored over activated 3Å molecular sieves before use. Pinacolborane (Oakwood) and trimethylsilyl cyanide (Aldrich) were used as received.

Tetramethyldisiloxa[3]metallocenophane compounds **4–6** were prepared according to a literature procedure.[1]

Solution NMR spectroscopy was performed using a Bruker AVANCE III 400 MHz NMR spectrometer at 25 °C. ^{1}H NMR spectra were calibrated internally to resonances for the residual proteo solvent relative to tetramethylsilane. ^{11}B, ^{13}C{^{1}H}, ^{19}F{^{1}H}, and ^{31}P{^{1}H} NMR spectra were referenced using the absolute reference function of MestReNova version 14.2.0 software.

Synthesis of Cp*$_2$M Compounds (1–3)

Synthesis of Cp*$_2$Ge (**1**)

The following synthesis was adapted from a procedure reported by Weidenbruch and co-workers.[2]

In a glovebox, germanium(II) chloride dioxane complex (1:1) (0.500 g, 2.16 mmol) was dissolved in 4 mL of THF in a scintillation vial. In a separate scintillation vial equipped with a magnetic stir bar, Cp*Li (0.614 g, 4.32 mmol) was suspended in 10 mL of THF. Both vials were cooled in a –35 °C glovebox freezer for 15 minutes. After removing both vials from the glovebox freezer, the germanium(II) chloride solution was added dropwise to the stirred suspension of Cp*Li. The reaction mixture was stirred for 24 hours at 25 °C then dried *in vacuo*. Pentane (15 mL) was added to the resulting pale yellow solid, and the mixture was filtered. The filtrate was dried *in vacuo* to afford Cp*$_2$Ge (**1**) as a pale-yellow powder (0.559 g, 76 % yield). ^{1}H NMR (400 MHz, C$_6$D$_6$) δ 1.95 (s). ^{13}C{^{1}H} NMR (101 MHz, C$_6$D$_6$) δ 117.85, 9.89. Spectroscopic data agree with those previously reported.[2]

Synthesis of Cp*$_2$Sn (**2**)

The following synthesis was adapted from a procedure reported by Jutzi and co-workers.[3]

In a glovebox, tin(II) chloride (0.409 g, 2.16 mmol) was dissolved in 6 mL of THF in a scintillation vial. In a separate scintillation vial equipped with a magnetic stir bar, Cp*Li (0.614 g, 4.32 mmol) was suspended in 6 mL of THF. Both vials were cooled in a –35 °C glovebox freezer for 15 minutes. After removing both vials from the glovebox freezer, the tin(II) chloride solution was added dropwise to the stirred suspension of Cp*Li. The reaction mixture was stirred for 26 hours at 25 °C then dried *in vacuo*. Pentane (18 mL) was added to the resulting yellow solid, and the mixture was filtered. The filtrate was dried *in vacuo* to afford Cp*$_2$Sn (**2**) as a bright yellow

powder (0.620 g, 74 % yield). ^{1}H NMR (400 MHz, C$_6$D$_6$) δ 2.03 (s with ^{119}Sn satellites, J_{SnH} = 3.7 Hz). ^{13}C{^{1}H} NMR (101 MHz, C$_6$D$_6$) δ 116.81 (s with ^{119}Sn satellites, J_{SnC} = 11.3 Hz), 10.16 (s with ^{119}Sn satellites, J_{SnC} = 22.9 Hz). Spectroscopic data agree with those previously reported.[3]

Synthesis of Cp*$_2$Pb (**3**)

The following synthesis was adapted from a procedure reported by Jutzi and co-workers.[4]

In a glovebox, lead(II) chloride (0.600 g, 2.16 mmol) was dissolved in 8 mL of THF in a scintillation vial. In a separate scintillation vial equipped with a magnetic stir bar, Cp*Li (0.614 g, 4.32 mmol) was suspended in 10 mL of THF. Both vials were cooled in a –35 °C glovebox freezer for 15 minutes. After removing both vials from the glovebox freezer, the lead(II) chloride solution was added dropwise to the stirred suspension of Cp*Li. The reaction mixture was stirred for 22 hours at 25 °C then dried *in vacuo*. Pentane (20 mL) was added to the resulting red solid, and the mixture was filtered. The filtrate was dried *in vacuo* to afford Cp*$_2$Pb (**3**) as a bright red powder (0.655 g, 64 % yield). ^{1}H NMR (400 MHz, C$_6$D$_6$) δ 2.19 (s with ^{207}Pb satellites, J_{PbH} = 11.1 Hz). ^{13}C{^{1}H} NMR (101 MHz, C$_6$D$_6$) δ 117.45 (s with ^{207}Pb satellites, J_{PbC} = 36.8 Hz), 9.80 (s with ^{207}Pb satellites, J_{PbC} = 24.0 Hz). Spectroscopic data agree with those previously reported.[4]

General Procedure for Aldehyde and Ketone Hydroboration Catalysis
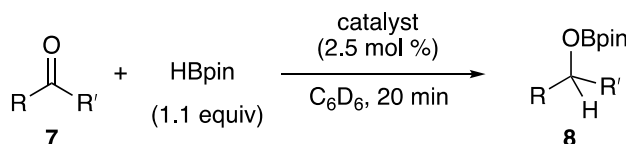
In a glovebox, a J. Young NMR tube was charged with 0.50 mL of benzene-d_6, aldehyde or ketone (0.24 mmol), pinacolborane (0.27 mmol), catalyst (0.0060 mmol), and hexamethylbenzene (0.040 mmol) as an internal standard. The reaction progress was monitored by ^{1}H NMR spectroscopy, and the reaction yield was determined by ^{1}H NMR integration relative to the hexamethylbenzene internal standard.

General Procedure for Aldehyde Cyanosilylation Catalysis
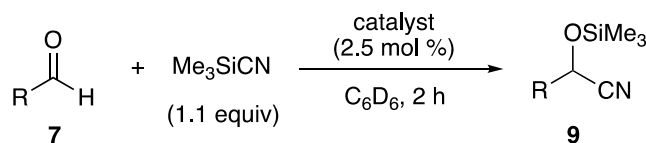
In a glovebox, a J. Young NMR tube was charged with 0.50 mL of benzene-d_6, aldehyde (0.24 mmol), trimethylsilyl cyanide (0.27 mmol), catalyst (0.0060 mmol), and hexamethylbenzene (0.040 mmol) as an internal standard. The reaction progress was monitored by ^{1}H NMR spectroscopy, and the reaction yield was determined by ^{1}H NMR integration relative to the hexamethylbenzene internal standard.

Competition Hydroboration Reactions for *para*-Substituted Benzaldehyde Derivatives

In a glovebox, a J. Young NMR tube was charged with 0.50 mL of benzene-d_6, benzaldehyde (0.24 mmol), a *para*-substituted benzaldehyde derivative (0.24 mmol), pinacolborane (0.048 mmol), catalyst **5** (0.0060 mmol), and hexamethylbenzene (0.040 mmol).

Average yields from two experiments were determined after 1 h at 25 °C by ^{1}H NMR integration relative to the hexamethylbenzene internal standard with a 10 s relaxation delay.

Table S1. Relative rates for the hydroboration of *para*-substituted benzaldehydes derivatives.

Para Substituent (X)	σ	k_X/k_H	$\log(k_X/k_H)$
–OCH$_3$	–0.268	0.59	–0.23
–CH$_3$	–0.170	0.72	–0.14
–Cl	+0.227	1.23	+0.09
–Br	+0.232	1.44	+0.16
–CN	+1.00	5.67	+0.75
–NO$_2$	+1.27	8.09	+0.91

Stoichiometric Reactions Between Catalysts 4–6 and Substrates

Stochiometric Reactions of Compounds **4–6** with 4-(Trifluoromethyl)Benzaldehyde

In a glovebox, a J. Young NMR tube was charged with 0.50 mL of benzene-d_6, 4-(trifluoromethyl)benzaldehyde (0.025 mmol), and **4–6** (0.025 mmol).

^{1}H NMR spectra indicated a <0.01 ppm change in chemical shift for the aldehydic signal. ^{13}C{^{1}H} NMR spectra indicated a ≤0.43 ppm change in chemical shift for the carbonyl signal.

Table S2. NMR results for stoichiometric reactions of compounds **4–6** with 4-(trifluoromethyl)benzaldehyde.

Experiment	^{1}H NMR signal for the aldehydic C*H*O (ppm)	^{13}C{^{1}H} NMR signal for the aldehydic *C*HO (ppm)
4-(trifluoromethyl) benzaldehyde	9.39	189.81
Ge compound **4** + 4-(trifluoromethyl) benzaldehyde	9.39	190.24
Sn compound **5** + 4-(trifluoromethyl) benzaldehyde	9.40	190.16
Pb compound **6** + 4-(trifluoromethyl) benzaldehyde	9.40	190.18

Stochiometric Reactions of Compounds **4–6** with Pinacolborane

In a glovebox, a J. Young NMR tube was charged with 0.50 mL of benzene-d_6, pinacolborane (0.025 mmol), and **4–6** (0.025 mmol).

^{1}H NMR spectra indicated <0.01 ppm changes in chemical shifts for the pinacolborane signals. ^{11}B NMR spectra indicated a <0.01 ppm change in chemical shift for the boron signal.

Stochiometric Reactions of Compounds **4–6** with Trimethylsilyl Cyanide

In a glovebox, a J. Young NMR tube was charged with 0.50 mL of dichloromethane-d_2, trimethylsilyl cyanide (0.025 mmol), and **4–6** (0.025 mmol).

^{13}C{^{1}H} NMR spectra indicated ≤0.02 ppm changes in chemical shift for the cyanide signal.

Table S3. NMR results for stoichiometric reactions of compounds **4–6** with trimethylsilyl cyanide.

Experiment	^{13}C{^{1}H} NMR signal for the cyano group (ppm)
TMSCN	127.47
Ge compound **4** + TMSCN	127.46
Sn compound **5** + TMSCN	127.47
Pb compound **6** + TMSCN	127.45

Lewis Acidity Measurements

Gutmann-Beckett Assessment of Compounds **4–6** with Triethylphosphine Oxide

In a glovebox, a J. Young NMR tube was charged with 0.50 mL of benzene-d_6, triethyl phosphine oxide (0.025 mmol), and **4–6** (0.075 mmol; 3 equiv).

^{31}P{^{1}H} NMR data were collected after 15 min at 25 °C.

Table S4. NMR results for combinations of compounds **4–6** with triethylphosphine oxide.

Lewis Acid	Et$_3$PO ^{31}P δ (ppm)	Et$_3$PO ^{31}P Δδ (ppm)
None	45.4	—
Ge compound **4**	46.7	1.3
Sn compound **5**	49.5	4.1
Pb compound **6**	50.7	5.3
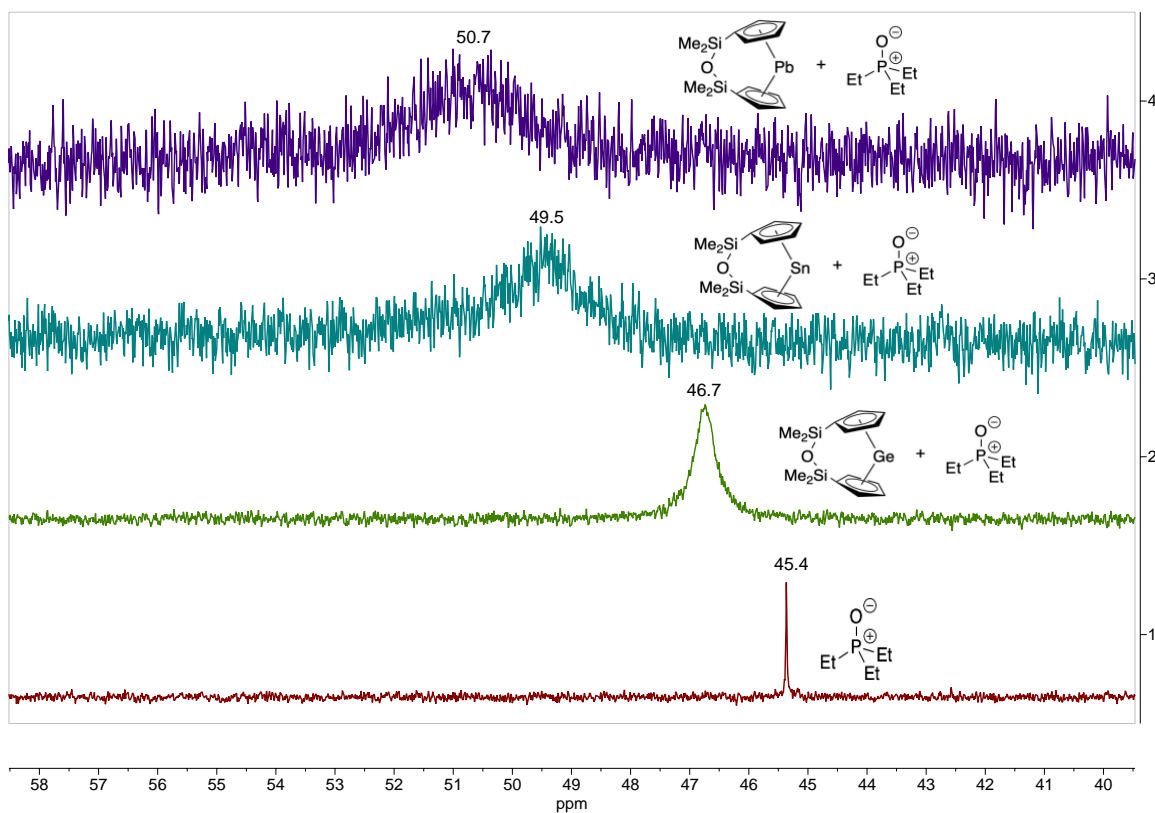
Figure S1. ^{31}P{^{1}H} NMR spectra of compounds **4–6** combined with Et$_3$PO in a 3:1 ratio in benzene-d_6.

Stoichiometric Reactions of Compounds **4–6** with *N*,*N*-Dimethylacetamide

In a glovebox, a J. Young NMR tube was charged with 0.50 mL of benzene-d_6, *N*,*N*-dimethylacetamide (0.025 mmol), and **4–6** (0.025 mmol).

^{13}C{^{1}H} NMR data were collected after 15 min at 25 °C.

Table S5. NMR results for combinations of compounds **4–6** with *N*,*N*-dimethylacetamide.

Lewis Acid	C=O signal ^{13}C δ (ppm)	C=O signal ^{13}C Δδ (ppm)
None	168.8	—
Ge compound **4**	169.1	0.3
Sn compound **5**	168.8	0.0
Pb compound **6**	168.9	0.1

Stoichiometric Reactions of Compounds **4–6** with 1,3-Dimethyl-2-oxohexahydropyrimidine

In a glovebox, a J. Young NMR tube was charged with 0.50 mL of benzene-d_6, 1,3-dimethyl-2-oxohexahydropyrimidine (0.025 mmol), and **4–6** (0.025 mmol).

^{13}C{^{1}H} NMR data were collected after 15 min at 25 °C.

Table S6. NMR results for combinations of compounds **4–6** with 1,3-dimethyl-2-oxohexahydropyrimidine.

Lewis Acid	C=O signal ^{13}C δ (ppm)	C=O signal ^{13}C Δδ (ppm)
None	156.4	—
Ge compound **4**	156.3	0.1
Sn compound **5**	155.9	0.5
Pb compound **6**	155.9	0.5

NMR Characterization Data for Aldehyde and Ketone Hydroboration Products
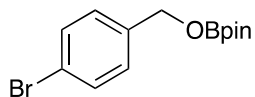
2-((4-bromobenzyl)oxy)-4,4,5,5-tetramethyl-1,3,2-dioxaborolane (8a).[5] ^{1}H NMR (400 MHz, C_6D_6) δ 7.26 (d, J = 8.5 Hz, 2H), 6.98 (d, J = 8.5 Hz, 2H), 4.78 (s, 2H), 1.08 (s, 12H). ^{13}C{^{1}H} NMR (101 MHz, C_6D_6) δ 138.6, 131.4, 128.4, 121.1, 82.6, 65.8, 24.6. ^{11}B NMR (128 MHz, C_6D_6) δ 22.8.
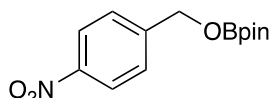
4,4,5,5-tetramethyl-2-((4-nitrobenzyl)oxy)-1,3,2-dioxaborolane (8b).[6] ^{1}H NMR (400 MHz, C_6D_6) δ 7.79 (d, J = 8.7 Hz, 2H), 6.92 (d, J = 8.8 Hz, 2H), 4.69 (s, 2H), 1.04 (s, 12H). ^{13}C{^{1}H} NMR (101 MHz, C_6D_6) δ 147.1, 146.2, 126.4, 123.2, 82.8, 65.3, 24.3. ^{11}B NMR (128 MHz, C_6D_6) δ 22.7.
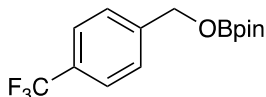
4,4,5,5-tetramethyl-2-((4-(trifluoromethyl)benzyl)oxy)-1,3,2-dioxaborolane (8c).[7] ^{1}H NMR (400 MHz, C_6D_6) δ 7.30 (d, J = 8.1 Hz, 2H), 7.08 (d, J = 8.1 Hz, 2H), 4.78 (s, 2H), 1.05 (s, 12H). ^{13}C{^{1}H} NMR (101 MHz, C_6D_6) δ 143.5, 129.2 (q, J = 32.1 Hz), 126.5, 125 (q, J = 3.9 Hz), 82.6, 65.6, 24.2. ^{11}B NMR (128 MHz, C_6D_6) δ 22.8. ^{19}F{^{1}H} NMR (377 MHz, C_6D_6) δ -62.2.
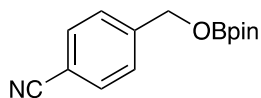
4-(((4,4,5,5-tetramethyl-1,3,2-dioxaborolan-2-yl)oxy)methyl)benzonitrile (8d).[8] ^{1}H NMR (400 MHz, C_6D_6) δ 7.00 (d, J = 8.3 Hz, 2H), 6.88 (d, J = 8.3 Hz, 2H), 4.66 (s, 2H), 1.03 (s, 12H). ^{13}C{^{1}H} NMR (101 MHz, C_6D_6) δ 144.2, 131.7, 126.4, 118.5, 111.2, 82.7, 65.5, 24.3. ^{11}B NMR (128 MHz, C_6D_6) δ 22.7.
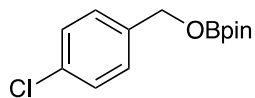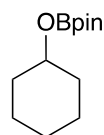

2-((4-chlorobenzyl)oxy)-4,4,5,5-tetramethyl-1,3,2-dioxaborolane (8e).[8] ^{1}H NMR (400 MHz, C_6D_6) δ 7.06 (d, J = 8.4 Hz, 2H), 6.99 (d, J = 8.4 Hz, 2H), 4.76 (s, 2H), 1.03 (s, 12H). ^{13}C{^{1}H} NMR (101 MHz, C_6D_6) δ 138.1, 133.0, 128.4, 128.0, 82.5, 65.7, 24.3. ^{11}B NMR (128 MHz, C_6D_6) δ 22.8.
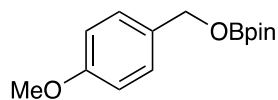
2-((4-methoxybenzyl)oxy)-4,4,5,5-tetramethyl-1,3,2-dioxaborolane (8f).[5] ^{1}H NMR (400 MHz, C_6D_6) δ 7.25 (d, J = 8.6 Hz, 2H), 6.74 (d, J = 8.6 Hz, 2H), 4.92 (s, 2H), 3.28 (s, 3H), 1.04 (s, 12H). ^{13}C{^{1}H} NMR (101 MHz, C_6D_6) δ 159.3, 131.8, 128.5, 113.7, 82.3, 66.4, 54.4, 24.4. ^{11}B NMR (128 MHz, C_6D_6) δ 22.8.
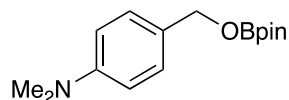
_N_,_N_-dimethyl-4-(((4,4,5,5-tetramethyl-1,3,2-dioxaborolan-2-yl)oxy)methyl)aniline (8g).[8] ^{1}H NMR (400 MHz, C_6D_6) δ 7.33 (d, J = 8.7 Hz, 2H), 6.55 (d, J = 8.8 Hz, 2H), 5.00 (s, 2H), 2.49 (s, 6H), 1.06 (s, 12H). ^{13}C{^{1}H} NMR (101 MHz, C_6D_6) δ 150.2, 128.6, 127.7, 112.4, 82.2, 66.9, 39.9, 24.4. ^{11}B NMR (128 MHz, C_6D_6) δ 22.9.
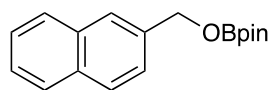
4,4,5,5-tetramethyl-2-(naphthalen-2-ylmethoxy)-1,3,2-dioxaborolane (8h).[6] ^{1}H NMR (400 MHz, C_6D_6) δ 7.77 (d, J = 1.4 Hz, 1H), 7.66 – 7.50 (overlapping signals, 3H), 7.39 (dd, J = 8.5, 1.8 Hz, 1H), 7.29 – 7.19 (overlapping signals, 2H), 5.10 (s, 2H), 1.05 (s, 12H). ^{13}C{^{1}H} NMR (101 MHz, C_6D_6) δ 137.2, 133.6, 133.1, 128.1, 128.0, 127.7, 125.9, 125.6, 125.4, 124.9, 82.5, 66.7, 24.4. ^{11}B NMR (128 MHz, C_6D_6) δ 23.0.
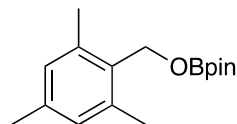
4,4,5,5-tetramethyl-2-((2,4,6-trimethylbenzyl)oxy)-1,3,2-dioxaborolane (8i).[8] ^{1}H NMR (400 MHz, C_6D_6) δ 6.72 (s, 2H), 5.03 (s, 2H), 2.37 (s, 6H), 2.12 (s, 3H), 1.04 (s, 12H). ^{13}C{^{1}H} NMR (101 MHz, C_6D_6) δ 137.4, 137.0, 132.6, 129.0, 82.2, 61.2, 24.3, 20.7, 19.3. ^{11}B NMR (128 MHz, C_6D_6) δ 22.7.
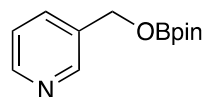
3-(((4,4,5,5-tetramethyl-1,3,2-dioxaborolan-2-yl)oxy)methyl)pyridine (8j).[5] ^{1}H NMR (400 MHz, C_6D_6) δ 8.66 (s, 1H), 8.44 (d, J = 4.8 Hz, 1H), 7.31 (d, J = 7.9 Hz, 1H), 6.71 (dd, J = 7.8, 4.8 Hz, 1H), 4.72 (s, 2H), 1.00 (s, 12H). ^{13}C{^{1}H} NMR (101 MHz, C_6D_6) δ 149.0, 148.9, 134.5, 133.9, 122.9, 82.6, 64.3, 24.3. ^{11}B NMR (128 MHz, C_6D_6) δ 22.8.
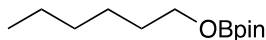
2-(hexyloxy)-4,4,5,5-tetramethyl-1,3,2-dioxaborolane (8k).[9] ^{1}H NMR (400 MHz, C$_6$D$_6$) δ 3.93 (t, J = 6.6 Hz, 2H), 1.51 (m, 2H), 1.29 (m, 2H), 1.18 (m, 4H), 1.08 (s, 12H), 0.82 (t, J = 6.9 Hz, 3H). ^{13}C{^{1}H} NMR (101 MHz, C$_6$D$_6$) δ 82.0, 64.8, 31.7, 31.5, 25.4, 24.4, 22.6, 13.9. ^{11}B NMR (128 MHz, C$_6$D$_6$) δ 22.6.
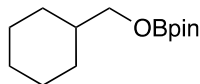
2-(cyclohexylmethoxy)-4,4,5,5-tetramethyl-1,3,2-dioxaborolane (8l).[8] ^{1}H NMR (400 MHz, C$_6$D$_6$) δ 3.76 (d, J = 6.4 Hz, 2H), 1.71 (m, 2H), 1.60 (m, 2H), 1.52(m, 2H), 1.11 (m, 2H), 1.06 (s, 12H), 1.00 (m, 1H), 0.90 (m, 2H). ^{13}C{^{1}H} NMR (101 MHz, C$_6$D$_6$) δ 82.0, 70.2, 39.5, 29.3, 26.5, 25.8, 24.4. ^{11}B NMR (128 MHz, C$_6$D$_6$) δ 22.6.
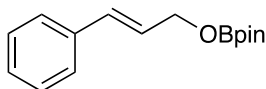
2-(cinnamyloxy)-4,4,5,5-tetramethyl-1,3,2-dioxaborolane (8m).[8] ^{1}H NMR (400 MHz, C$_6$D$_6$) δ 7.17 (m, 2H), 7.08 (m, 2H), 7.01 (m, 1H), 6.60 (dt, J = 15.9, 1.8 Hz, 1H), 6.16 (dt, J = 15.9, 5.3 Hz, 1H), 4.53 (dd, J = 5.3, 1.8 Hz, 2H), 1.05 (s, 12H). ^{13}C{^{1}H} NMR (101 MHz, C$_6$D$_6$) δ 137.0, 130.5, 128.4, 127.3, 127.2, 126.5, 82.3, 65.2, 24.6. ^{11}B NMR (128 MHz, C$_6$D$_6$) δ 22.8.
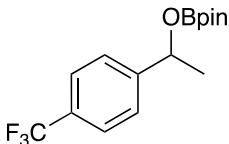
4,4,5,5-tetramethyl-2-(1-(4-(trifluoromethyl)phenyl)ethoxy)-1,3,2-dioxaborolane (8n).[10] ^{1}H NMR (400 MHz, C$_6$D$_6$) δ 7.31 (d, J = 8.1 Hz, 2H), 7.16 (d, J = 7.9 Hz, 2H), 5.26 (q, J = 6.5 Hz, 1H), 1.31 (d, J = 6.5 Hz, 3H), 1.01 (d, J = 13.0 Hz, 12H). ^{13}C{^{1}H} NMR (101 MHz, C$_6$D$_6$) δ 148.8, 129.1 (q, J = 32.2 Hz), 125.6, 125.1 (q, J = 3.8 Hz), 82.4, 71.9, 25.1, 24.2 (d, J = 2.8 Hz). ^{11}B NMR (128 MHz, C$_6$D$_6$) δ 22.5. ^{19}F{^{1}H} NMR (377 MHz, C$_6$D$_6$) δ -62.1.
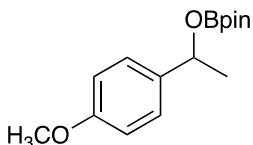
2-(1-(4-methoxyphenyl)ethoxy)-4,4,5,5-tetramethyl-1,3,2-dioxaborolane (8o).[10] ^{1}H NMR (400 MHz, C$_6$D$_6$) δ 7.29 (d, J = 8.7 Hz, 2H), 6.75 (d, J = 9.0 Hz, 2H), 5.39 (q, J = 5.9 Hz, 1H), 3.29 (s, 3H), 1.48 (d, J = 6.5 Hz, 3H), 1.02 (d, J = 8.3 Hz, 12H). ^{13}C{^{1}H} NMR (101 MHz, C$_6$D$_6$) δ 159.0, 137.1, 126.6, 113.6, 82.1, 72.3, 54.4, 25.4, 24.4, 24.3. ^{11}B NMR (128 MHz, C$_6$D$_6$) δ 22.6.
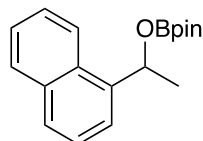
4,4,5,5-tetramethyl-2-(1-(naphthalen-1-yl)ethoxy)-1,3,2-dioxaborolane (8p).[11] ^{1}H NMR (400 MHz, C$_6$D$_6$) δ 7.94 (m, 1H), 7.87 (d, J = 7.2 Hz, 1H), 7.62 (m, 1H), 7.53 (d, J = 8.2 Hz, 1H), 7.27 (t, J = 7.7 Hz, 1H), 7.23 – 7.16 (overlapping signals, 2H), 6.18 (q, J = 6.4 Hz, 1H), 1.62 (d, J = 6.4 Hz, 3H), 1.00 (d, J = 16.9 Hz, 12H). ^{13}C{^{1}H} NMR (101 MHz, C$_6$D$_6$) δ 140.8, 134.0, 130.2, 128.8, 127.6, 125.7, 125.6, 125.2, 123.3, 122.4, 82.3, 70.0, 25.0, 24.2. ^{11}B NMR (128 MHz, C$_6$D$_6$) δ 22.6.

2-(cyclohexyloxy)-4,4,5,5-tetramethyl-1,3,2-dioxaborolane (8q).[12] ^{1}H NMR (400 MHz, C$_6$D$_6$) δ 4.19 (m, 1H), 1.88 (m, 2H), 1.60 (m, 2H), 1.46 (m, 2H), 1.28 (m, 1H), 1.33 (m, 2H), 1.06 (s, 12H), 1.00 (d, J = 4.5 Hz, 1H). ^{13}C{^{1}H} NMR (101 MHz, C$_6$D$_6$) δ 81.8, 72.4, 34.4, 25.4, 24.4, 23.8. ^{11}B NMR (128 MHz, C$_6$D$_6$) δ 22.4.
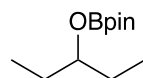
4,4,5,5-tetramethyl-2-(pentan-3-yloxy)-1,3,2-dioxaborolane (8r).[13] ^{1}H NMR (400 MHz, C$_6$D$_6$) δ 4.01 (m, 1H), 1.45 (m, 4H), 1.07 (s, 12H), 0.90 (t, J = 6.8 Hz, 6H). ^{13}C{^{1}H} NMR (101 MHz, C$_6$D$_6$) δ 81.8, 76.9, 28.9, 24.3, 9.7. ^{11}B NMR (128 MHz, C$_6$D$_6$) δ 22.5.

NMR Characterization Data for Aldehyde Cyanosilylation Products
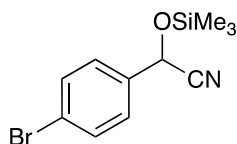
2-(4-bromophenyl)-2-((trimethylsilyl)oxy)acetonitrile (9a).[14] ^{1}H NMR (400 MHz, C$_6$D$_6$) δ 7.13 (d, J = 7.9 Hz, 2H), 6.91 (d, J = 8.0 Hz, 2H), 4.89 (s, 1H), -0.01 (s, 9H). ^{13}C{^{1}H} NMR (101 MHz, C$_6$D$_6$) δ 135.6, 131.9, 127.9, 123.2, 118.6, 62.9, -0.8.
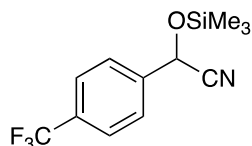
2-(4-(trifluoromethyl)phenyl)-2-((trimethylsilyl)oxy)acetonitrile (9b).[15] ^{1}H NMR (400 MHz, C$_6$D$_6$) δ 7.23 (d, J = 8.1 Hz, 2H), 7.11 (d, J = 8.1 Hz, 2H), 4.94 (s, 1H), 0.02 (s, 9H). ^{13}C{^{1}H} NMR (101 MHz, C$_6$D$_6$) δ 140.2, 131.0 (q, J = 32.5 Hz), 126.5, 125.7 (q, J = 3.8 Hz), 122.8, 118.4, 62.8, -0.9. ^{19}F{^{1}H} NMR (377 MHz, C$_6$D$_6$) δ -62.6.
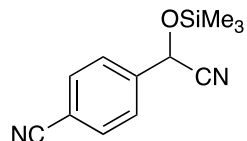
4-(cyano((trimethylsilyl)oxy)methyl)benzonitrile (9c).[15] ^{1}H NMR (400 MHz, C$_6$D$_6$) δ 6.97 (s, 4H), 4.92 (s, 1H), 0.01 (s, 9H). ^{13}C{^{1}H} NMR (101 MHz, C$_6$D$_6$) δ 140.7, 132.2, 126.5, 118.2, 117.9, 113.2, 62.7, -0.9.
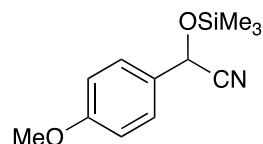
2-(4-methoxyphenyl)-2-((trimethylsilyl)oxy)acetonitrile (9d).[15] ^{1}H NMR (400 MHz, C$_6$D$_6$) δ 7.21 (d, J = 8.4 Hz, 2H), 6.64 (d, J = 8.4 Hz, 2H), 5.07 (s, 1H), 3.23 (s, 3H), –0.03 (s, 9H). ^{13}C{^{1}H} NMR (101 MHz, C$_6$D$_6$) δ 160.4, 128.8, 128.0, 119.4, 114.2, 63.4, 54.5, -0.7.
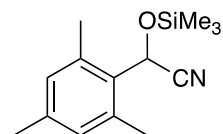
2-mesityl-2-((trimethylsilyl)oxy)acetonitrile (9e).[16] ^{1}H NMR (400 MHz, C$_6$D$_6$) δ 6.59 (s, 2H), 5.73 (s, 1H), 2.31 (s, 6H), 2.00 (s, 3H), 0.00 (s, 9H). ^{13}C{^{1}H} NMR (101 MHz, C$_6$D$_6$) δ 138.7, 136.6, 130.1, 130.0, 119.1, 59.1, 20.5, 19.6, -0.8.
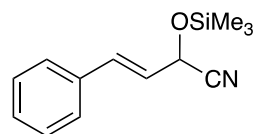
4-phenyl-2-((trimethylsilyl)oxy)but-3-enenitrile (9f).[15] ^{1}H NMR (400 MHz, C$_6$D$_6$) δ 7.04 (s, 5H), 6.57 (d, J = 15.8 Hz, 1H), 5.93 (dd, J = 17.0, 6.1 Hz, 1H), 4.63 (d, J = 6.5 Hz, 1H), 0.07 (d, J = 1.3 Hz, 9H). ^{13}C{^{1}H} NMR (101 MHz, C$_6$D$_6$) δ 135.1, 133.6, 128.5, 128.5, 126.9, 123.9, 118.4, 62.2, -0.6.

NMR Spectra
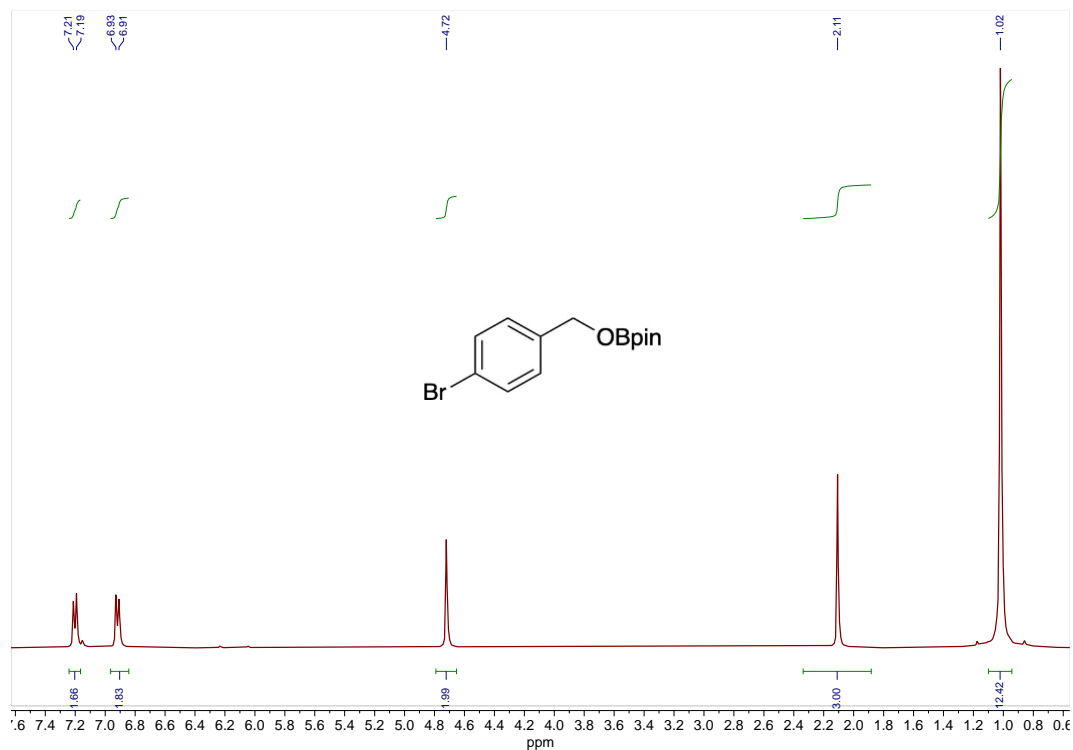
Figure S2. ^{1}H NMR spectrum of **8a** in benzene-d_6 with catalyst **5**. The signal at 2.1 ppm is the hexamethylbenzene internal standard.
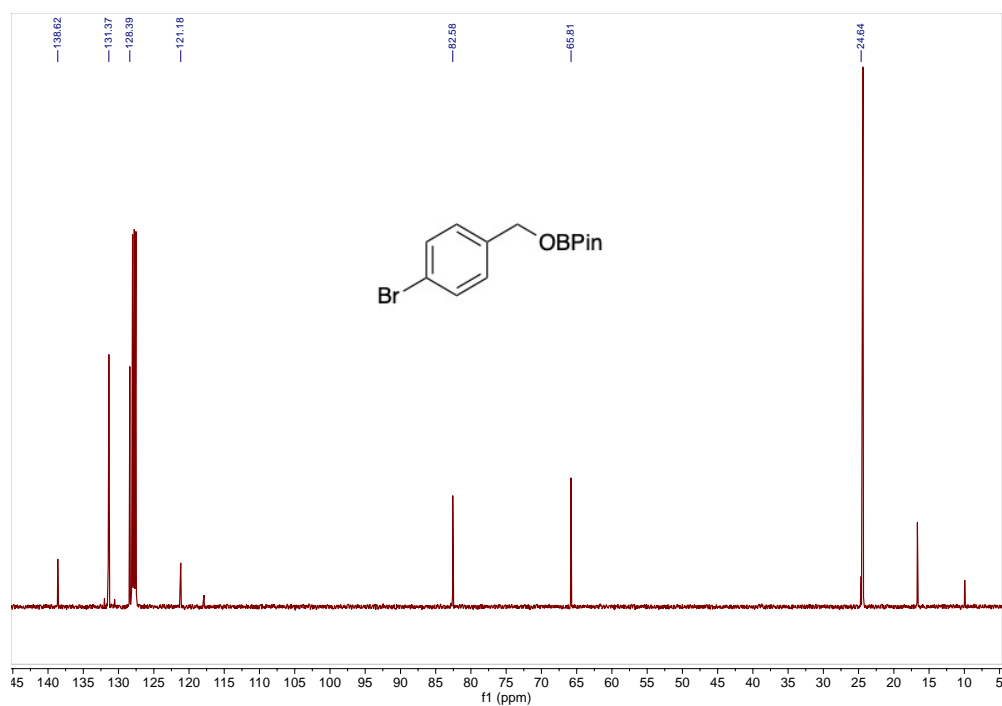
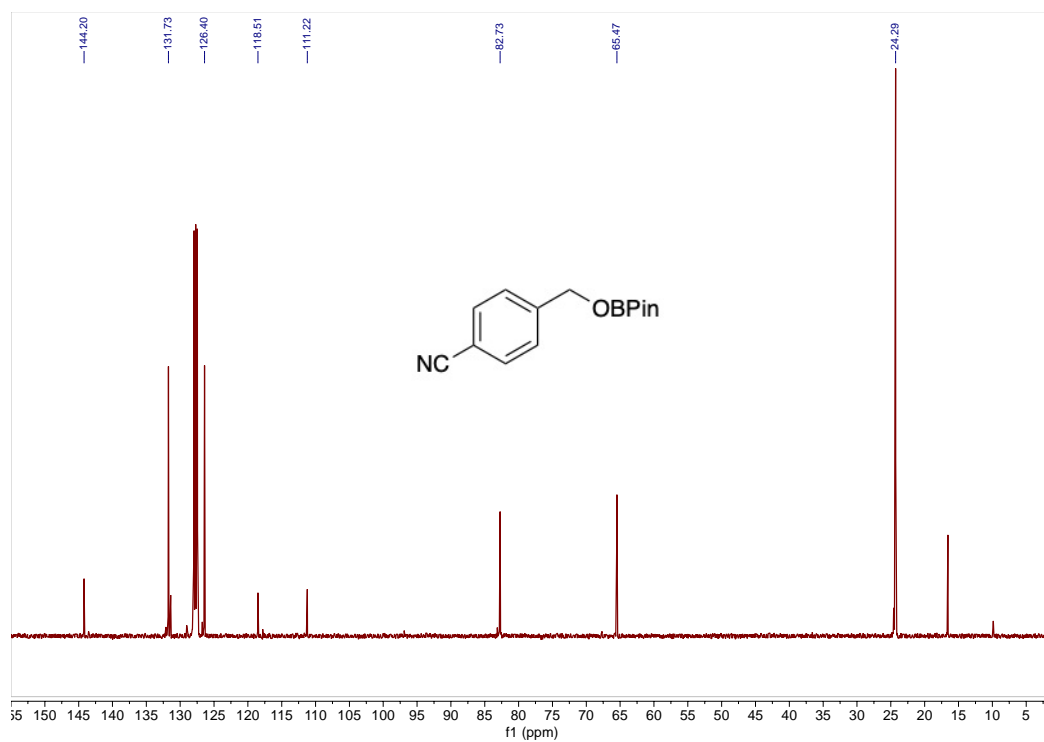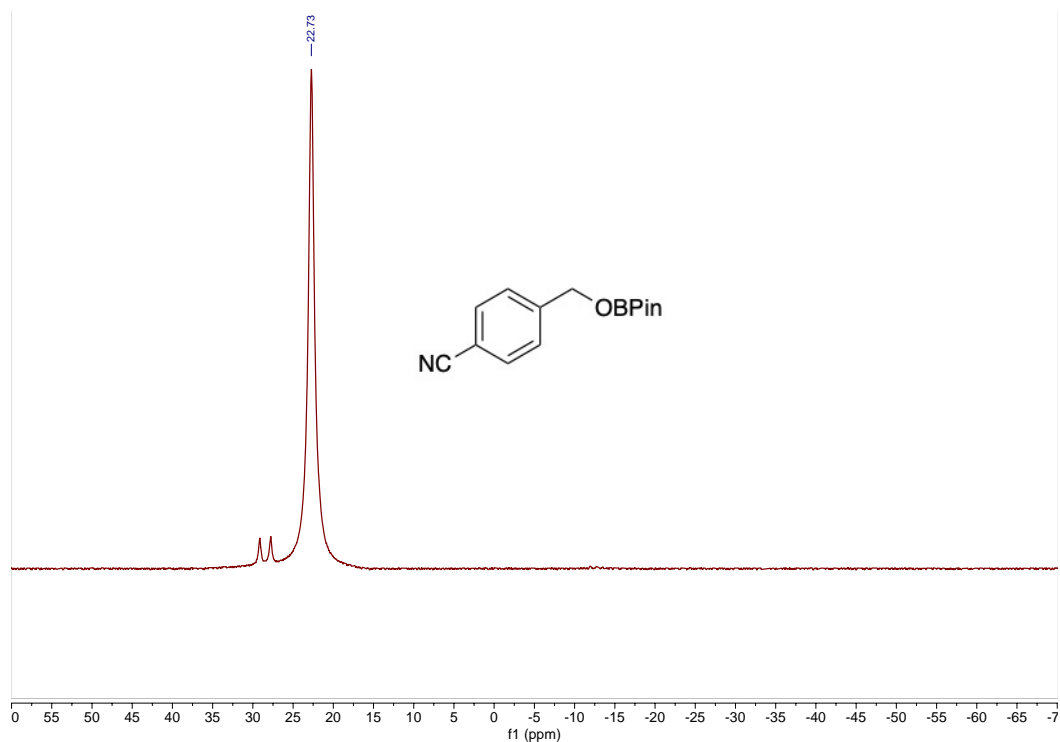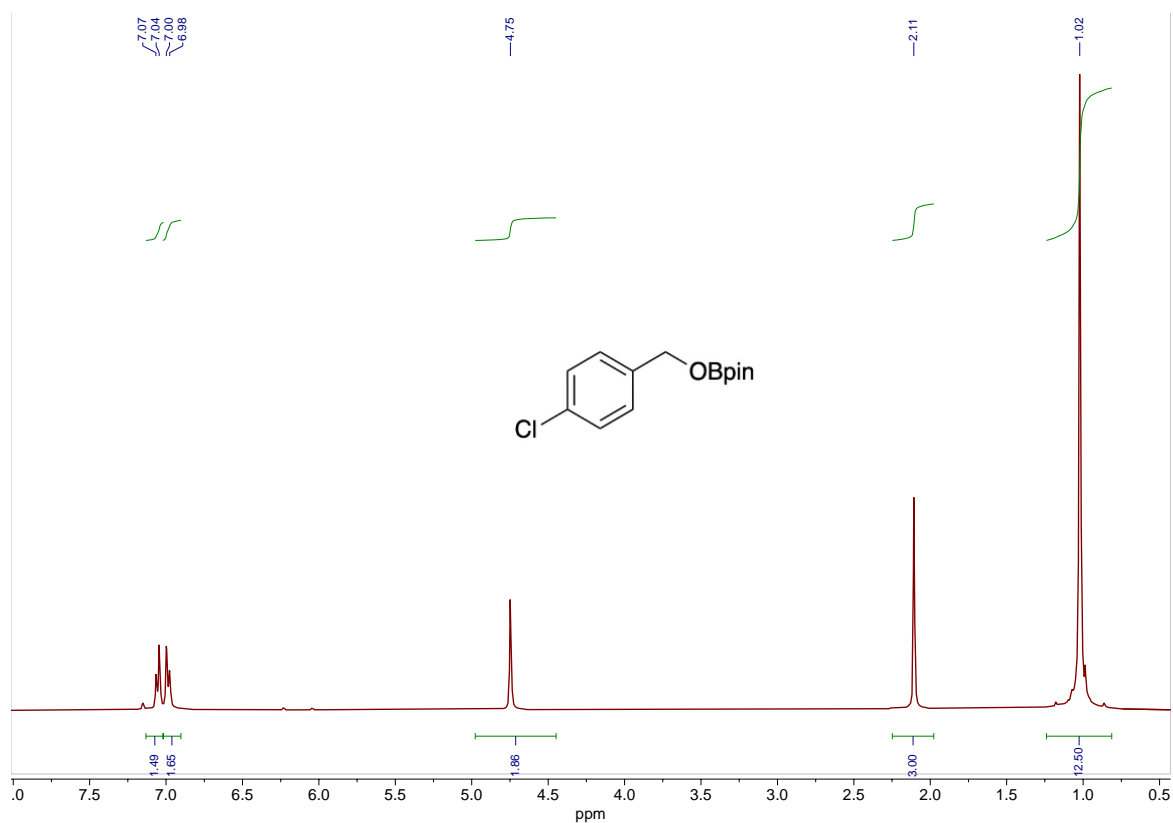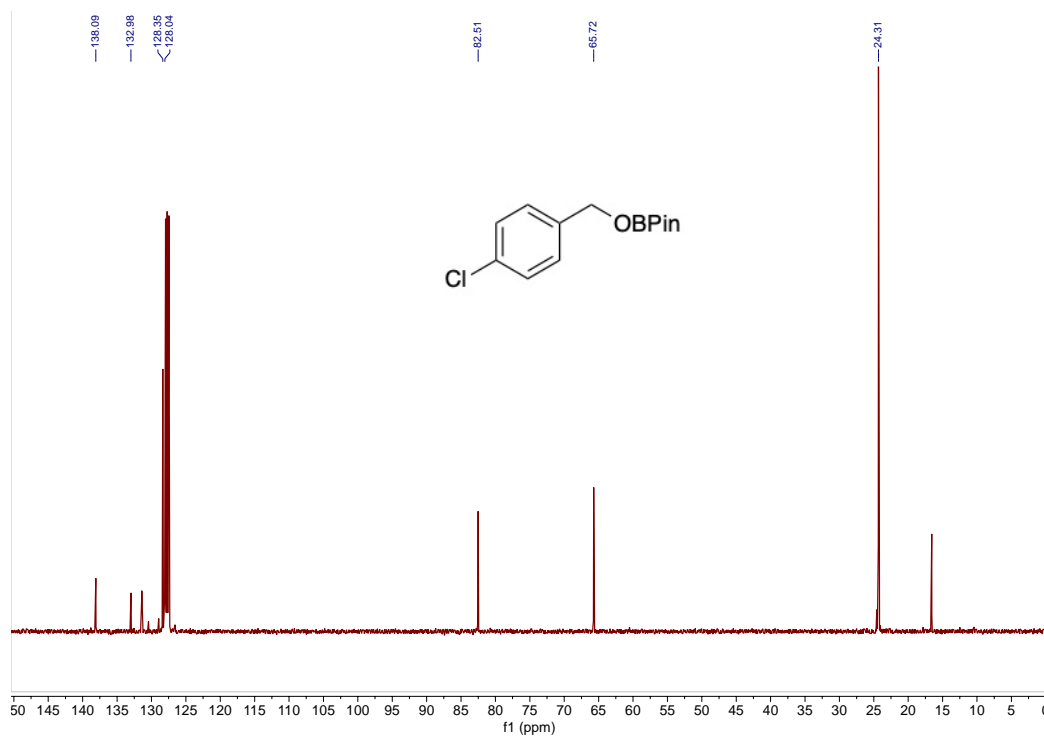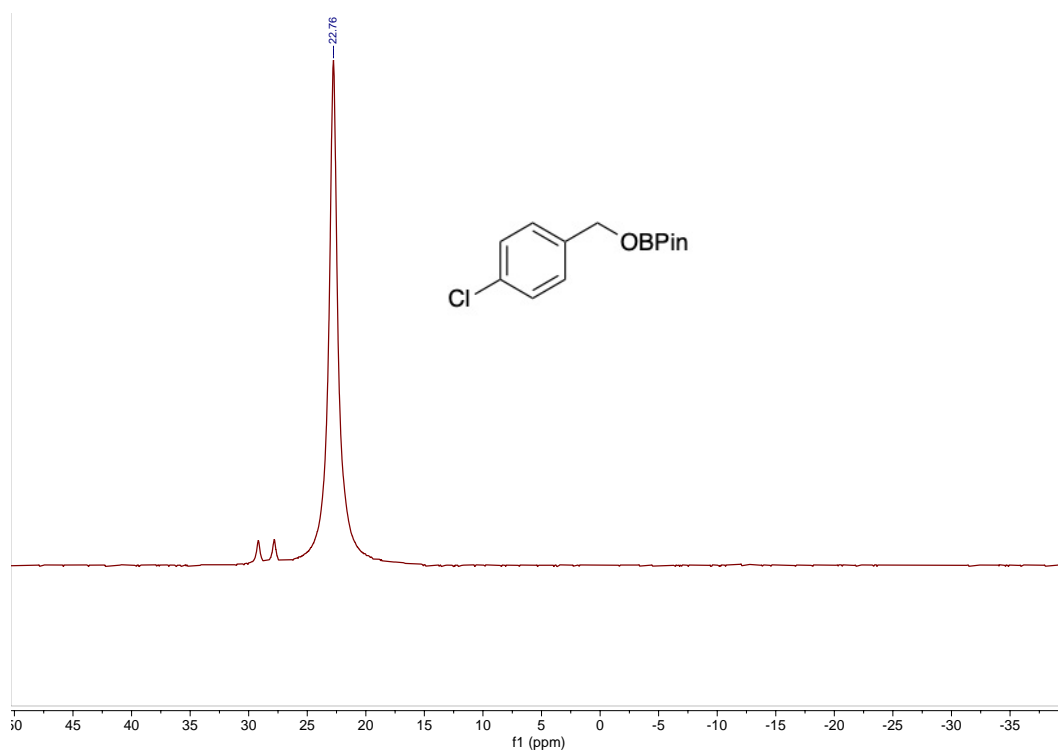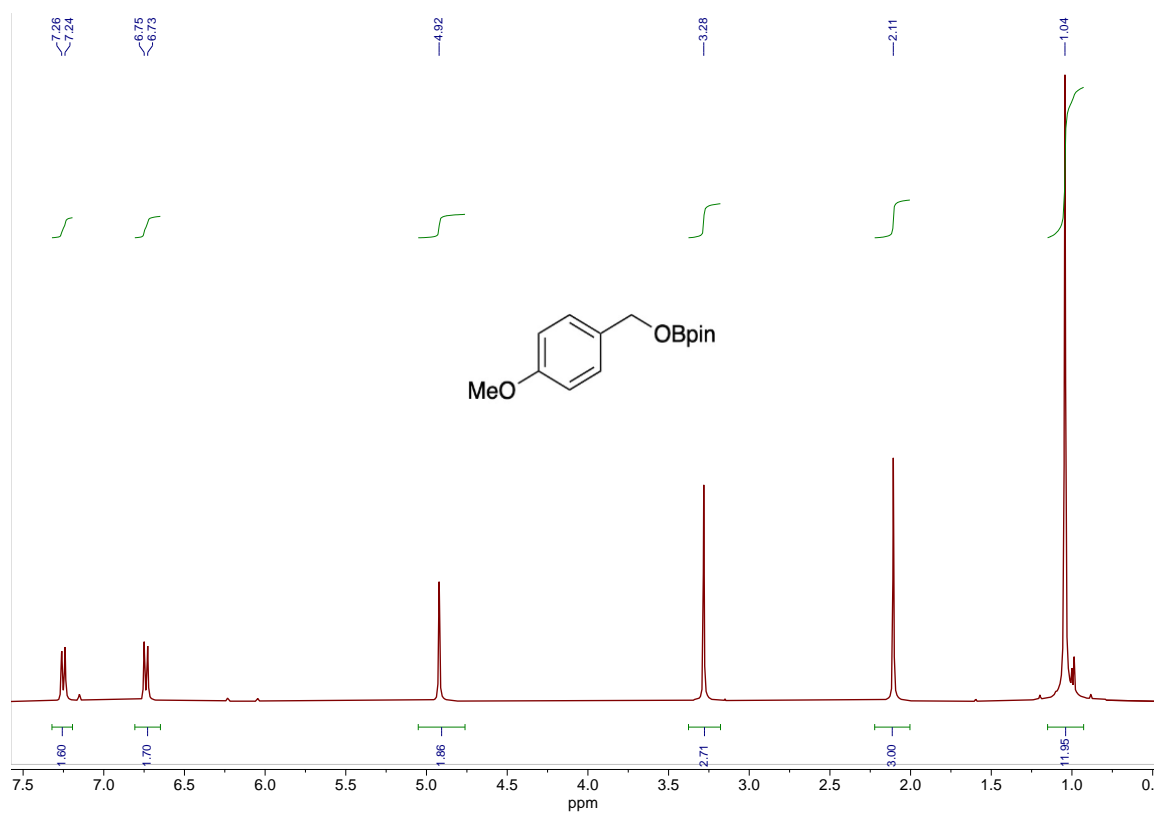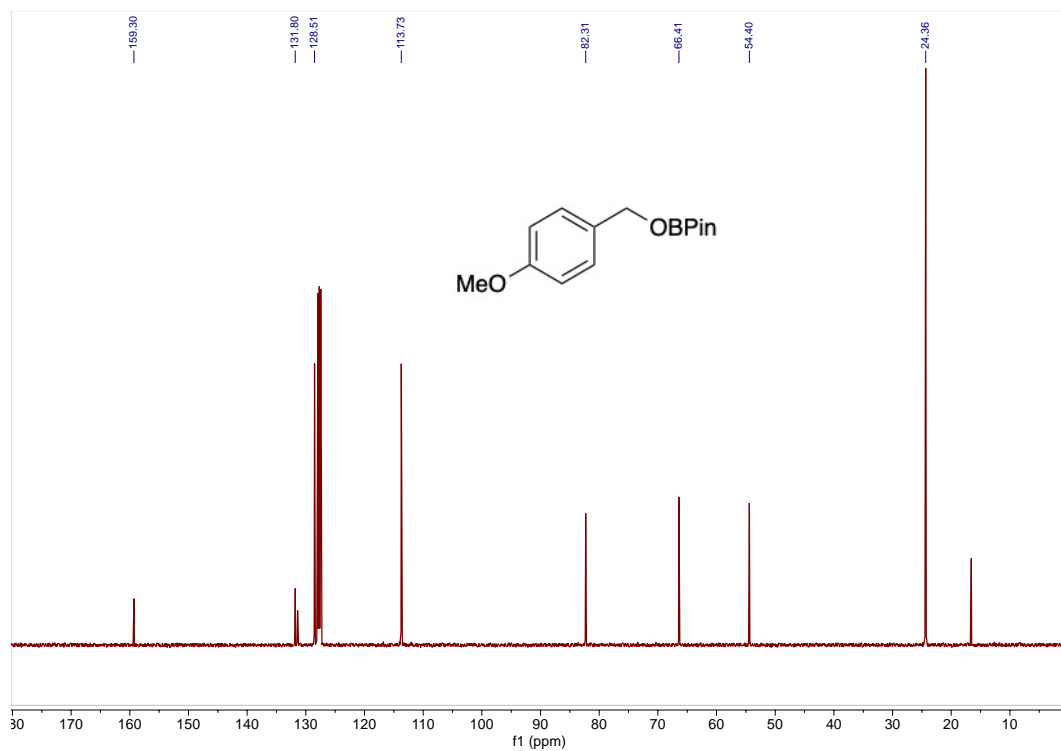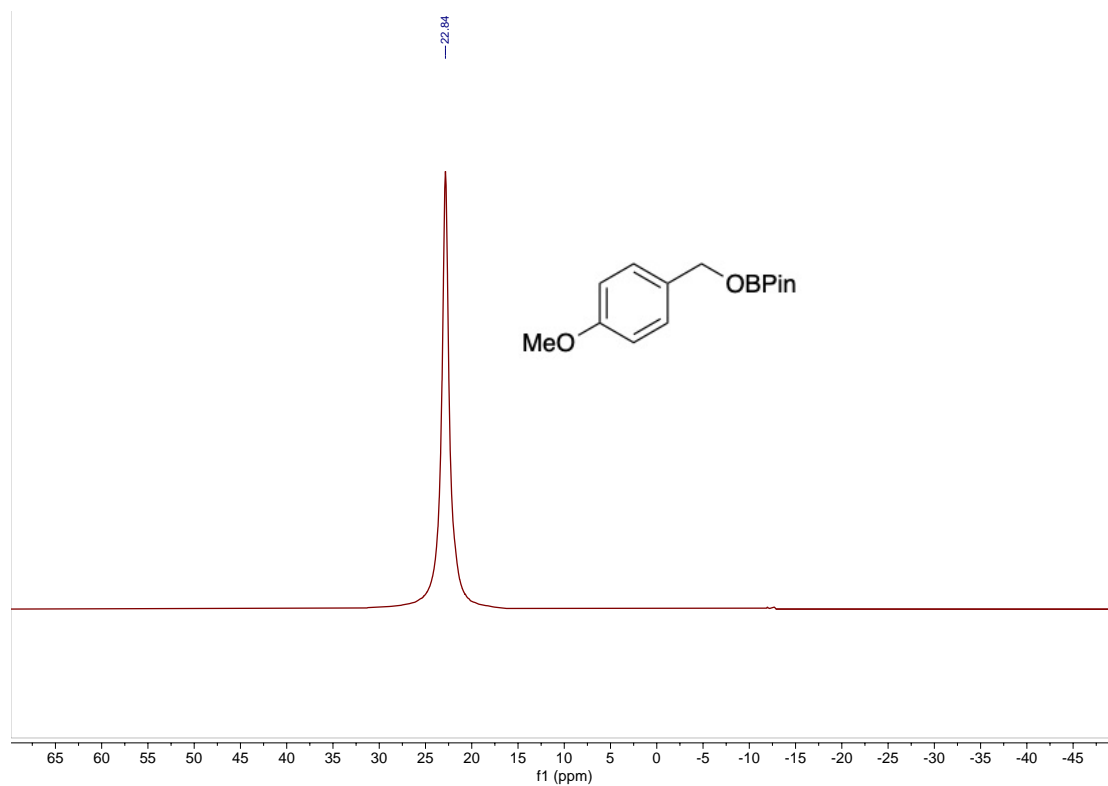**Figure S3.** ^{13}C{^{1}H} NMR spectrum of **8a** in benzene-d_6. The signals at 16.7 and 131.4 ppm are the hexamethylbenzene internal standard, and the signals at 10.0 and 118.0 ppm are the Cp*$_2$Sn catalyst.
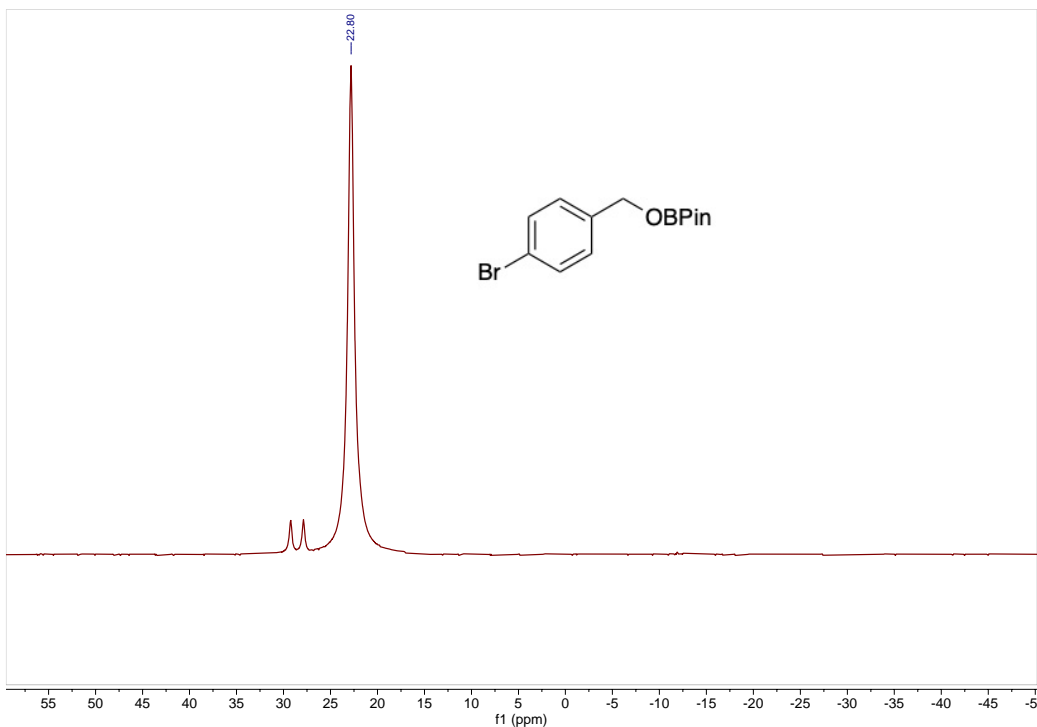
Figure S4. ^{11}B NMR spectrum of **8a** in benzene-d_6. The doublet signal at 28.5 ppm corresponds to HBpin.
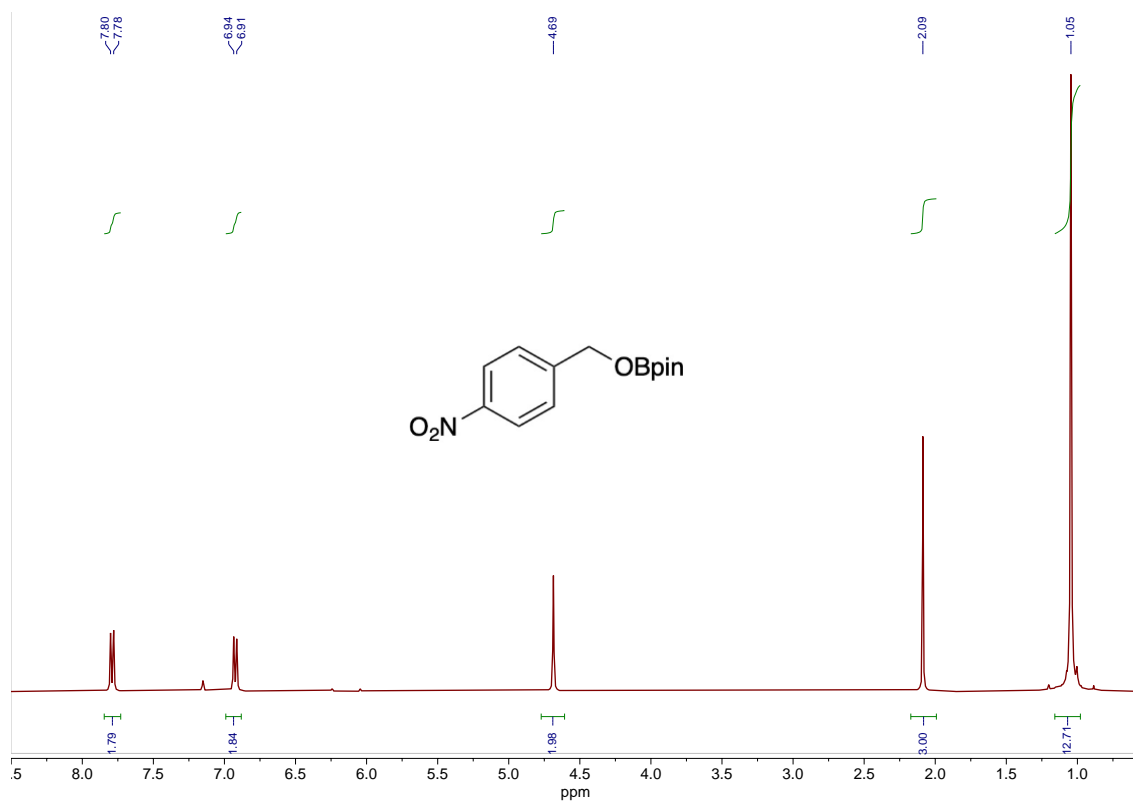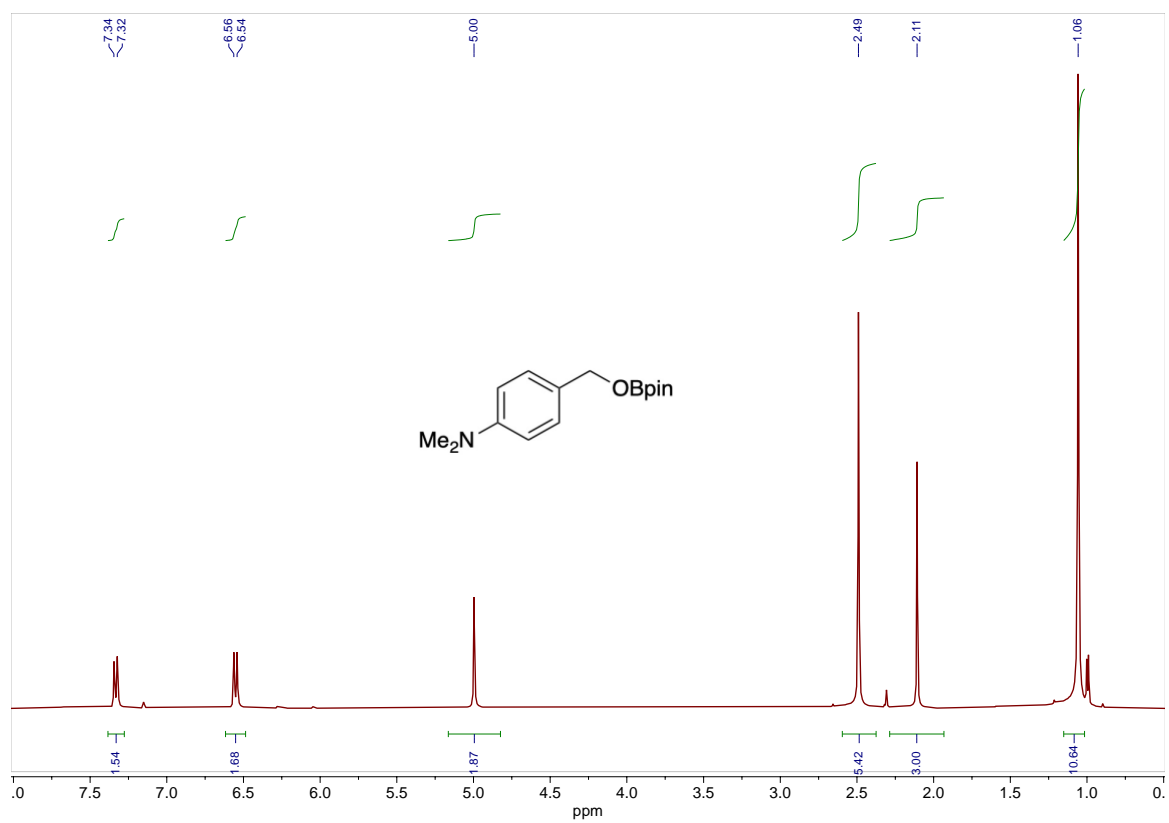

Figure S5. ^{1}H NMR spectrum of **8b** in benzene-d_6 using catalyst **6**. The signal at 2.1 ppm is the hexamethylbenzene internal standard.
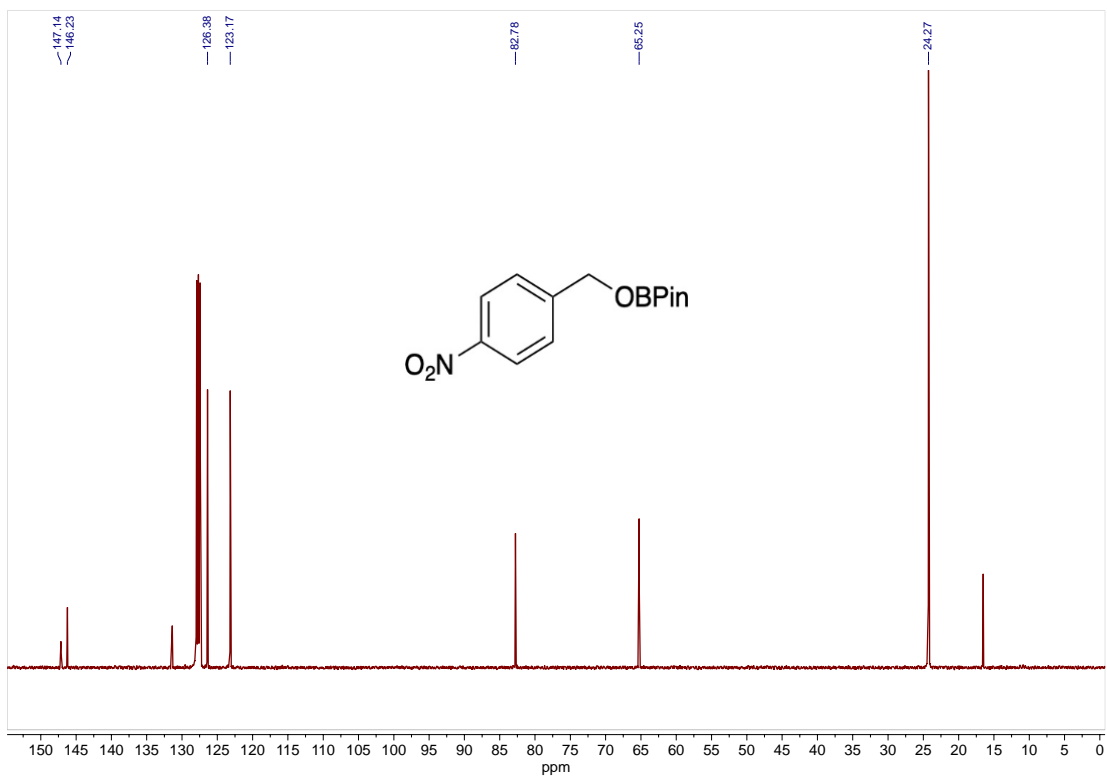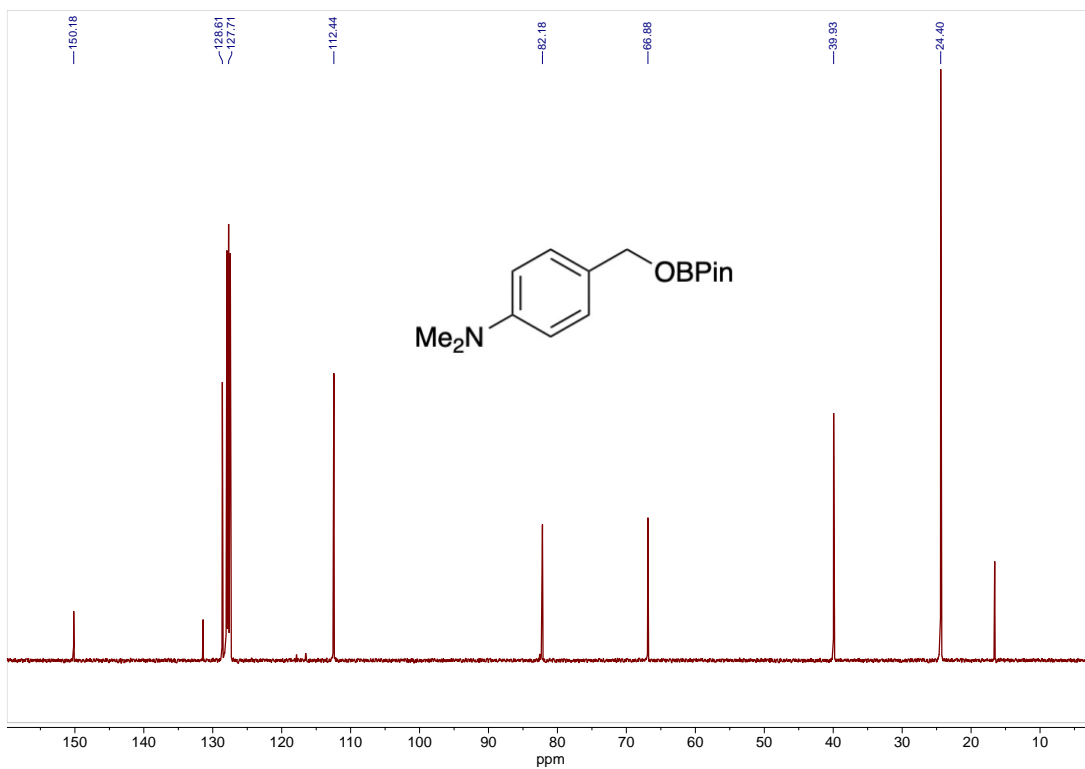
Figure S6. $^{13}C\{^1H\}$ NMR spectrum of **8b** in benzene-d_6. The signals at 16.7 and 131.4 ppm are the hexamethylbenzene internal standard.
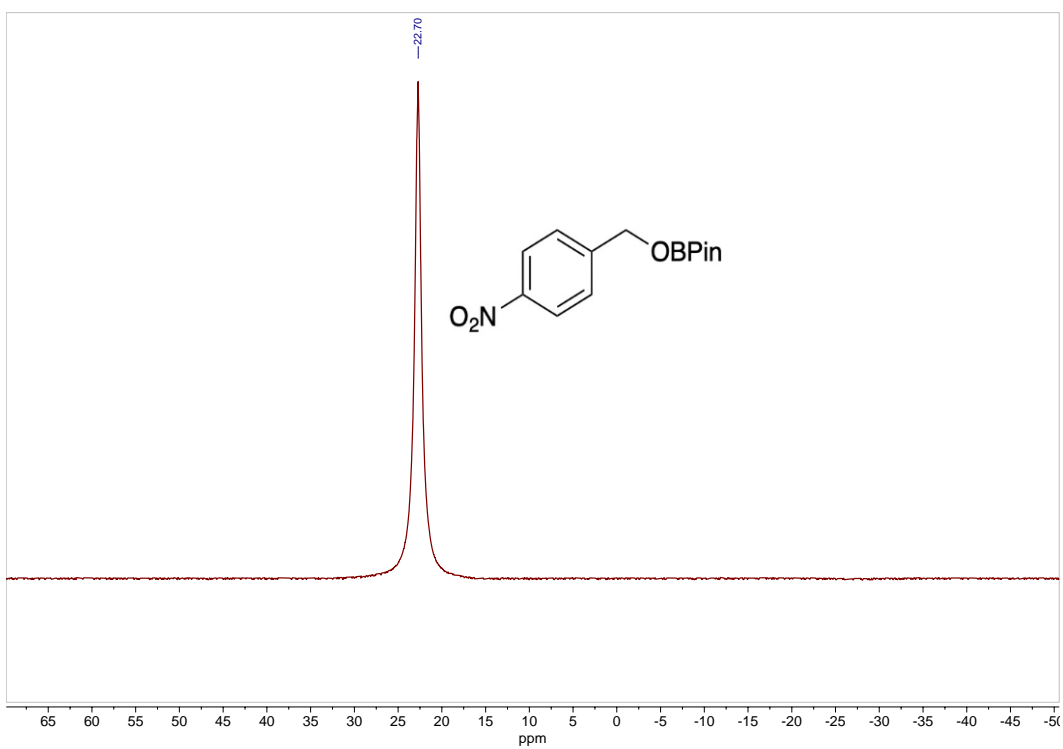
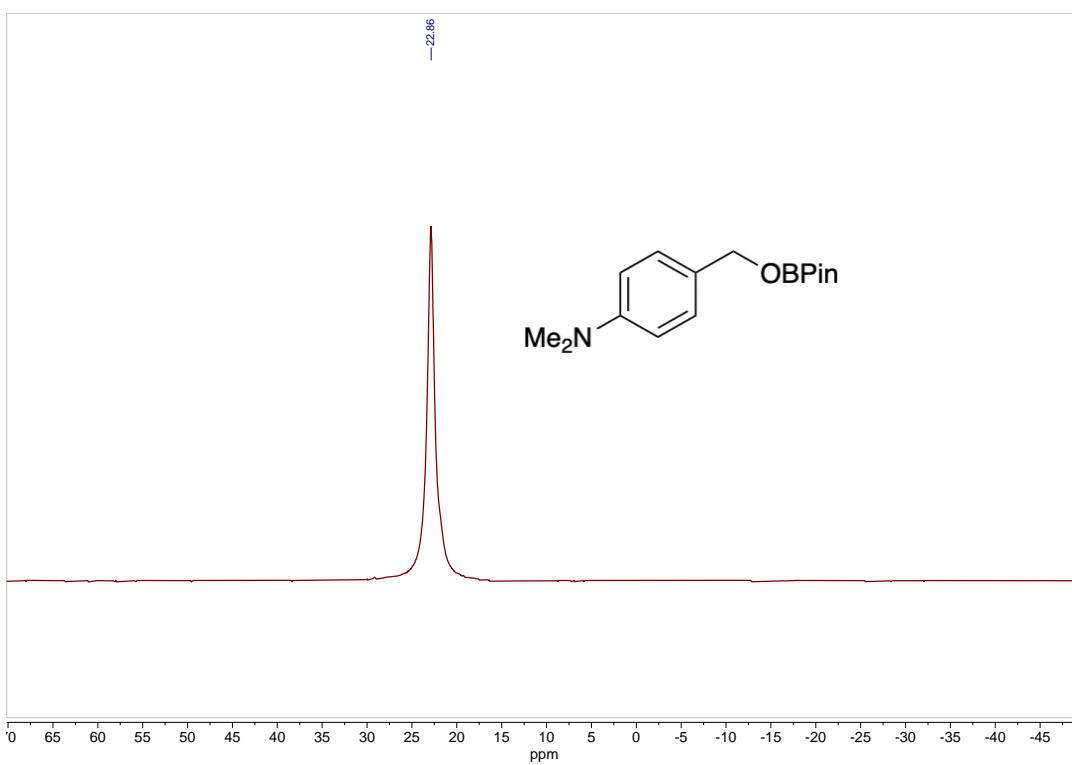**Figure S7.** ^{11}B NMR spectrum of **8b** in benzene-d_6.
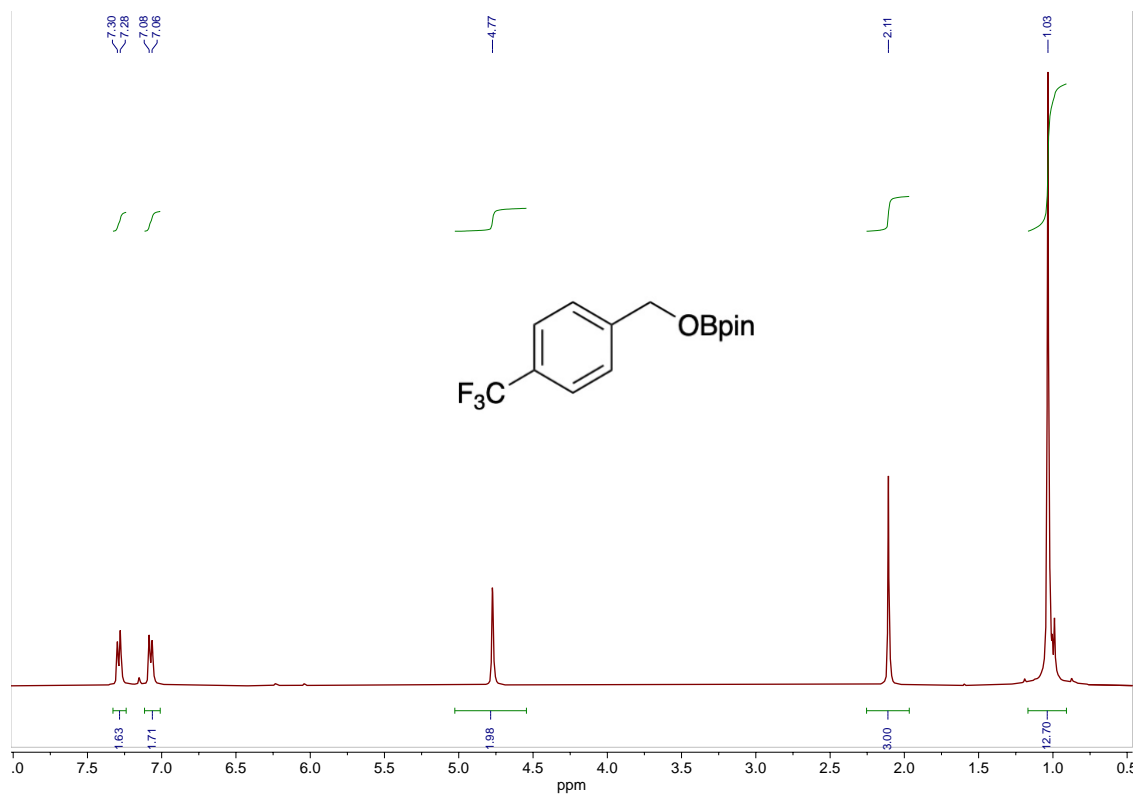
Figure S8. ^{1}H NMR spectrum of **8c** in benzene-d_6 with catalyst **6**. The signal at 2.1 ppm is the hexamethylbenzene internal standard.
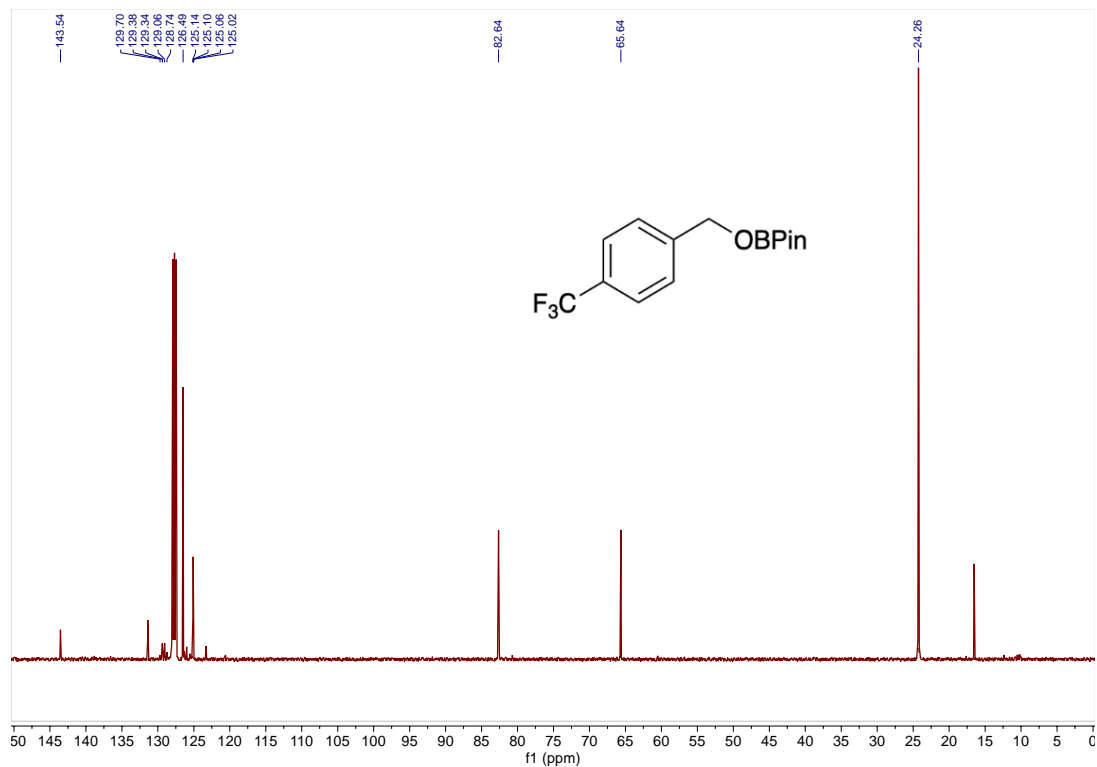
Figure S9. ^{13}C{^{1}H} NMR spectrum of **8c** in benzene-d_6. The signals at 16.7 and 131.4 ppm are the hexamethylbenzene internal standard.
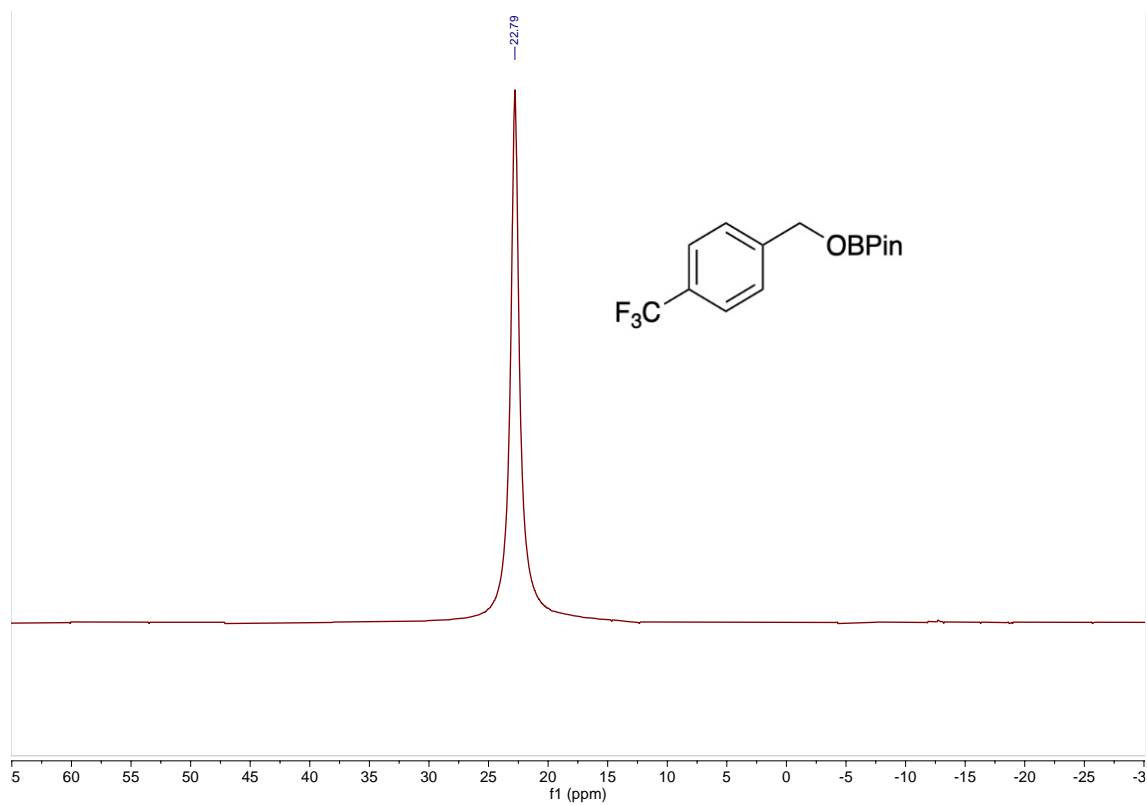
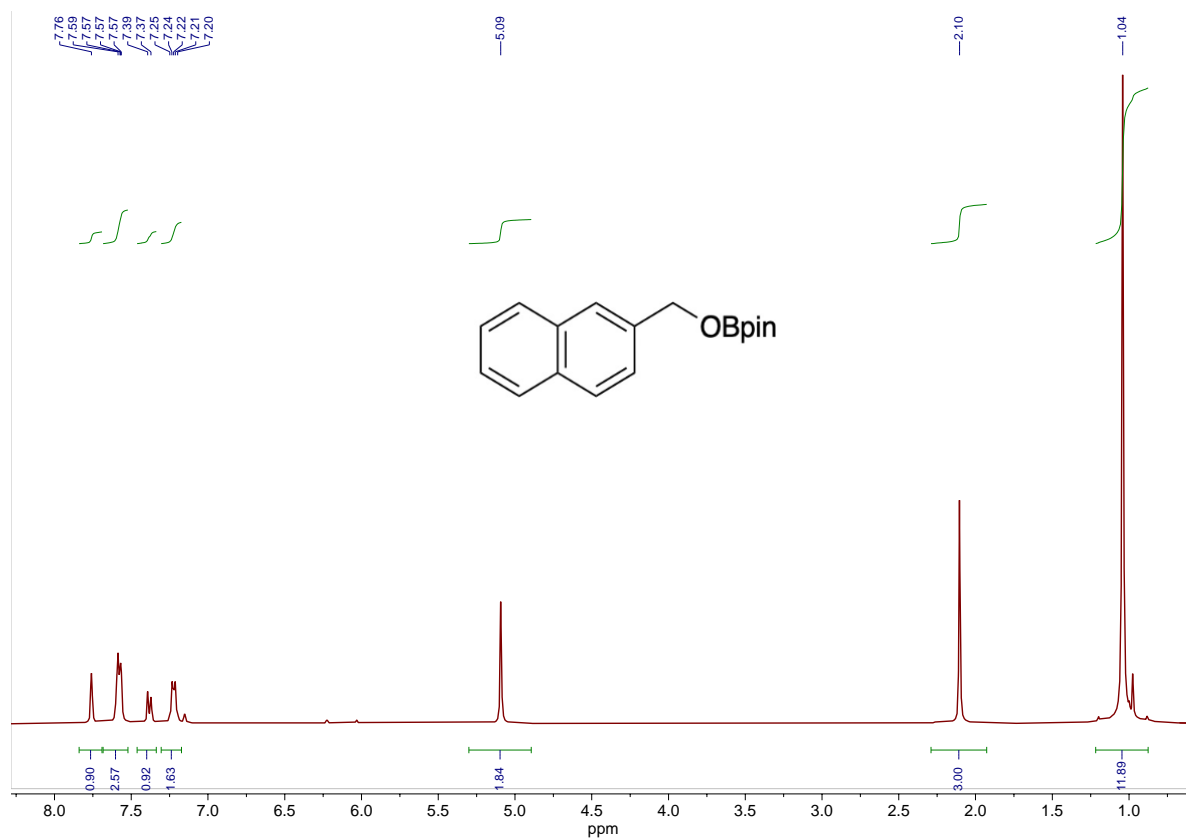**Figure S10.** ^{11}B NMR spectrum of **8c** in benzene-d_6.
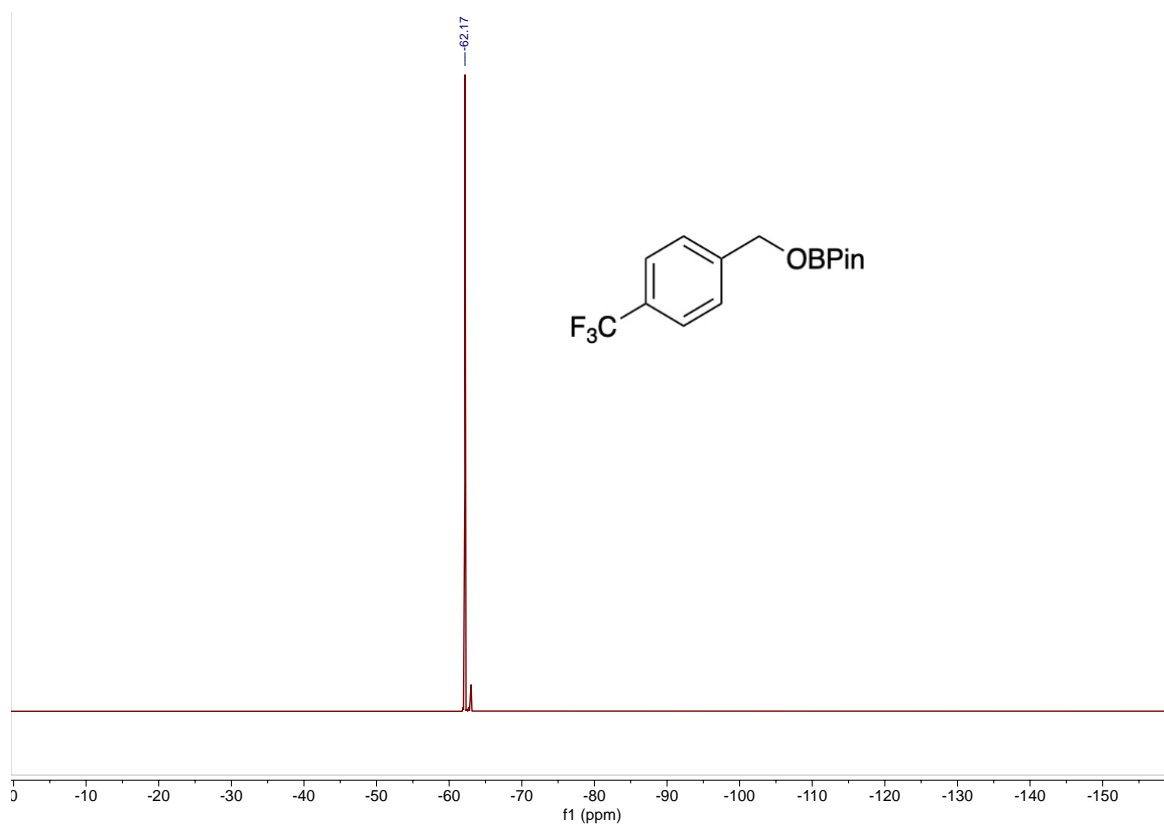
Figure S11. ^{19}F{^{1}H} NMR spectrum of **8c** in benzene-d_6.
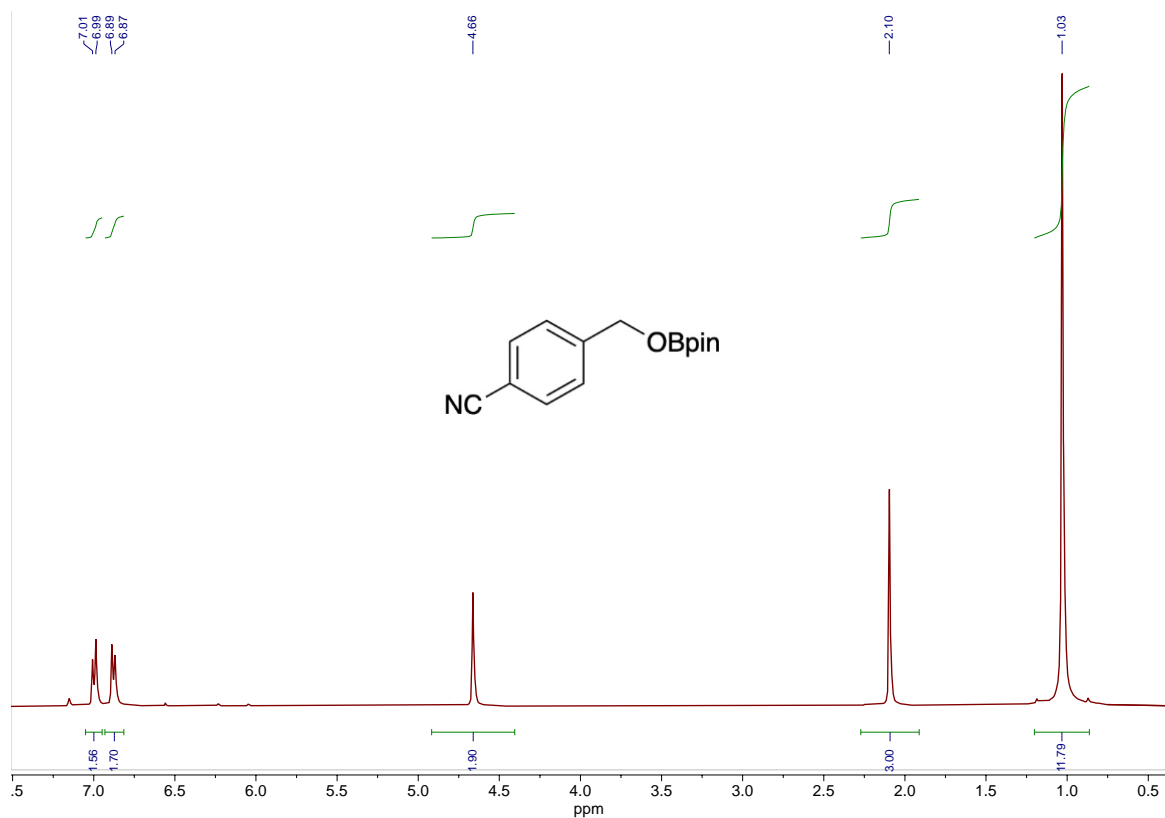
Figure S12. ^{1}H NMR spectrum of **8d** in benzene-d_6 using catalyst **5**. The signal at 2.1 ppm is the hexamethylbenzene internal standard.
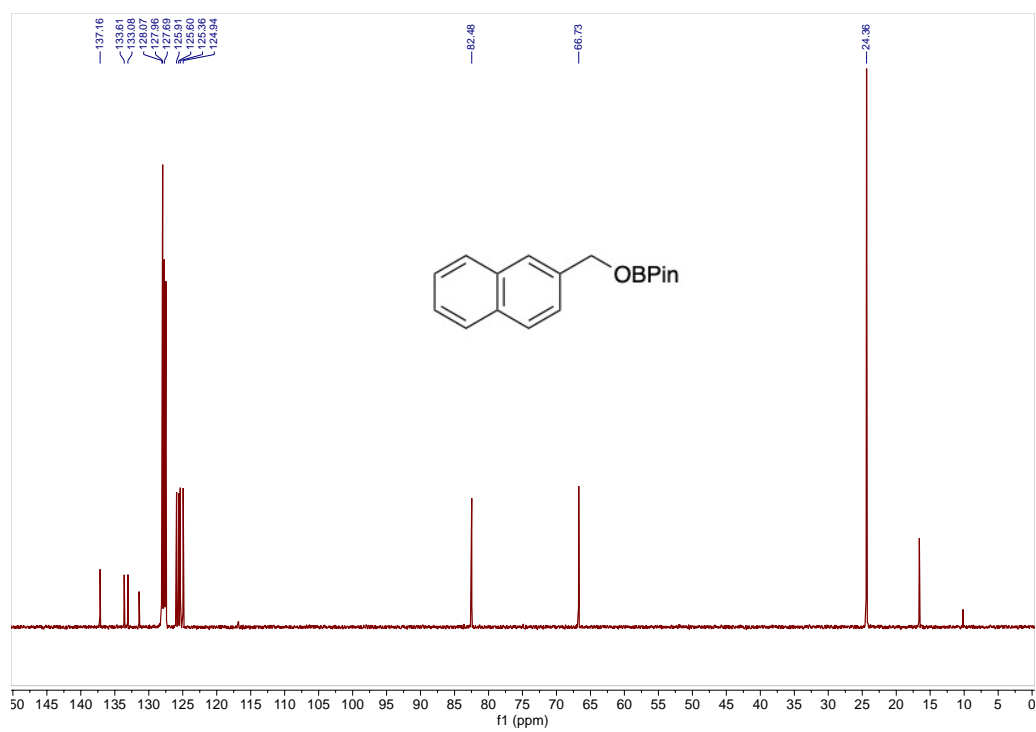

Figure S13. ^{13}C{^{1}H} NMR spectrum of **8d** in benzene-d_6. The signals at 16.7 and 131.4 ppm are the hexamethylbenzene internal standard.

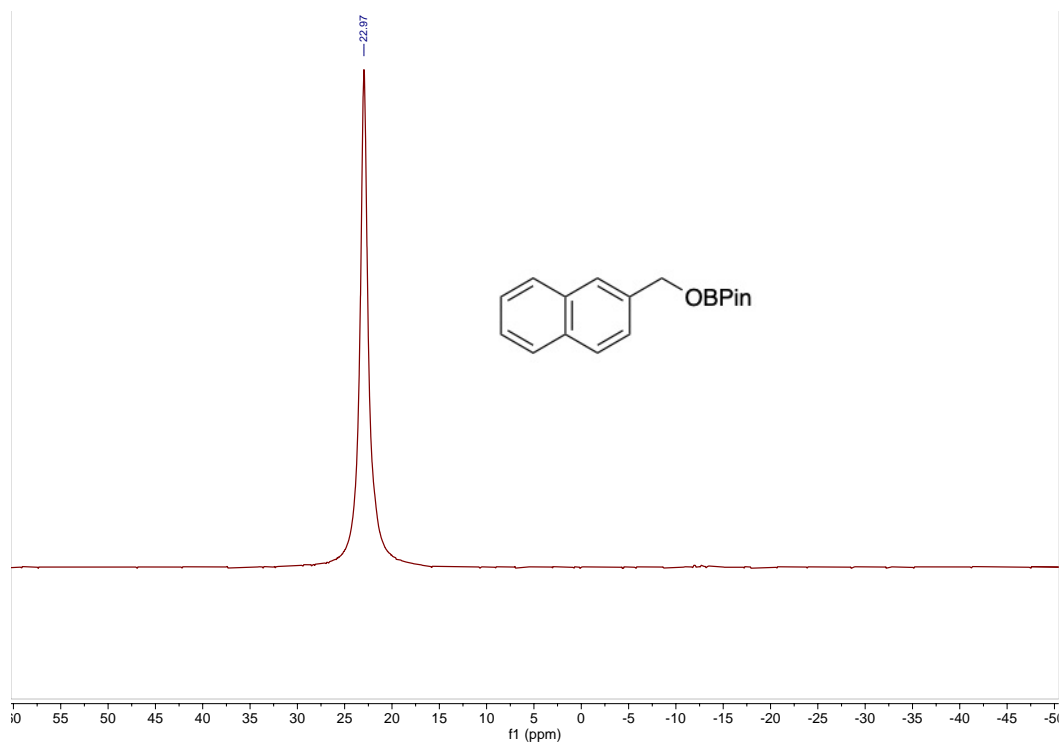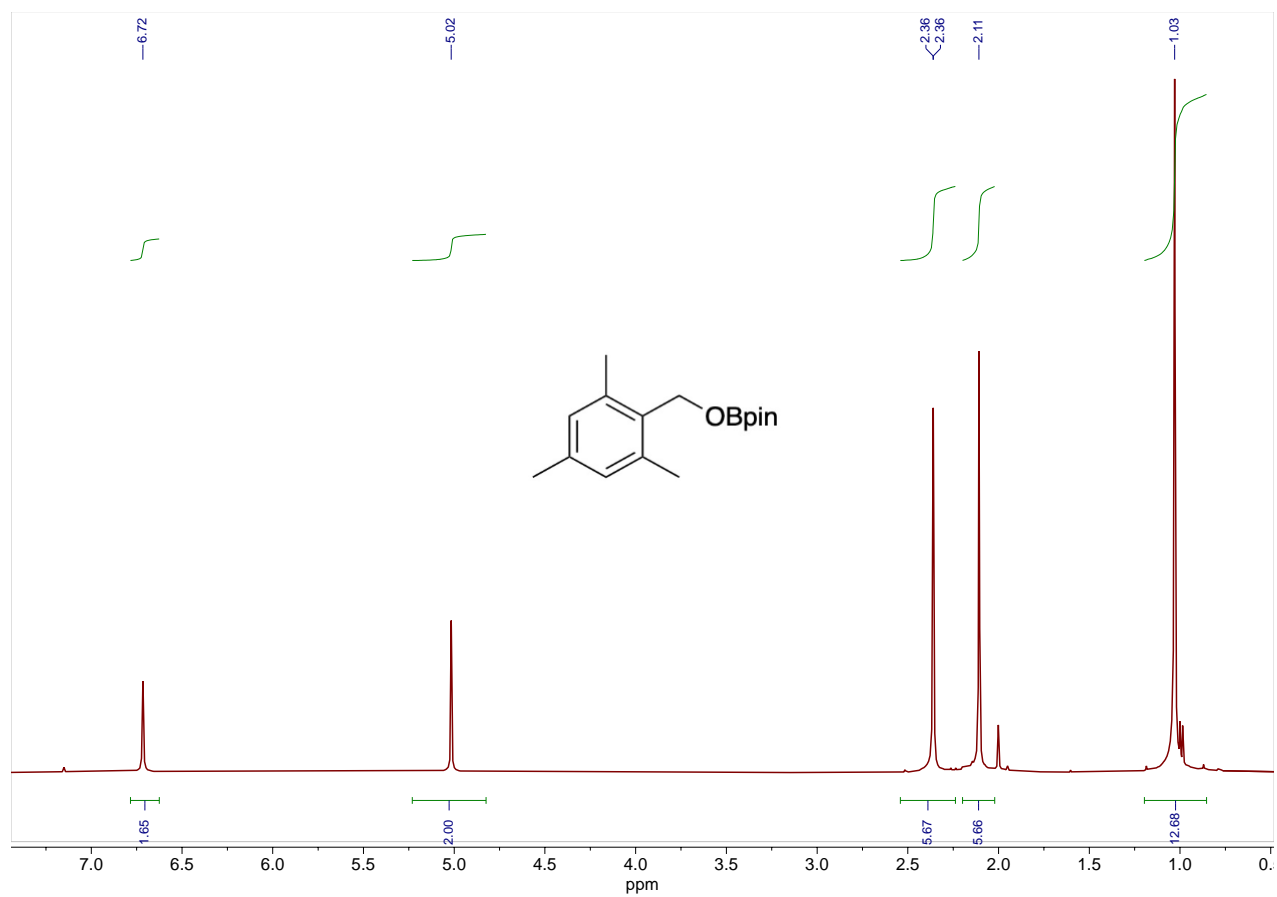**Figure S14.** ^{11}B NMR spectrum of **8d** in benzene-d_6. The doublet signal at 28.5 ppm corresponds to HBpin.

Figure S15. ^{1}H NMR spectrum of **8e** in benzene-d_6 using catalyst **5**. The signal at 2.1 ppm is the hexamethylbenzene internal standard.
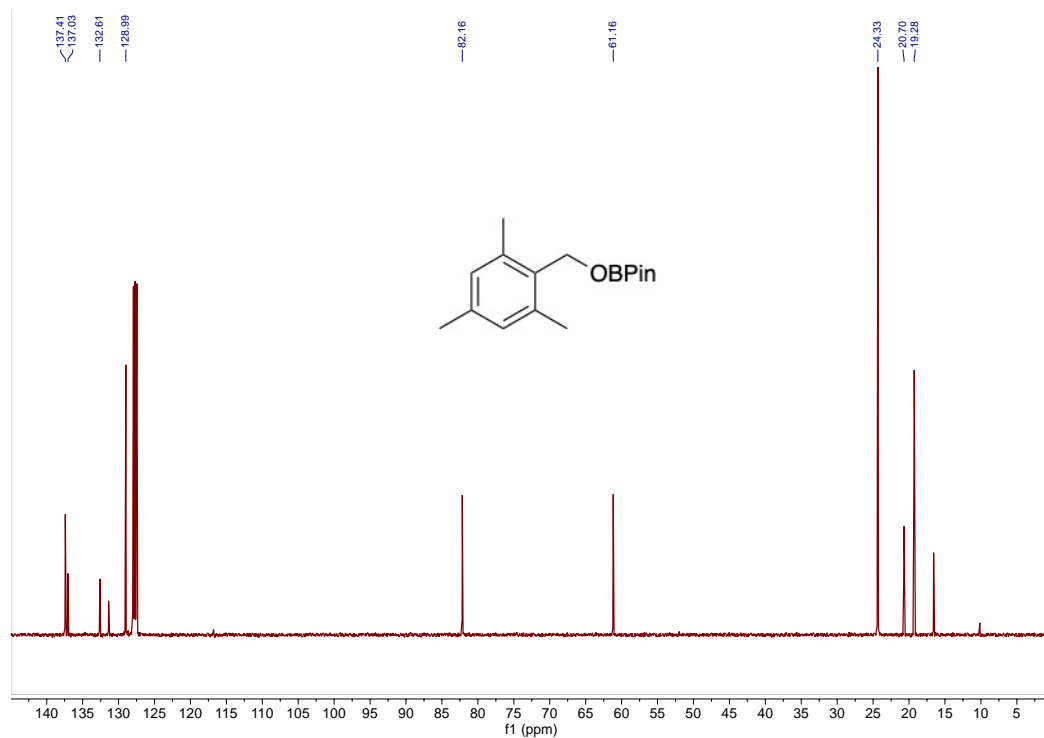
Figure S16. $^{13}C\{^1H\}$ NMR spectrum of **8e** in benzene-d_6. The signals at 16.7 and 131.4 ppm are the hexamethylbenzene internal standard.

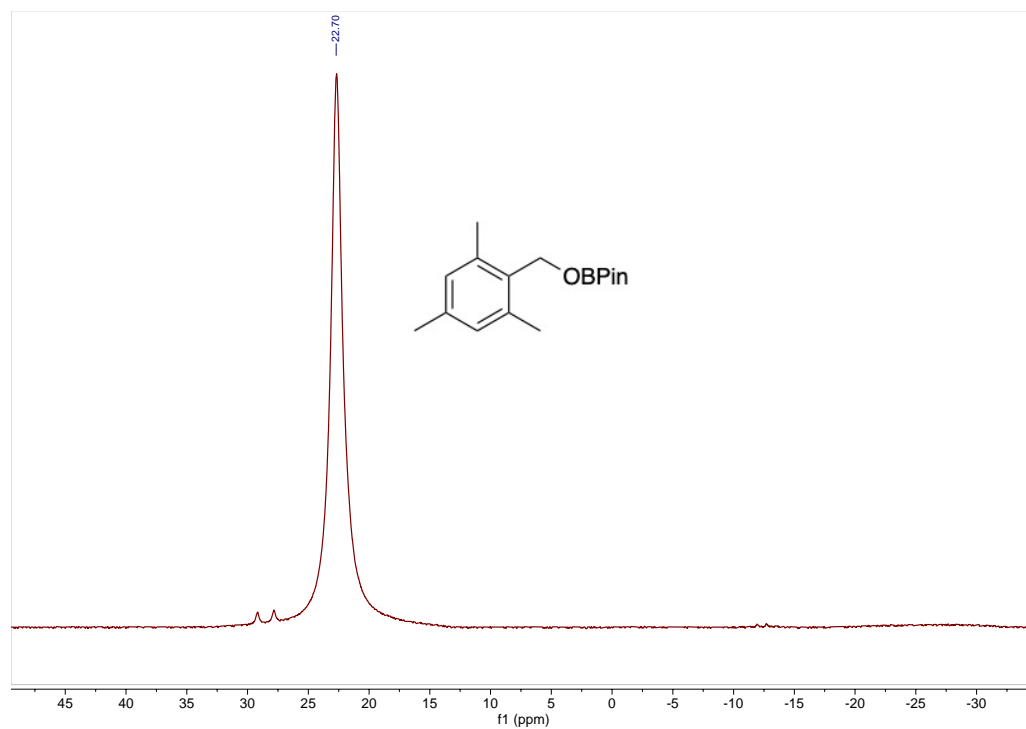**Figure S17.** ^{11}B NMR spectrum of **8e** in benzene-d_6. The doublet signal at 28.5 ppm corresponds to HBpin.
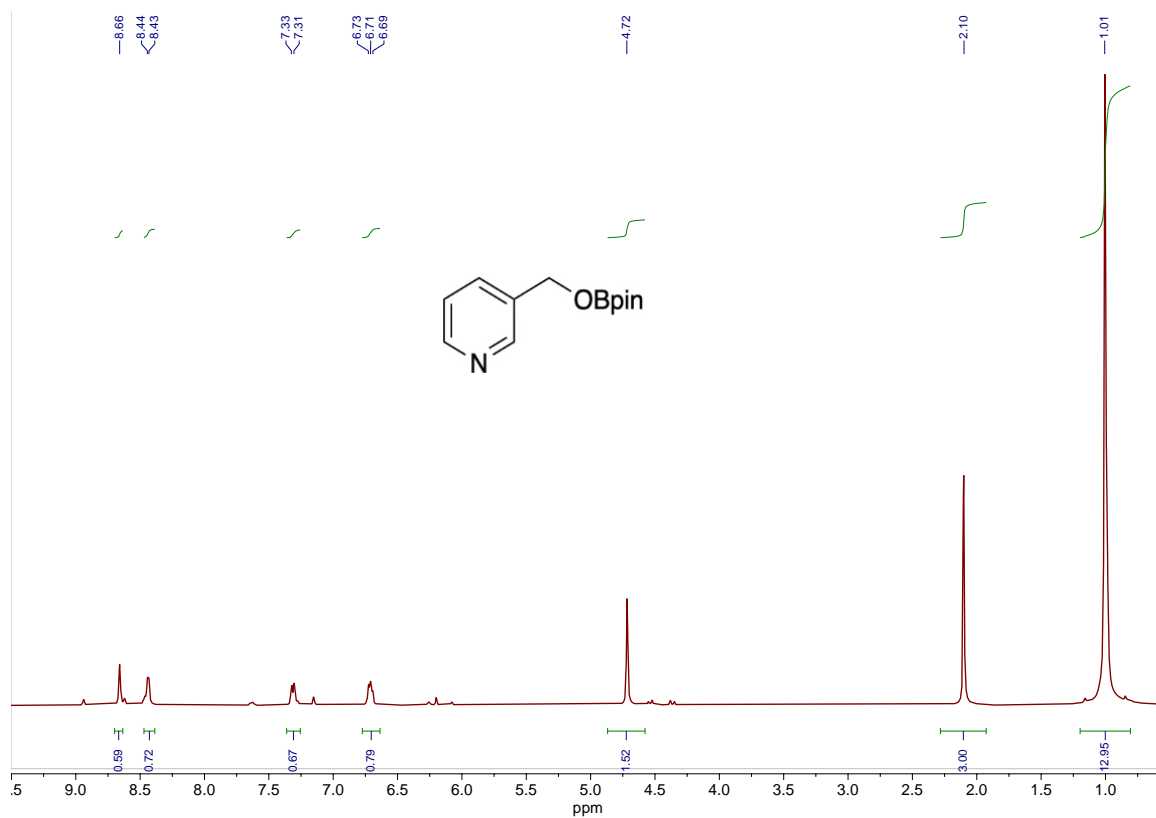
Figure S18. ^{1}H NMR spectrum of **8f** in benzene-d_6 using catalyst **5**. The signal at 2.1 ppm is the hexamethylbenzene internal standard.
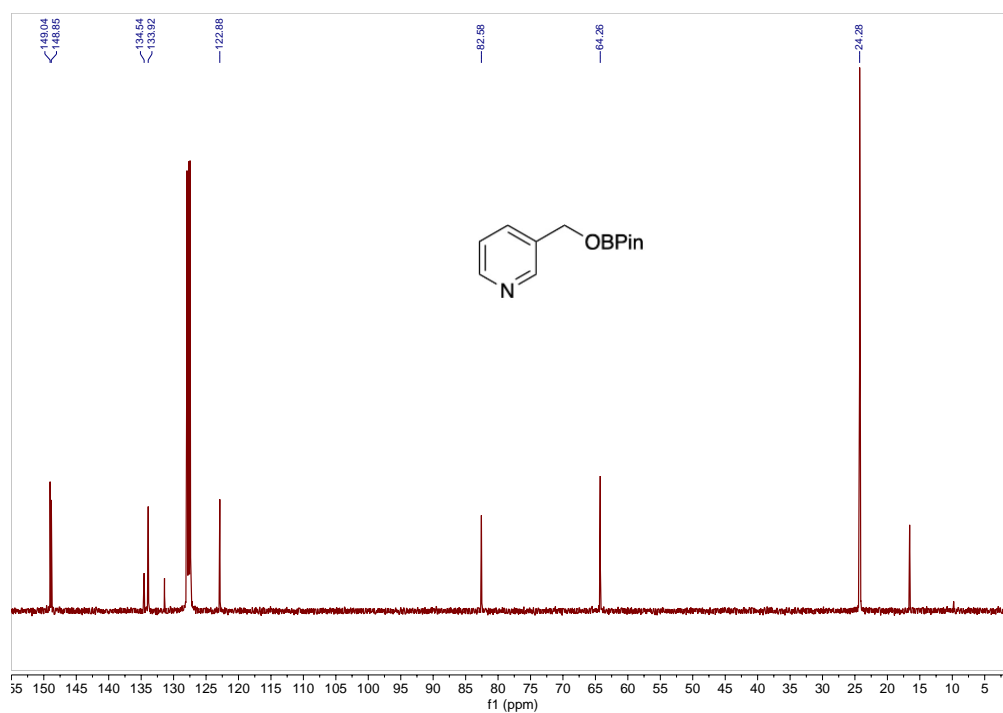

Figure S19. ^{13}C{^{1}H} NMR spectrum of **8f** in benzene-d_6. The signals at 16.7 and 131.4 ppm are the hexamethylbenzene internal standard.

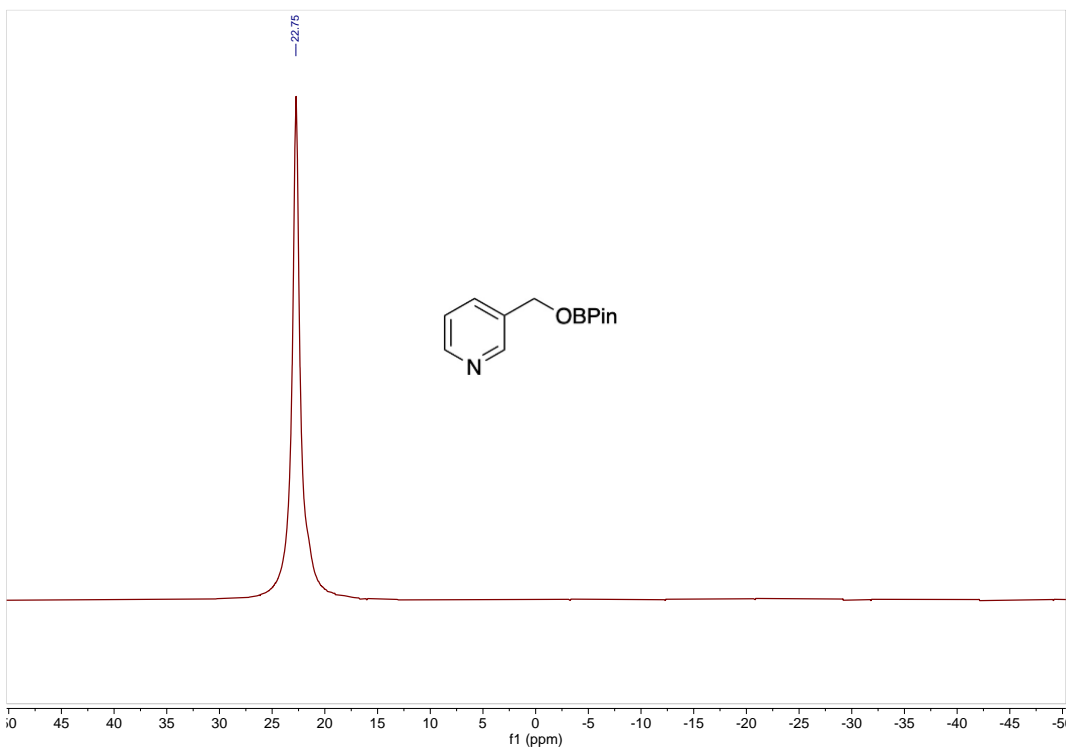**Figure S20.** ^{11}B NMR spectrum of **8f** in benzene-d_6.

Figure S21. ^{1}H NMR spectrum of **8g** in benzene-d_6 using catalyst **5**. The signal at 2.1 ppm is the hexamethylbenzene internal standard.

Figure S22. ^{13}C{^{1}H} NMR spectrum of **8g** in benzene-d_6. The signals at 16.7 and 131.4 ppm are the hexamethylbenzene internal standard.

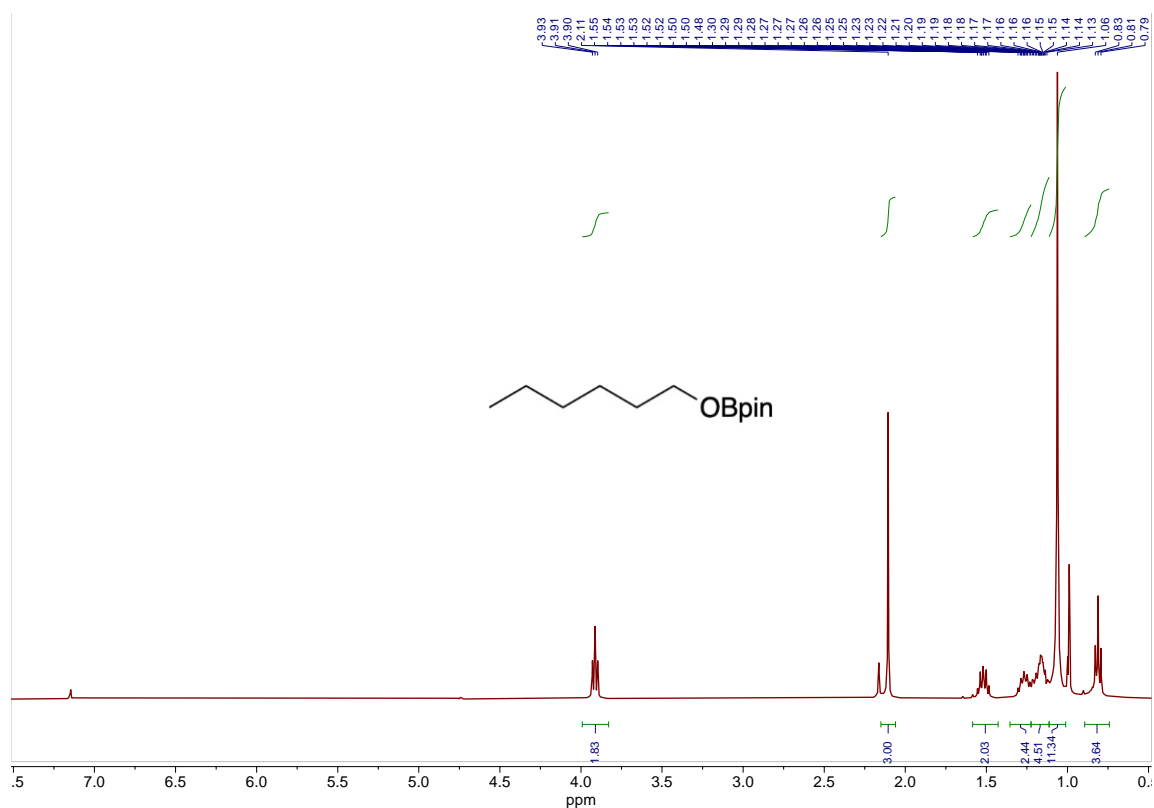**Figure S23.** ^{11}B NMR spectrum of **8g** in benzene-d_6.

Figure S24. ¹H NMR spectrum of **8h** in benzene-d_6 using catalyst **6**. The signal at 2.1 ppm is the hexamethylbenzene internal standard.
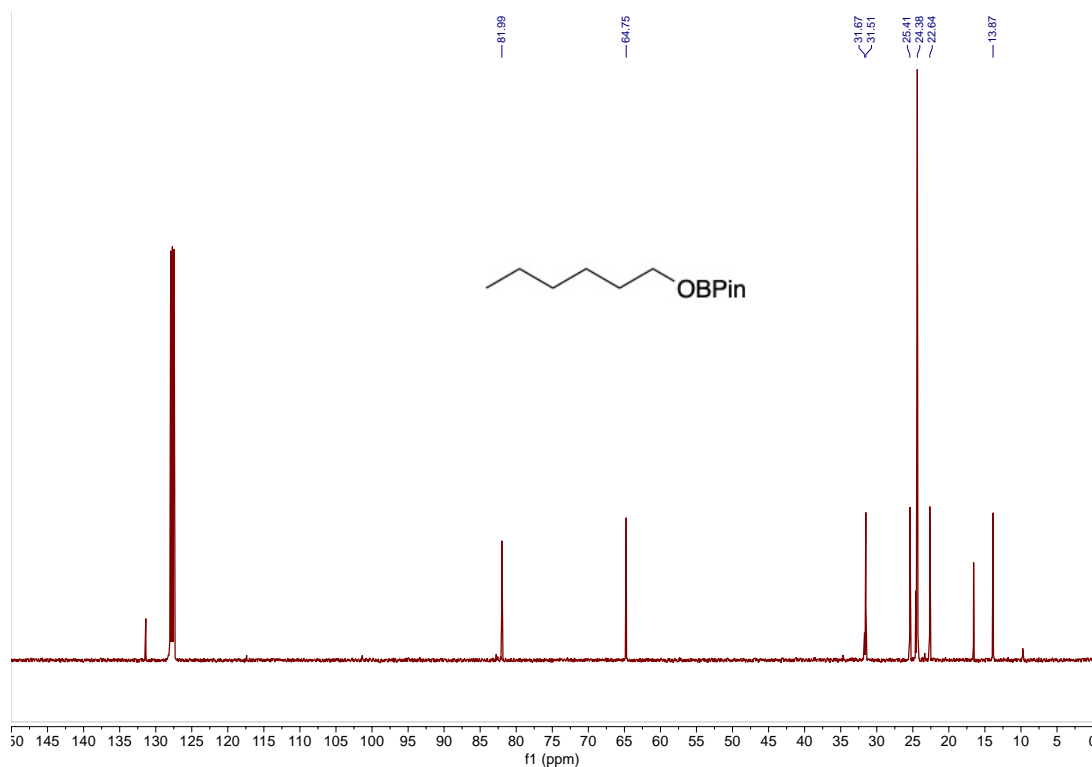

Figure S25. ¹³C{¹H} NMR spectrum of **8h** in benzene-d_6. The signals at 16.7 and 131.4 ppm are the hexamethylbenzene internal standard.

Figure S26. ^{11}B NMR spectrum of **8h** in benzene-d_6.

Figure S27. ^{1}H NMR spectrum of **8i** in benzene-d_6 using catalyst **5**.

Figure S28. $^{13}C\{^1H\}$ NMR spectrum of **8i** in benzene-d_6. The signals at 16.7 and 131.4 ppm are the hexamethylbenzene internal standard.
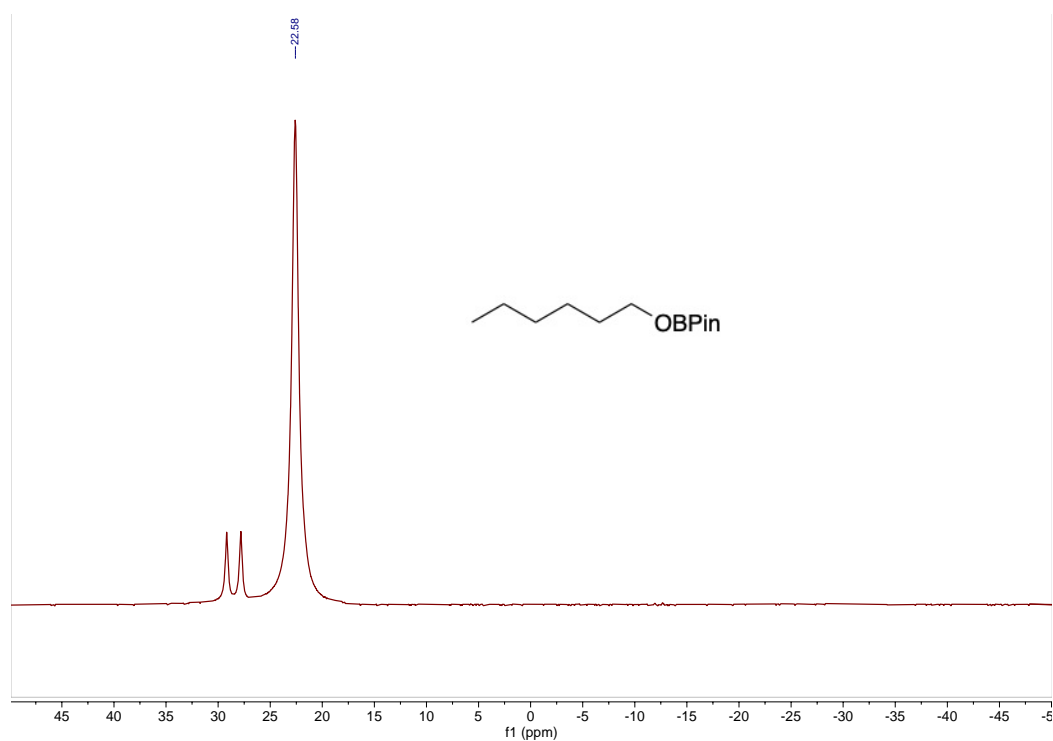

Figure S29. ^{11}B NMR spectrum of **8i** in benzene-d_6. The doublet signal at 28.5 ppm corresponds to HBpin.
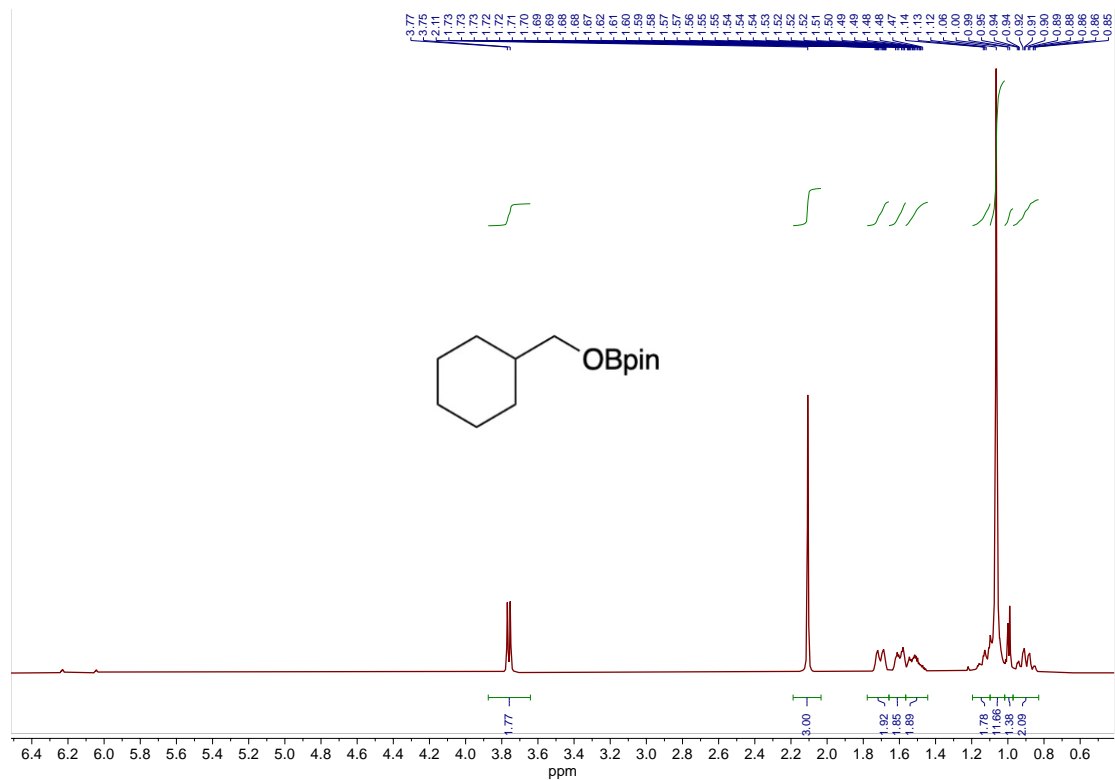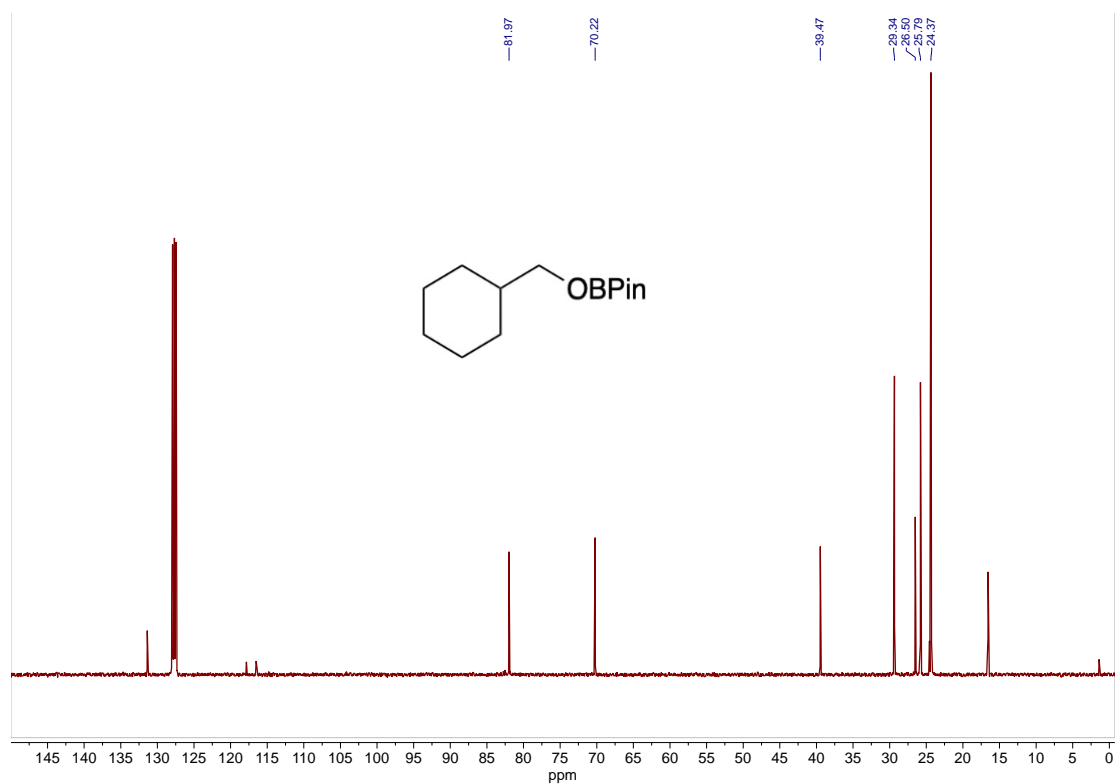
Figure S30. ^{1}H NMR spectrum of **8j** in benzene-d_6 using catalyst **6**. The signal at 2.1 ppm is the hexamethylbenzene internal standard.

Figure S31. ^{13}C{^{1}H} NMR spectrum of **8j** in benzene-d_6. The signals at 16.7 and 131.4 ppm are the hexamethylbenzene internal standard.

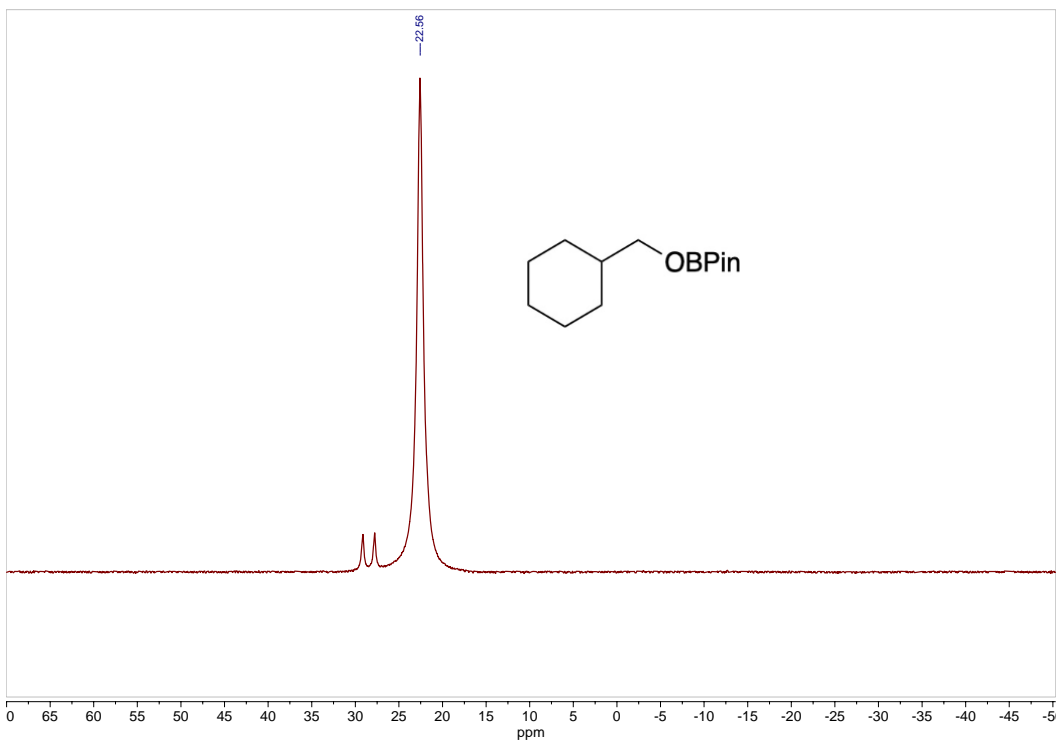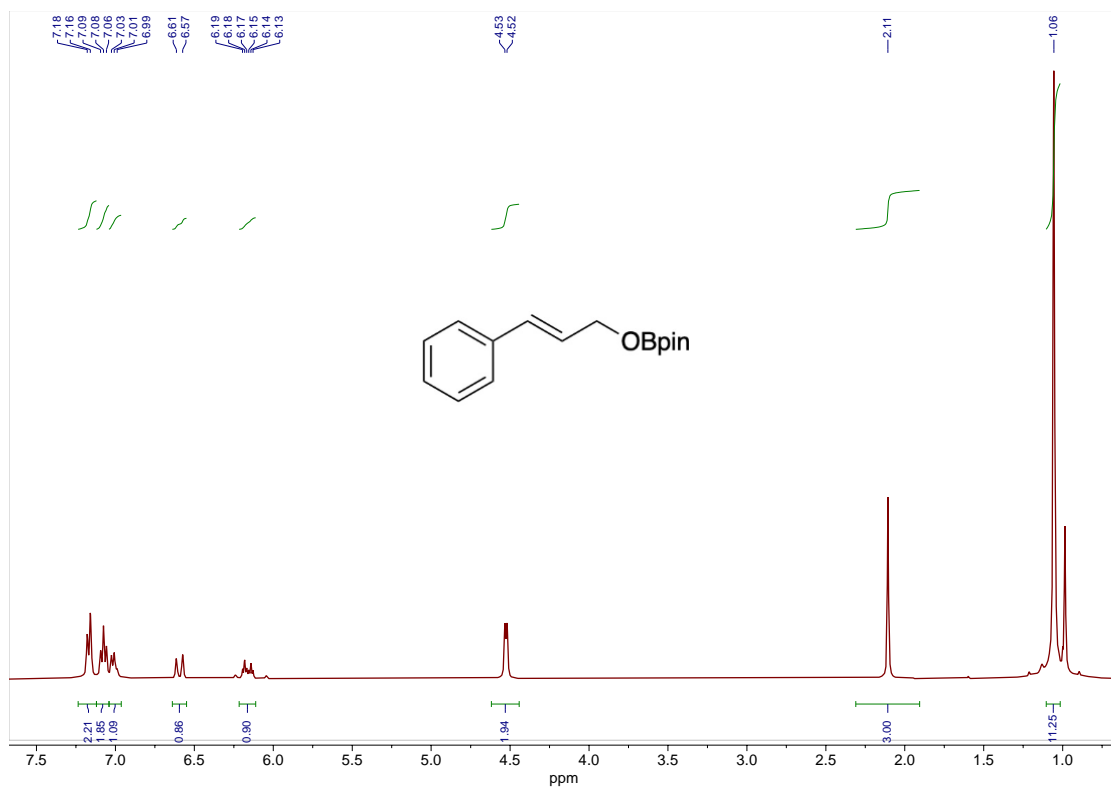**Figure S32.** ^{11}B NMR spectrum of **8j** in benzene-d_6.

Figure S33. ^{1}H NMR spectrum of **8k** in benzene-d_6 using catalyst **6**. The signal at 2.1 ppm is the hexamethylbenzene internal standard.
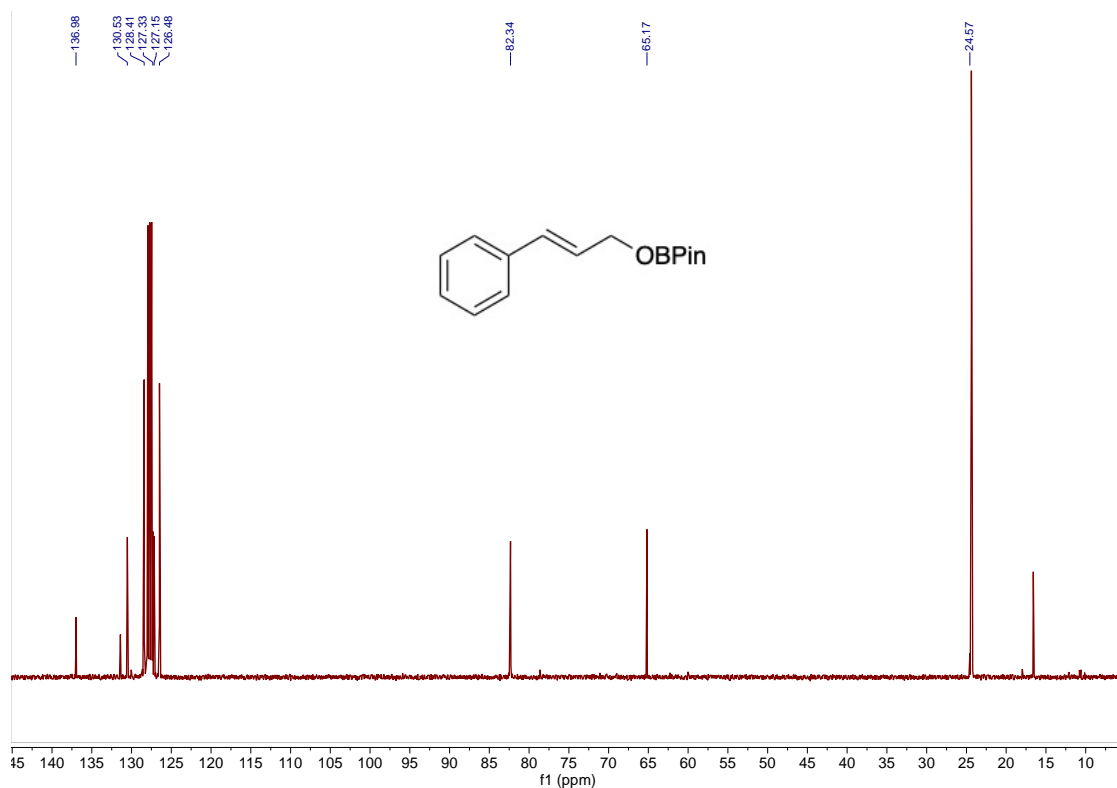
Figure S34. $^{13}C\{^1H\}$ NMR spectrum of **8k** in benzene-d_6. The signals at 16.7 and 131.4 ppm are the hexamethylbenzene internal standard.

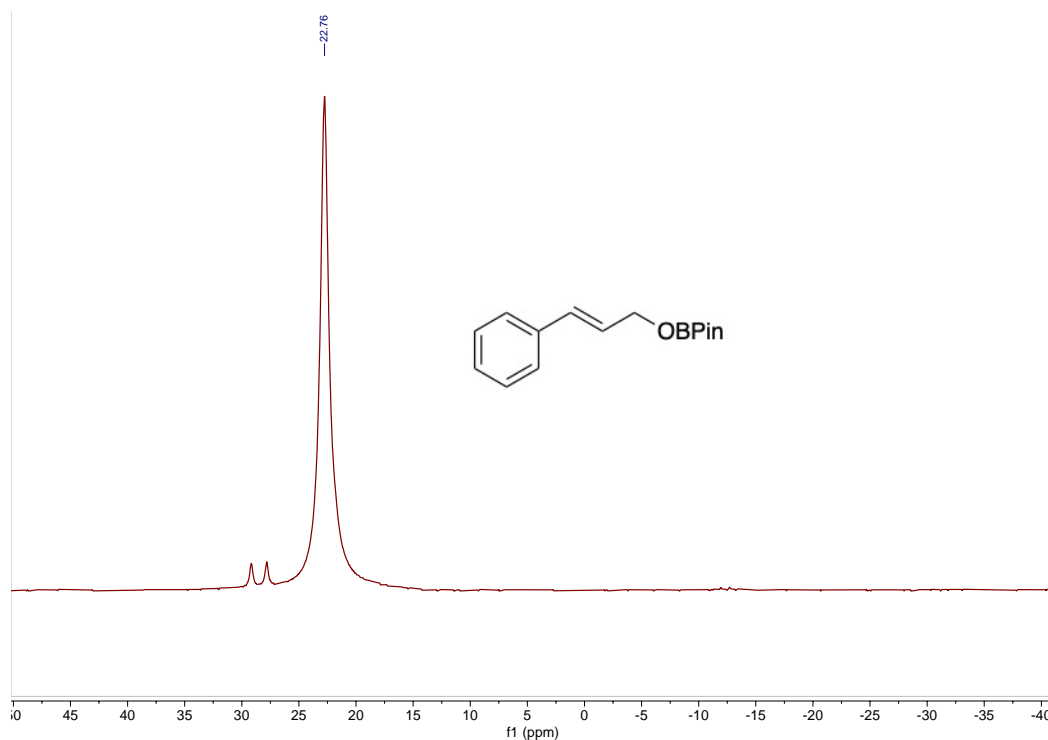**Figure S35.** ^{11}B NMR spectrum of **8k** in benzene-d_6. The doublet signal at 28.5 ppm corresponds to HBpin.

Figure S36. ^{1}H NMR spectrum of **8l** in benzene-d_6 with catalyst **5**. The signal at 2.1 ppm is the hexamethylbenzene internal standard.

Figure S37. ^{13}C{^{1}H} NMR spectrum of **8l** in benzene-d_6. The signals at 16.7 and 131.4 ppm are the hexamethylbenzene internal standard.

Figure S38. ^{11}B NMR spectrum of **8l** in benzene-d_6. The doublet signal at 28.5 ppm corresponds to HBpin.
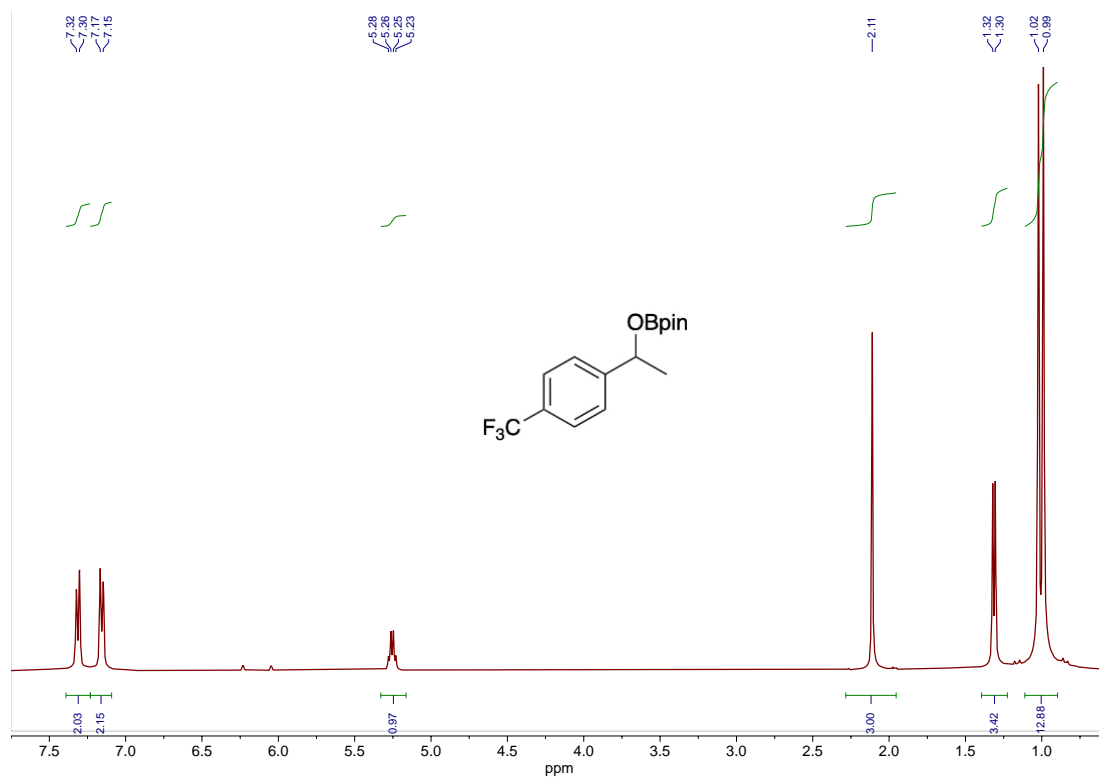

Figure S39. ^{1}H NMR spectrum of **8m** in benzene-d_6 using catalyst **5**. The signal at 2.1 ppm is the hexamethylbenzene internal standard.
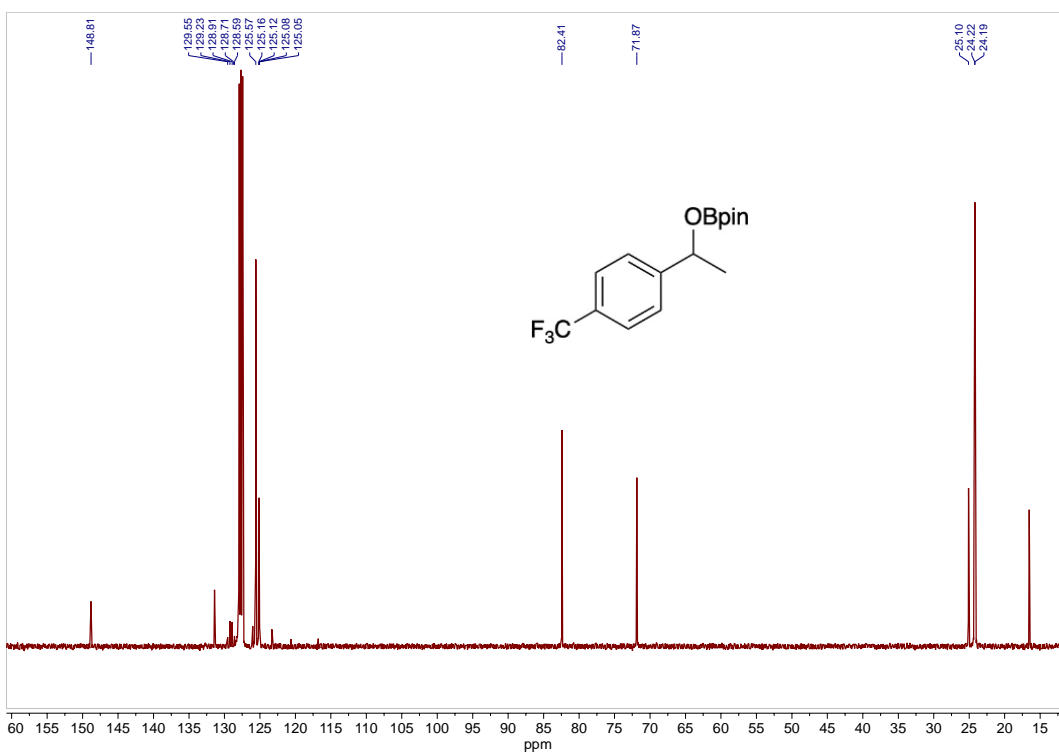
Figure S40. $^{13}C\{^1H\}$ NMR spectrum of **8m** in benzene-d_6. The signals at 16.7 and 131.4 ppm are the hexamethylbenzene internal standard.
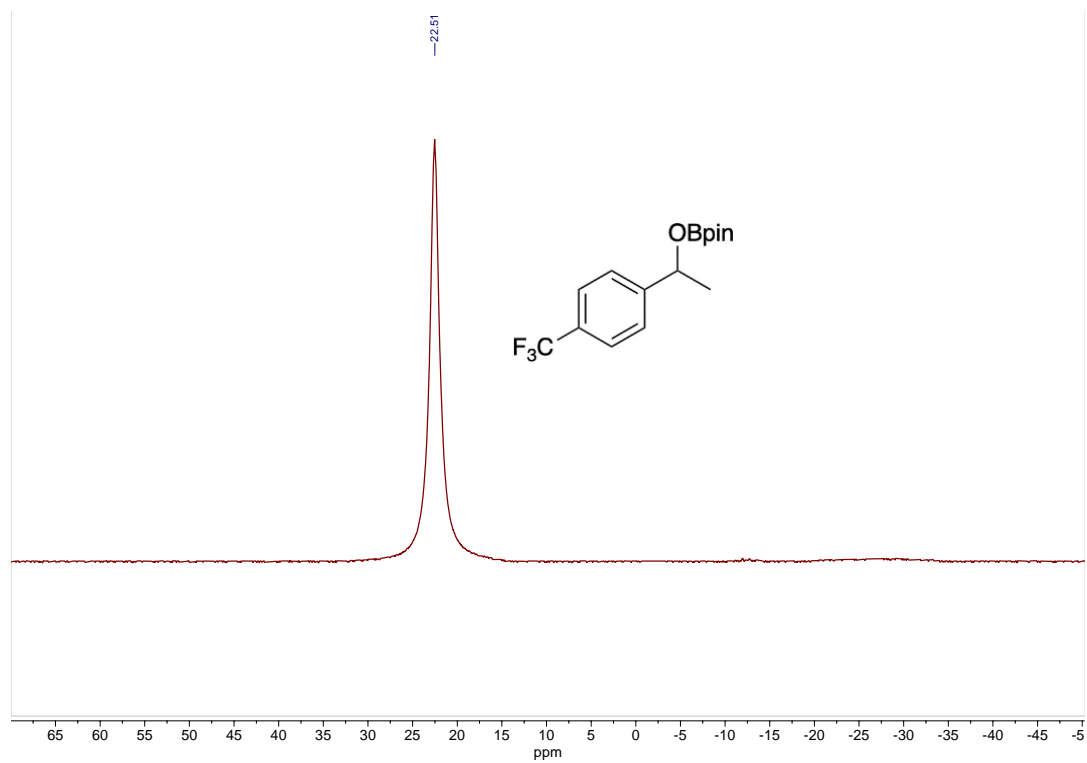

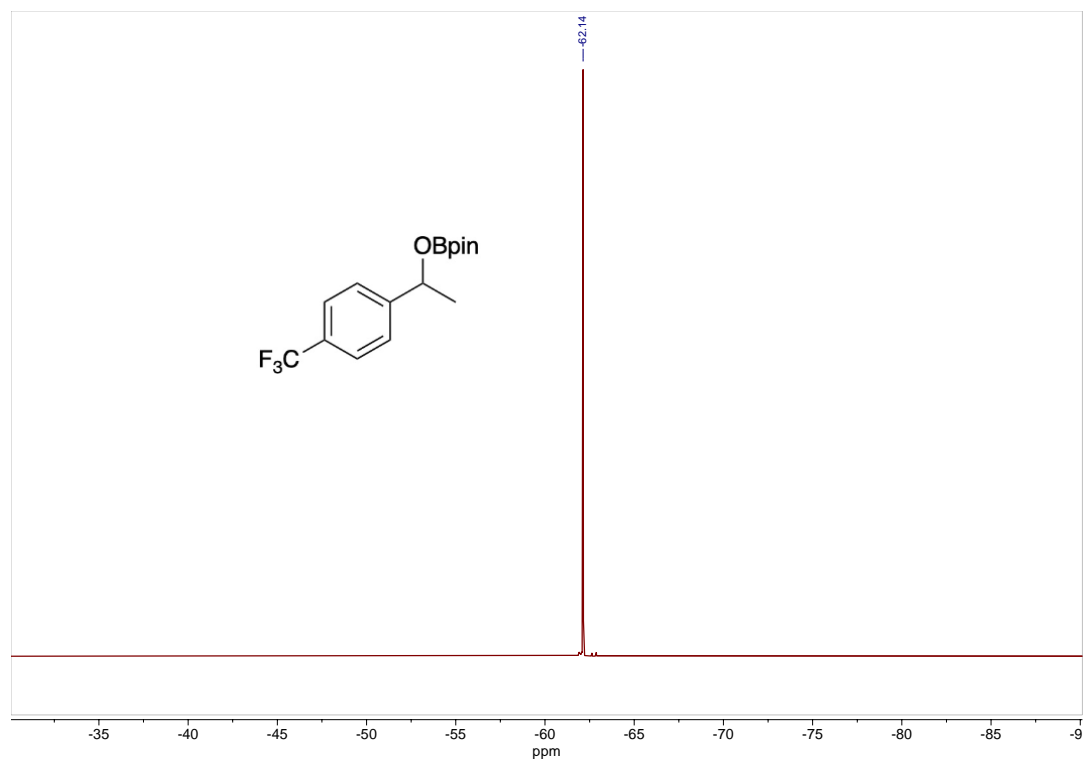**Figure S41.** ^{11}B NMR spectrum of **8m** in benzene-d_6. The doublet signal at 28.5 ppm corresponds to HBpin.

Figure S42. ^{1}H NMR spectrum of **8n** in benzene-d_6 using catalyst **5**. The signal at 2.1 ppm is the hexamethylbenzene internal standard.

Figure S43. ^{13}C{^{1}H} NMR spectrum of **8n** in benzene-d_6. The signals at 16.7 and 131.4 ppm are the hexamethylbenzene internal standard.

Figure S44. ^{11}B NMR spectrum of **8n** in benzene-d_6.

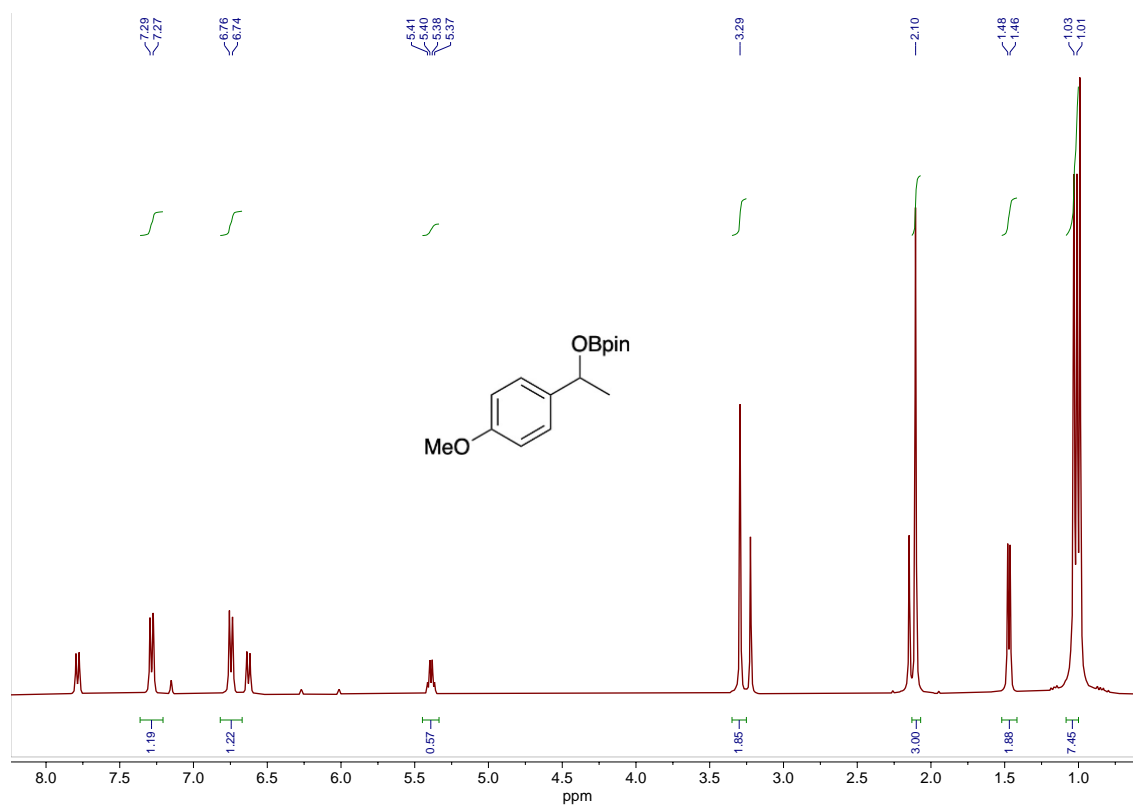**Figure S45.** ^{19}F{^{1}H} NMR spectrum of **8n** in benzene-d_6.

Figure S46. ^{1}H NMR spectrum of **8o** alongside remaining 4-methoxyacetophenone in benzene-d_6 using catalyst **4**. The signal at 2.1 ppm is the hexamethylbenzene internal standard.
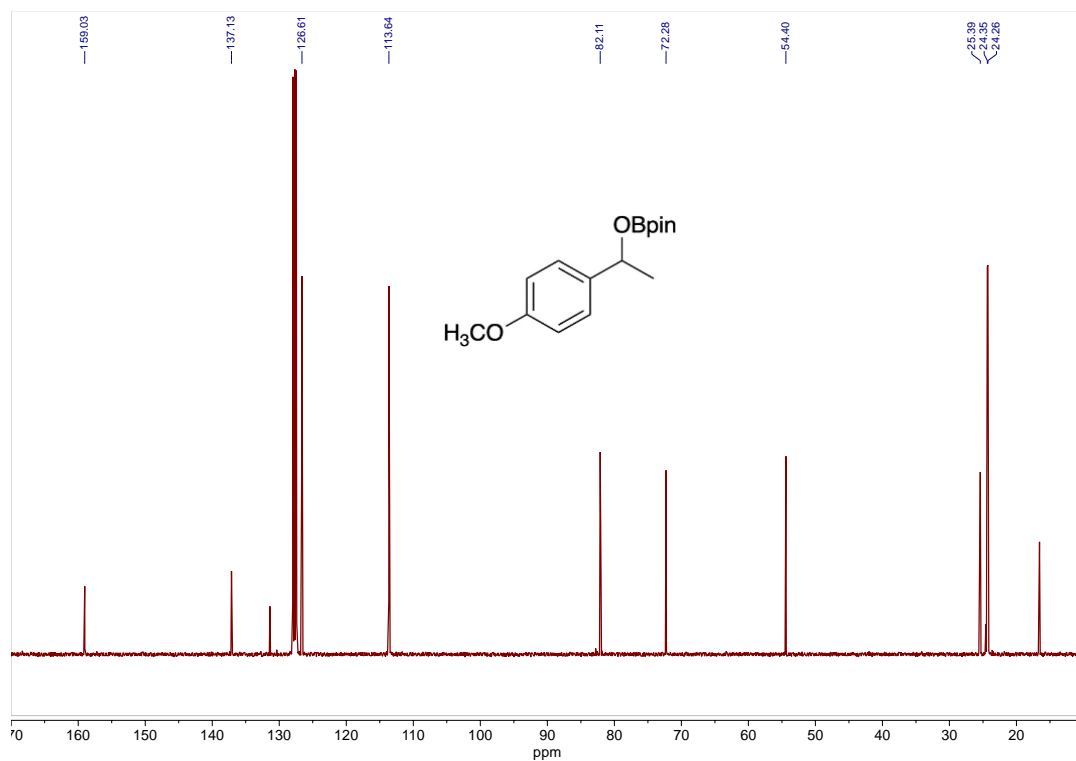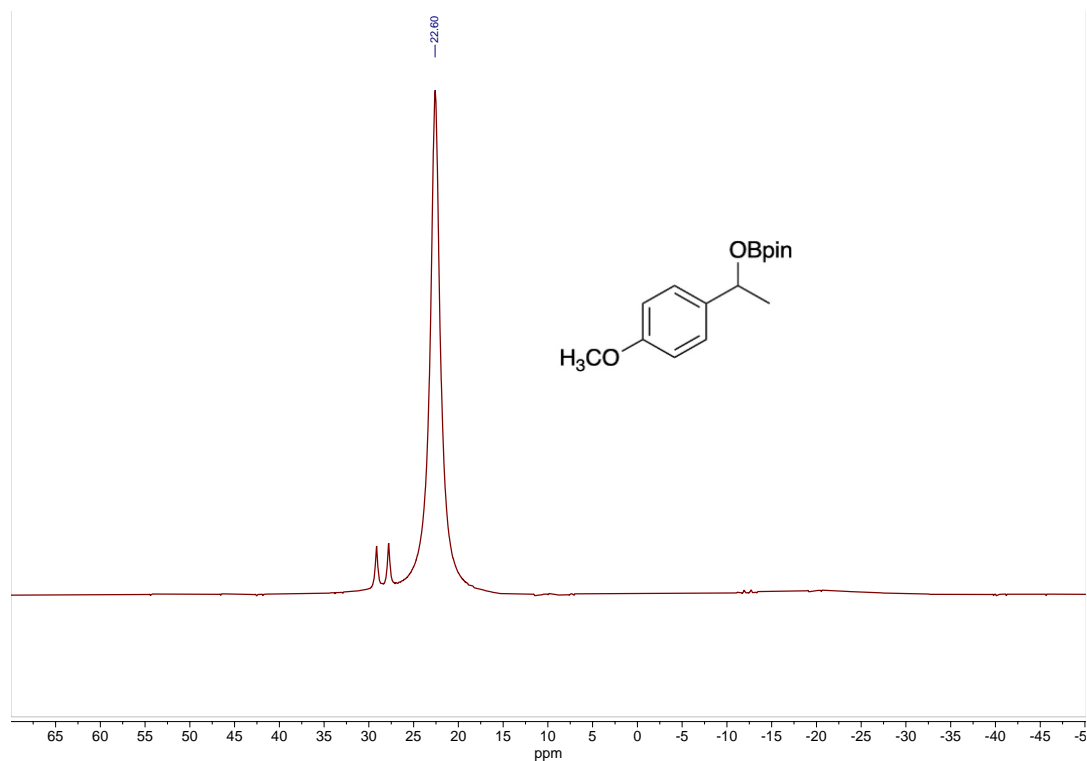

Figure S47. ^{13}C{^{1}H} NMR spectrum of **8o** in benzene-d_6. The signals at 16.7 and 131.4 ppm are the hexamethylbenzene internal standard.

Figure S48. ^{11}B NMR spectrum of **8o** in benzene-d_6. The doublet signal at 28.5 ppm corresponds to HBpin.
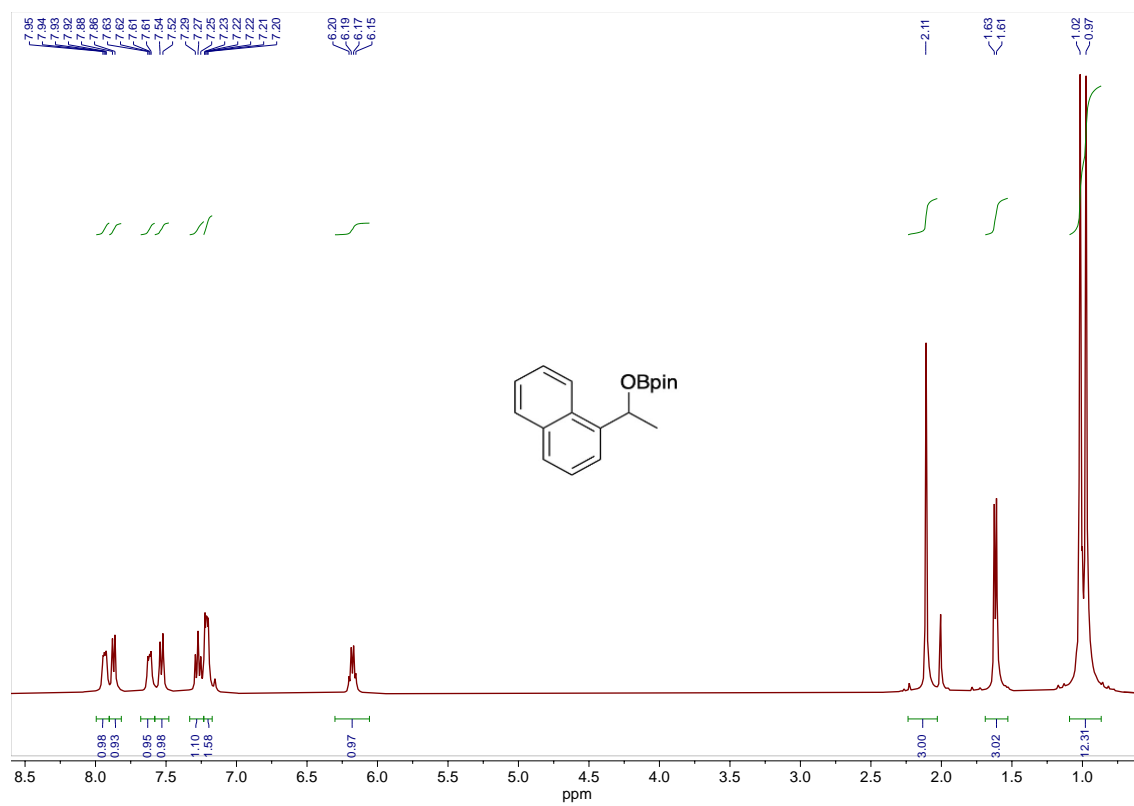

Figure S49. ^{1}H NMR spectrum of **8p** in benzene-d_6 using catalyst **5**. The signal at 2.1 ppm is the hexamethylbenzene internal standard.
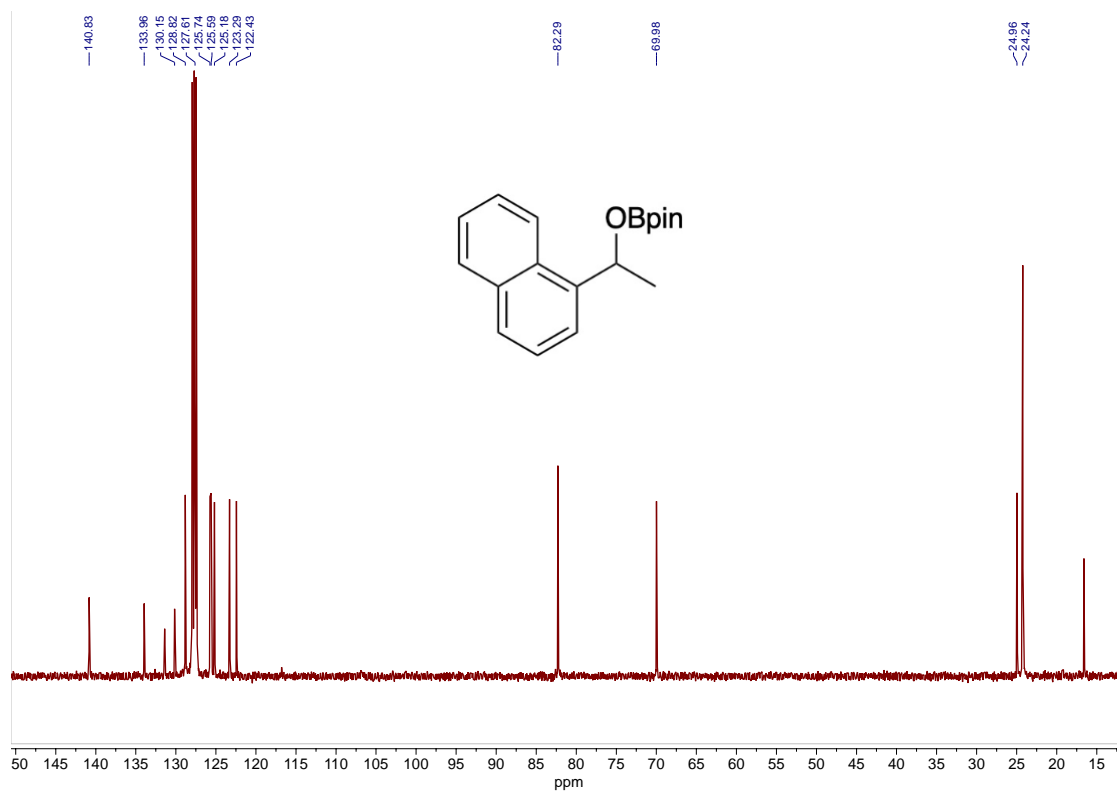
Figure S50. $^{13}C\{^1H\}$ NMR spectrum of **8p** in benzene-d_6. The signals at 16.7 and 131.4 ppm are the hexamethylbenzene internal standard.

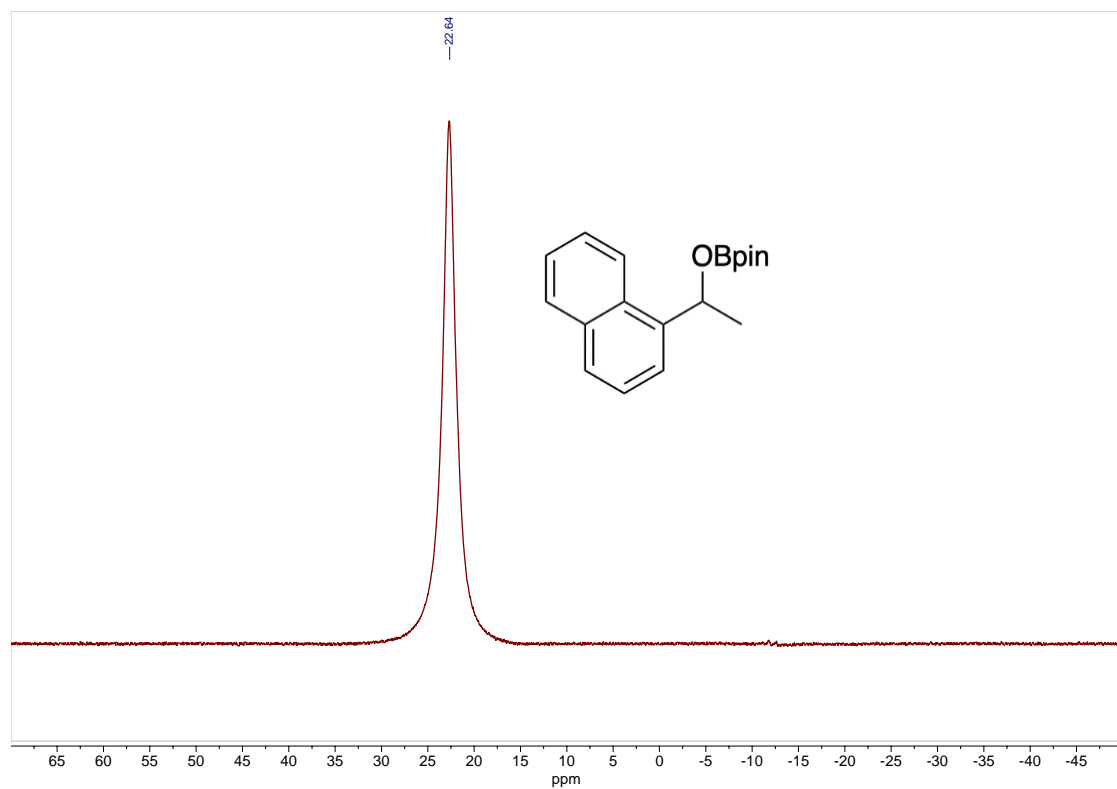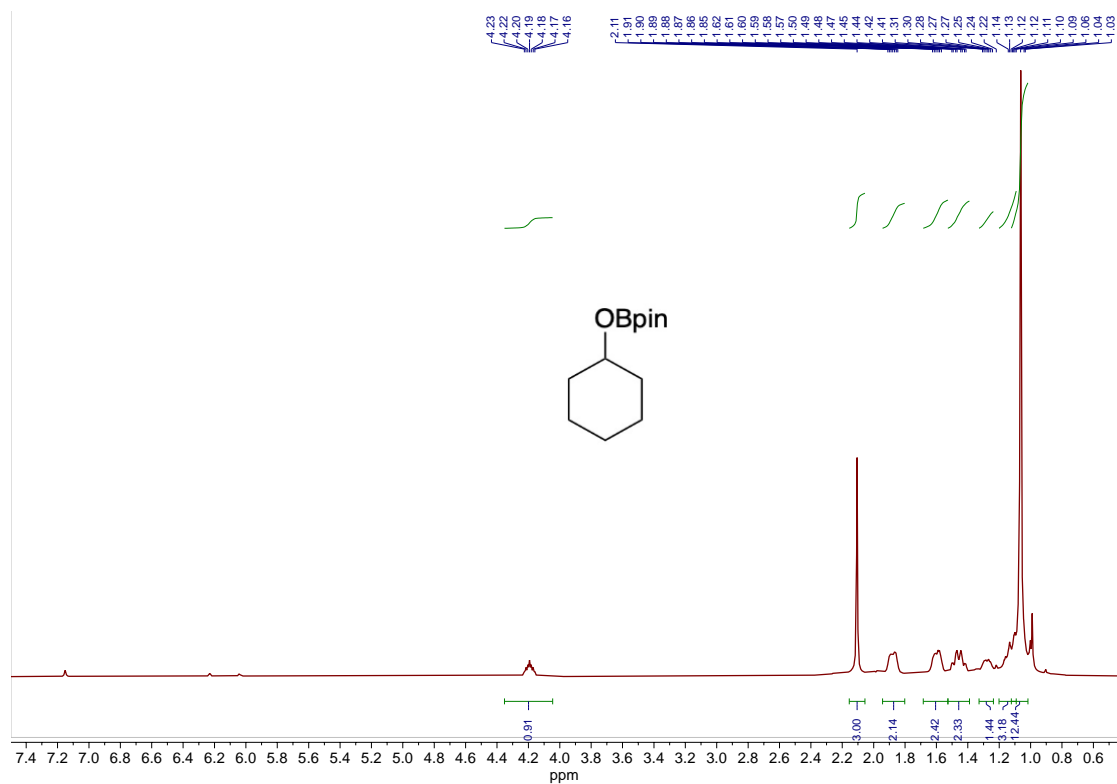**Figure S51.** ^{11}B NMR spectrum of **8p** in benzene-d_6.

Figure S52. ^{1}H NMR spectrum of **8q** in benzene-d_6 using catalyst **5**. The signal at 2.1 ppm is the hexamethylbenzene internal standard.
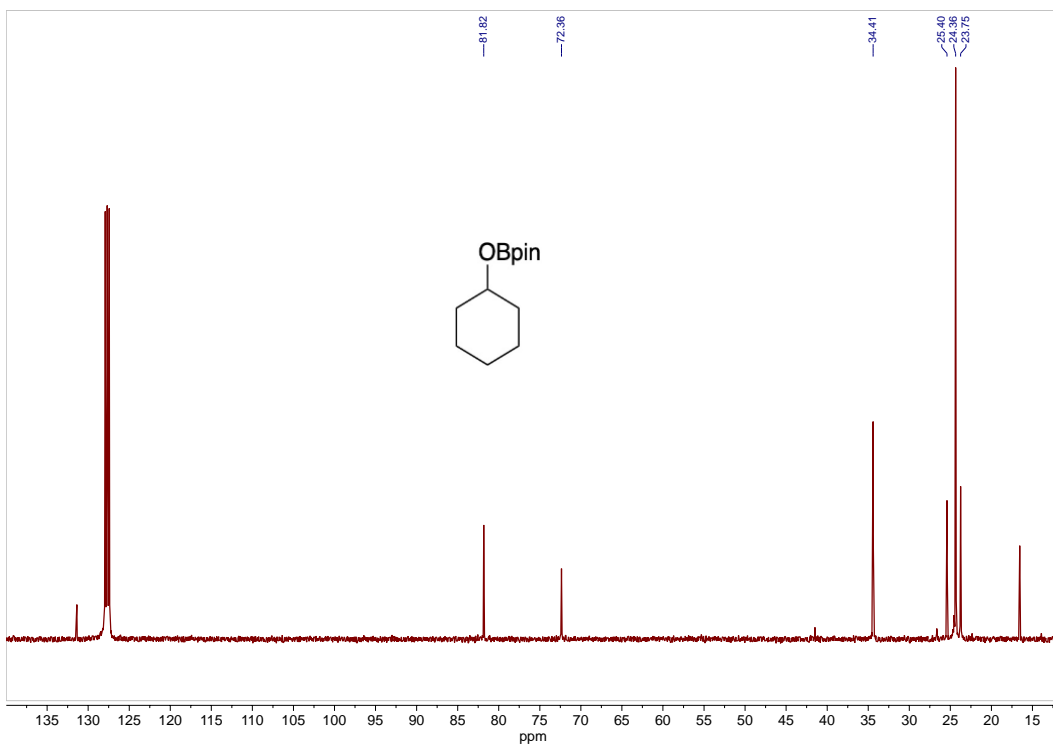

Figure S53. ^{13}C{^{1}H} NMR spectrum of **8q** in benzene-d_6. The signals at 16.7 and 131.4 ppm are the hexamethylbenzene internal standard.
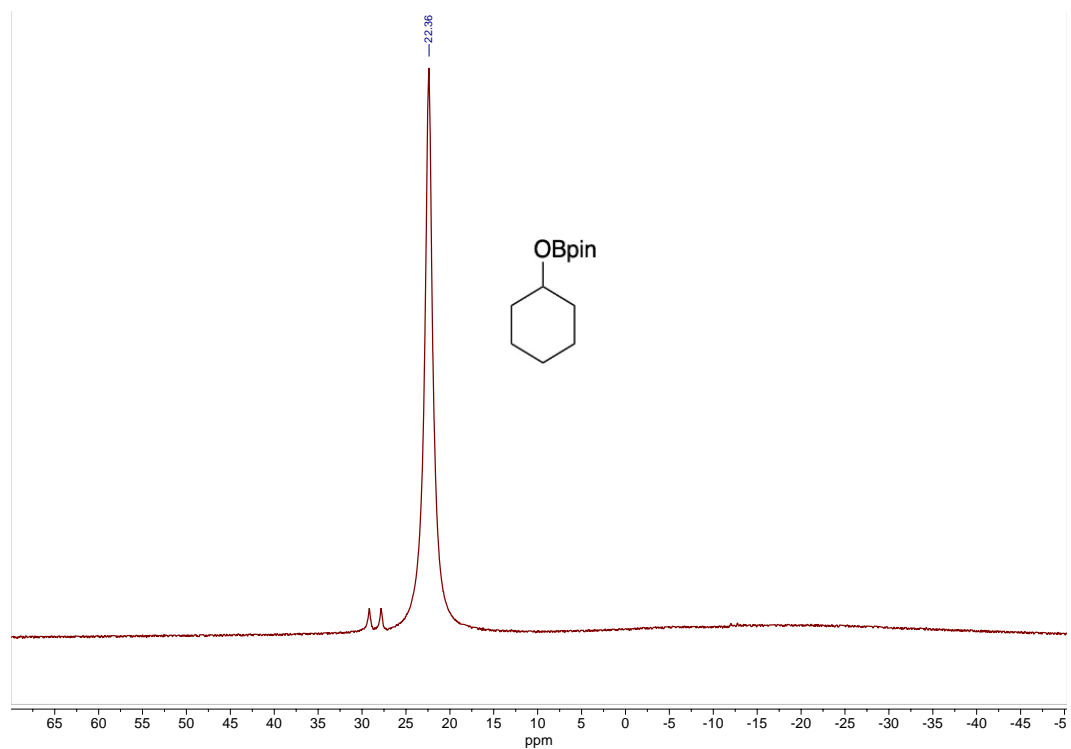
Figure S54. ^{11}B NMR spectrum of **8q** in benzene-d_6. The doublet signal at 28.5 ppm corresponds to HBpin.
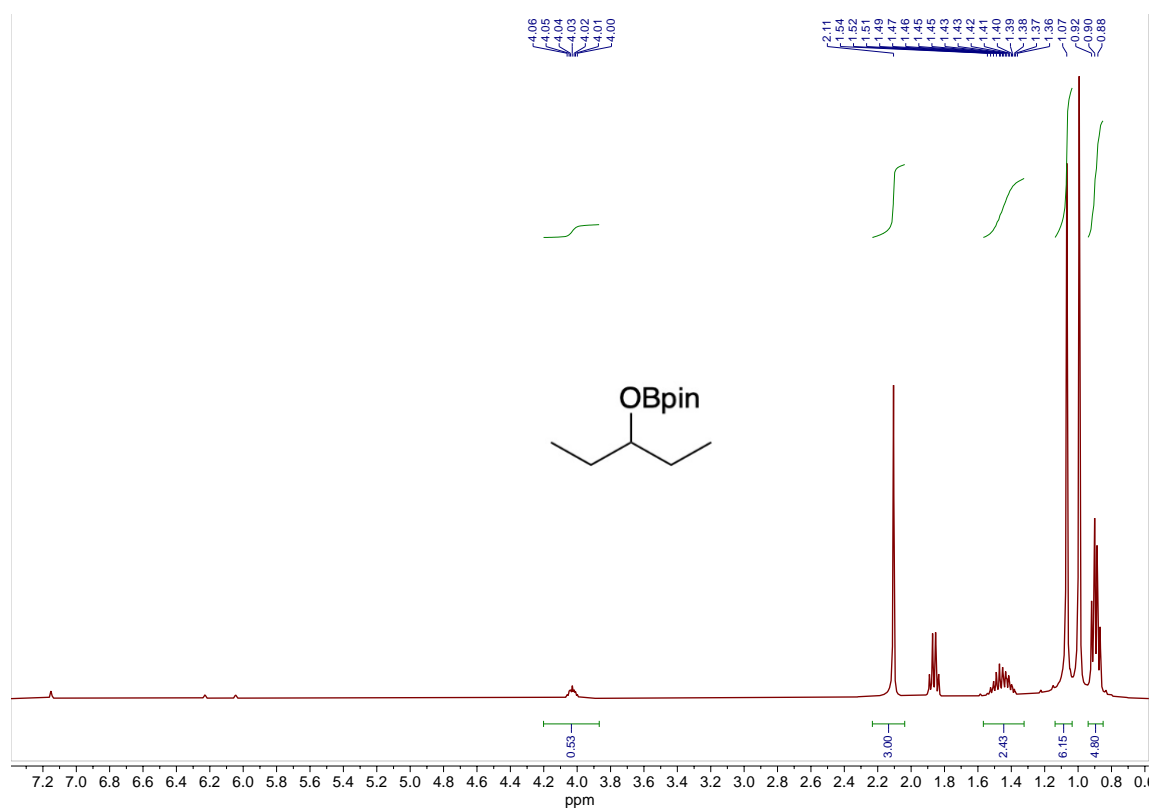

Figure S55. ^{1}H NMR spectrum of **8r** in benzene-d_6 alongside remaining 3-pentanone using catalyst **5**. The signal at 2.1 ppm is the hexamethylbenzene internal standard.
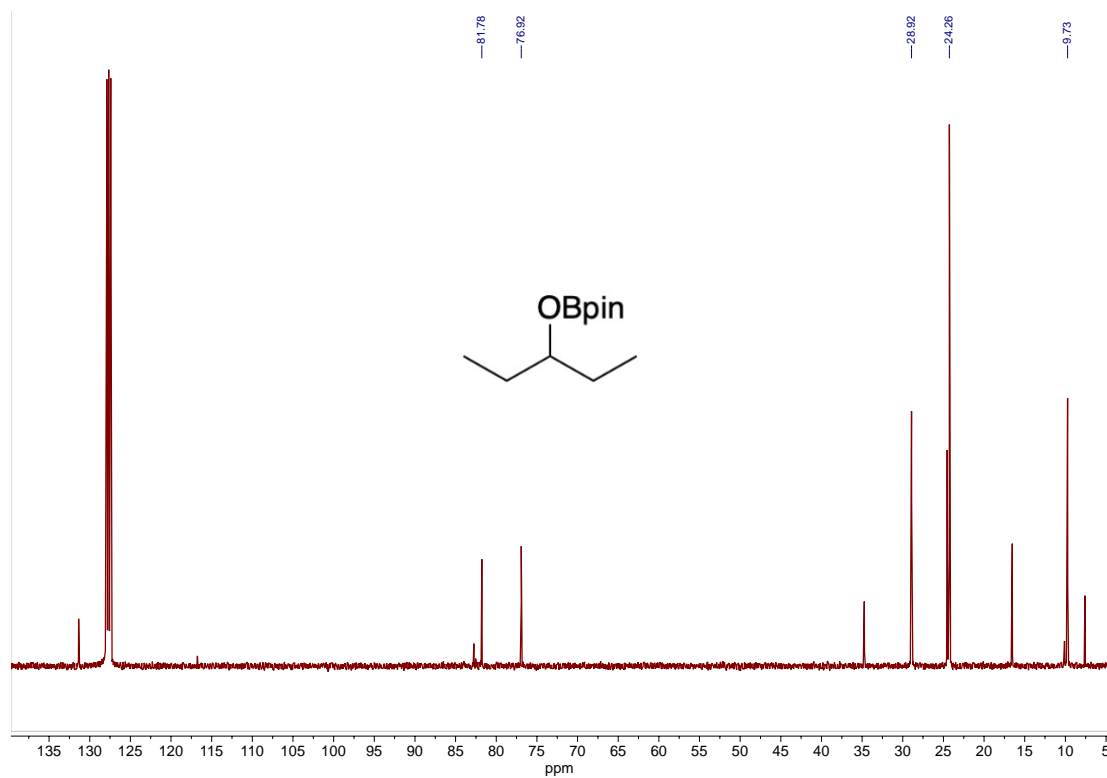
Figure S56. $^{13}C\{^1H\}$ NMR spectrum of **8r** in benzene-d_6 alongside residual 3-pentanone. The signals at 16.7 and 131.4 ppm are the hexamethylbenzene internal standard.
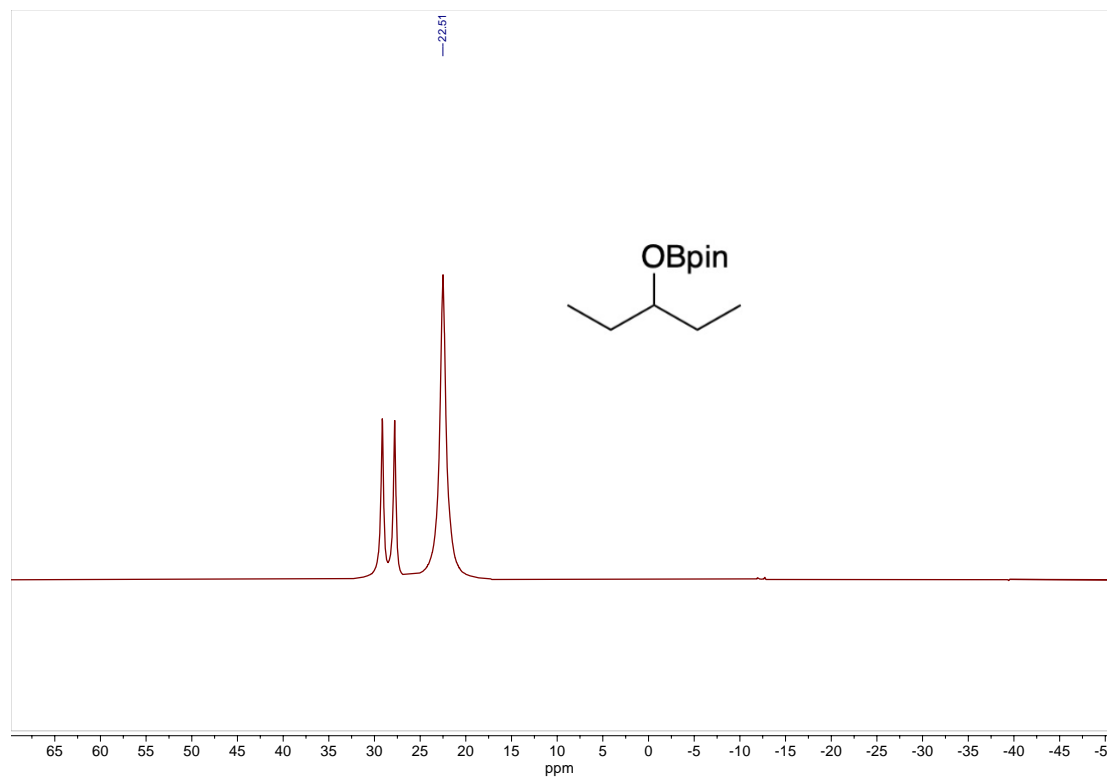

Figure S57. ^{11}B NMR spectrum of **8r** in benzene-d_6. The doublet signal at 28.5 ppm corresponds to HBpin.
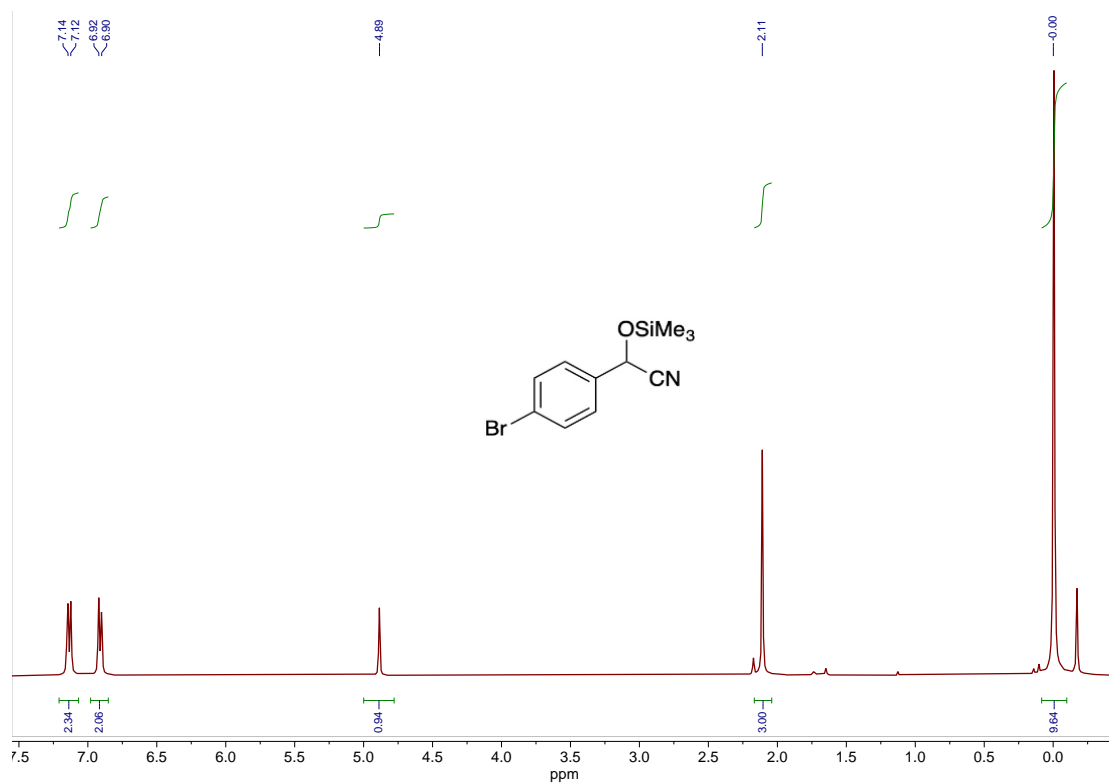
Figure S58. ¹H NMR spectrum of **9a** in benzene-d_6 using catalyst **5**. The signal at 2.1 ppm is the hexamethylbenzene internal standard.

Figure S59. ¹³C{¹H} NMR spectrum of **9a** in benzene-d_6. The signals at 16.7 and 131.4 ppm are the hexamethylbenzene internal standard.

Figure S60. ^{1}H NMR spectrum of **9b** in benzene-d_6 using catalyst **6**. The signal at 2.1 ppm is the hexamethylbenzene internal standard.
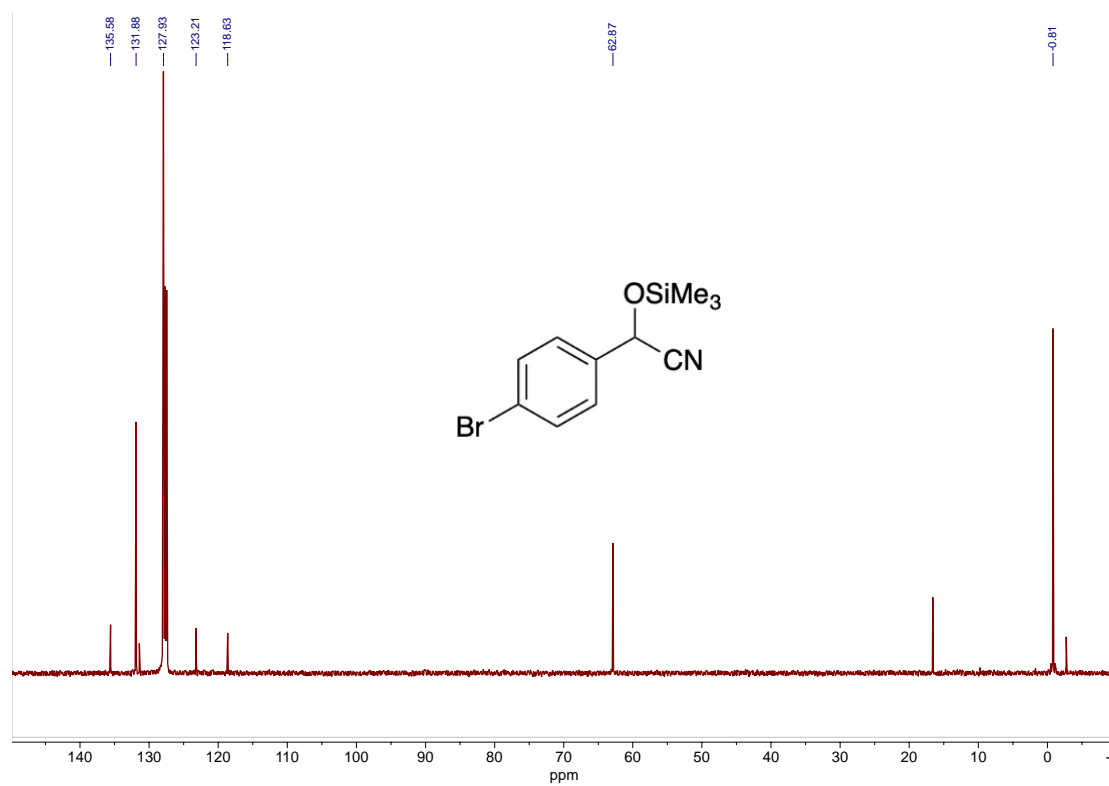

Figure S61. ^{13}C{^{1}H} NMR spectrum of **9b** in benzene-d_6. The signals at 16.7 and 131.4 ppm are the hexamethylbenzene internal standard.

Figure S62. $^{19}F\{^1H\}$ NMR spectrum of **9b** in benzene-d_6.

Figure S63. ^1H NMR spectrum of **9c** in benzene-d_6 using catalyst 5. The signal at 2.1 ppm is the hexamethylbenzene internal standard.

Figure S64. $^{13}C\{^1H\}$ NMR spectrum of **9c** in benzene-d_6. The signals at 16.7 and 131.4 ppm are the hexamethylbenzene internal standard.
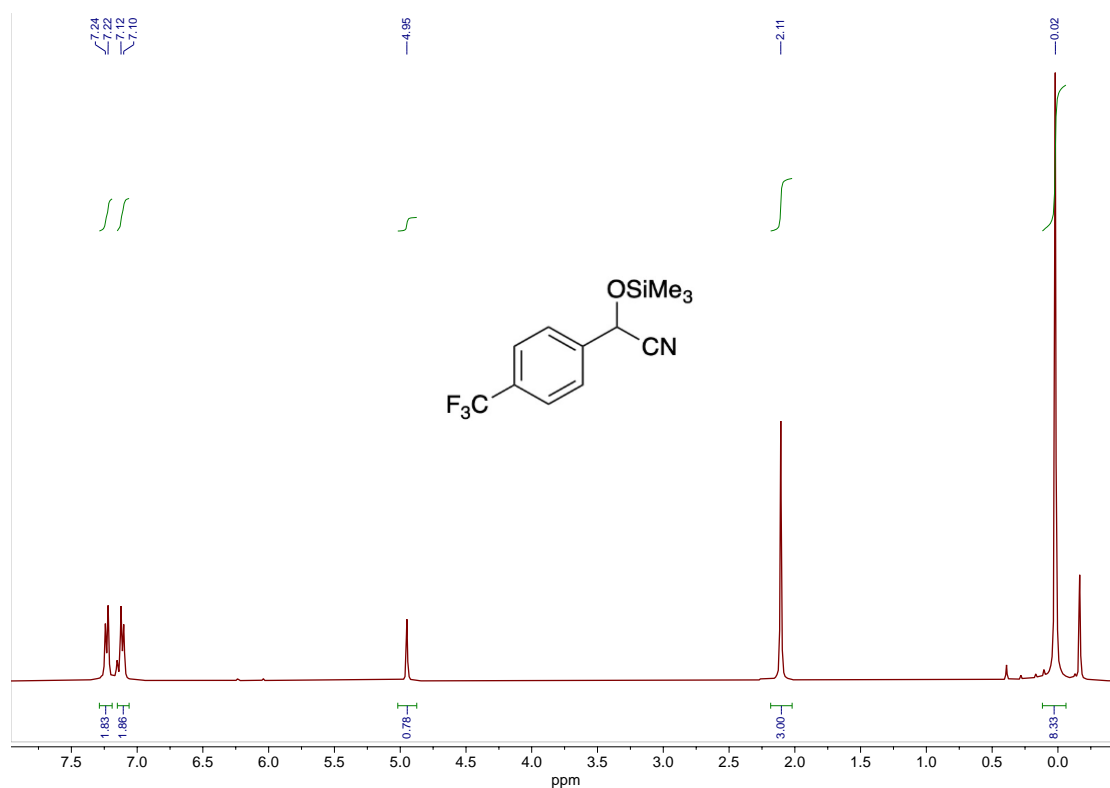

Figure S65. ^1H NMR spectrum of **9d** in benzene-d_6 using catalyst **5**. The signal at 2.1 ppm is the hexamethylbenzene internal standard.
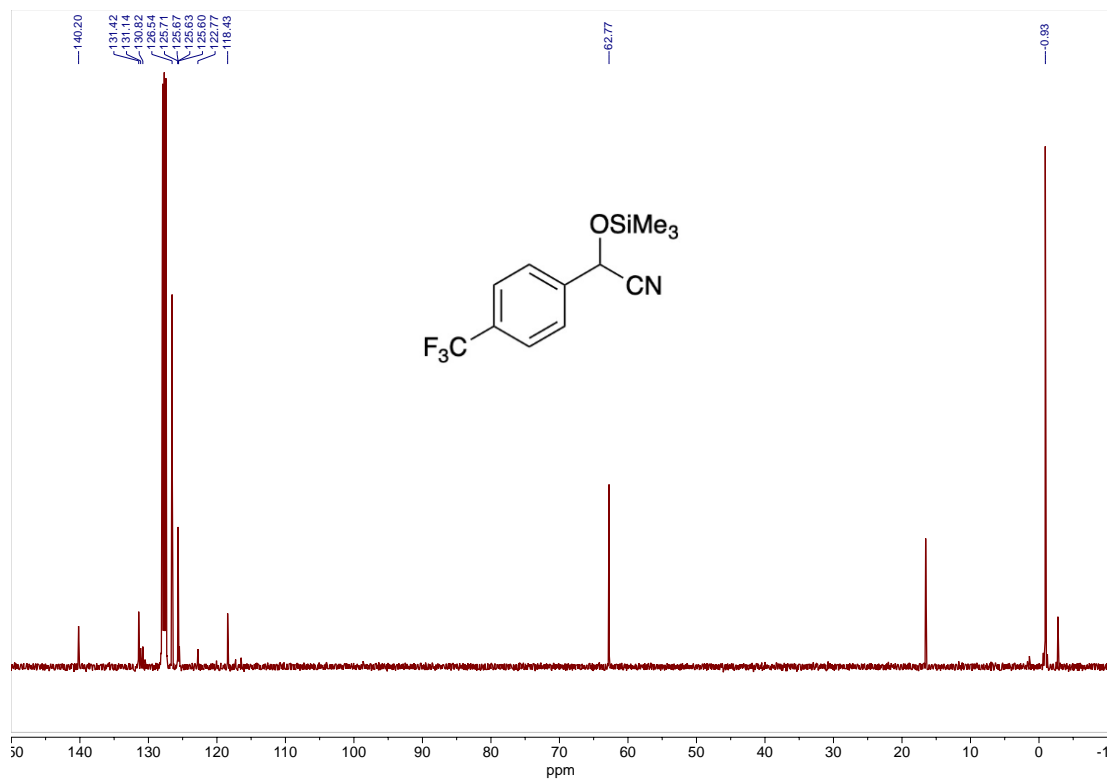
Figure S66. $^{13}C\{^1H\}$ NMR spectrum of **9d** in benzene-d_6. The signals at 16.7 and 131.4 ppm are the hexamethylbenzene internal standard.

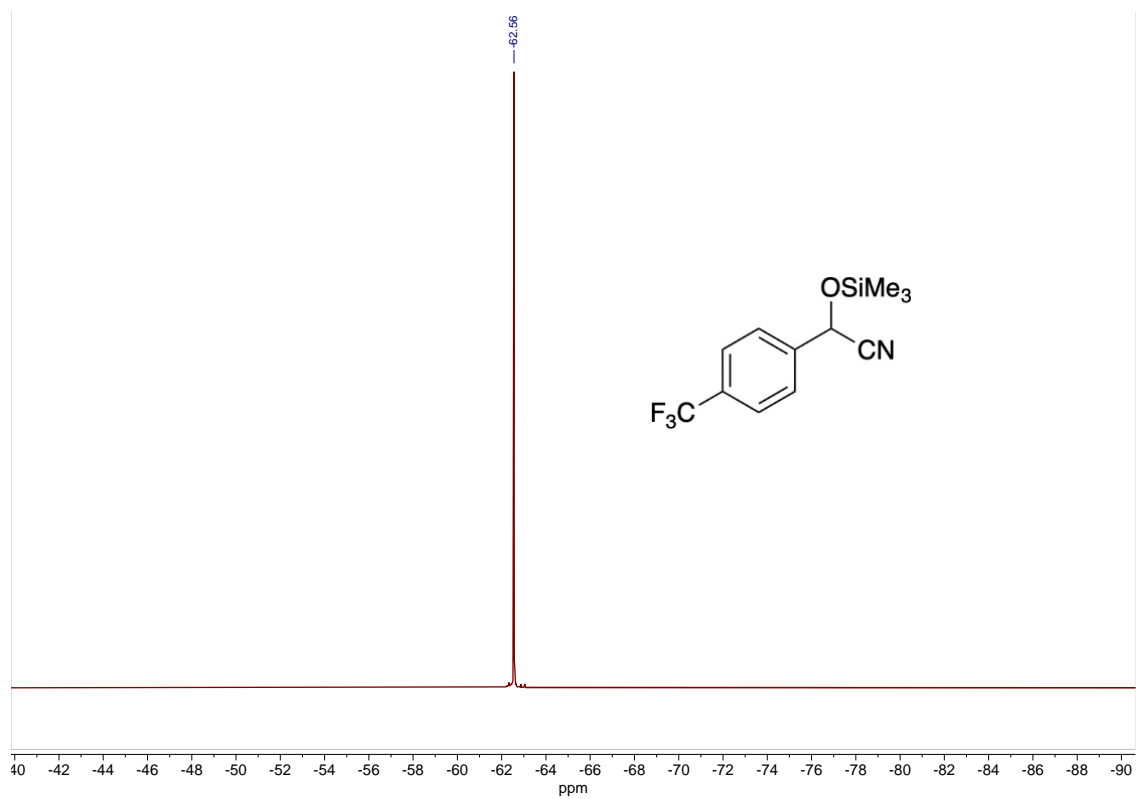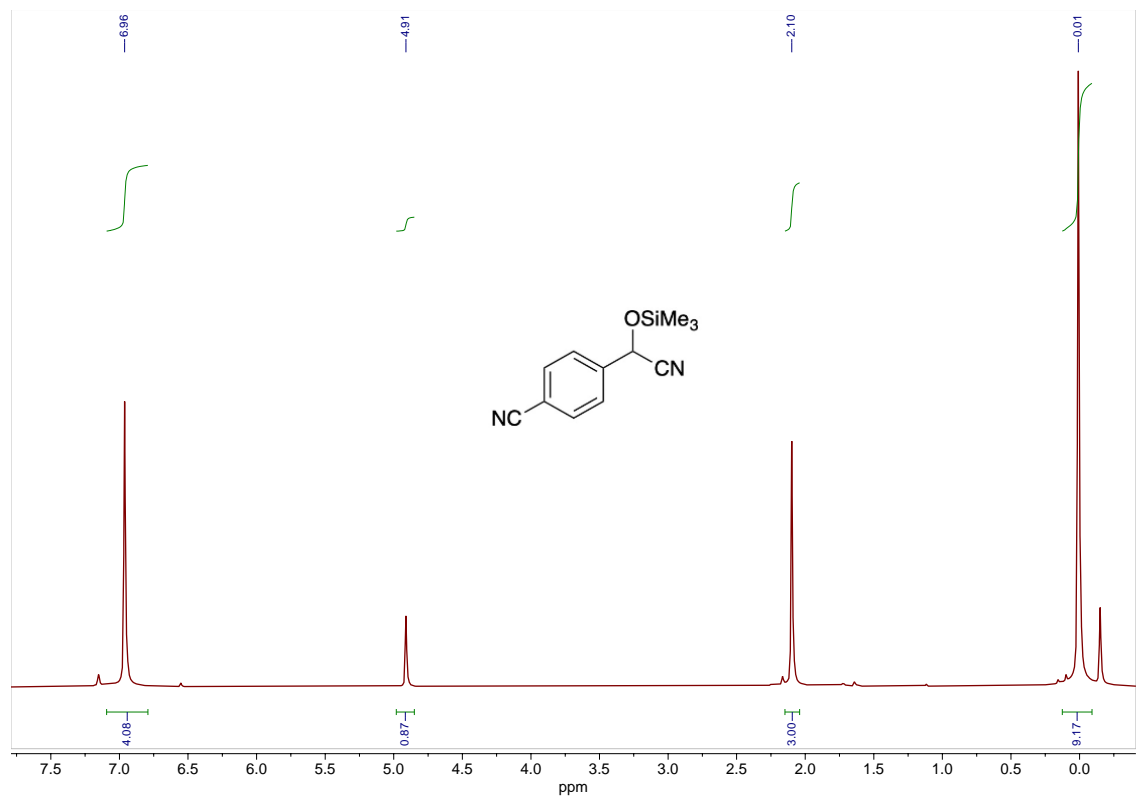**Figure S67.** ^1H NMR spectrum of **9e** in benzene-d_6 using catalyst **5**. The signal at 2.1 ppm is the hexamethylbenzene internal standard.

Figure S68. ^{13}C{^{1}H} NMR spectrum of **9e** in benzene-d_6. The signals at 16.7 and 131.4 ppm are the hexamethylbenzene internal standard.

Figure S69. ^{1}H NMR spectrum of **9f** in benzene-d_6 using catalyst **5**. The signal at 2.1 ppm is the hexamethylbenzene internal standard.
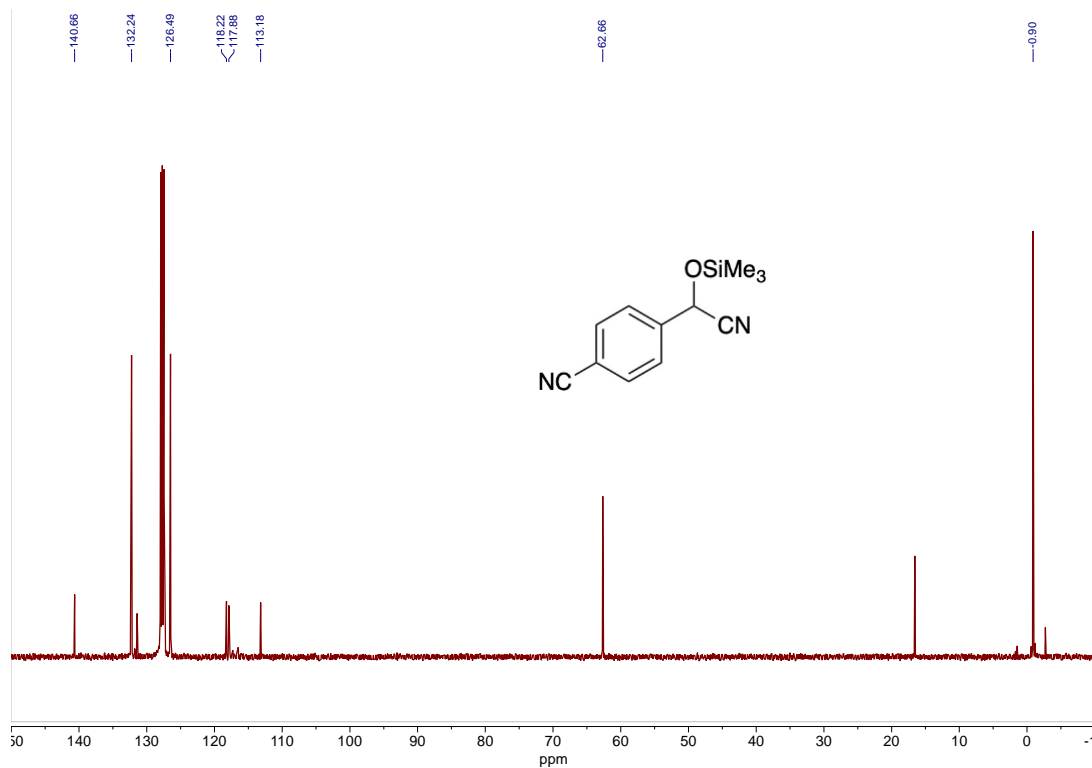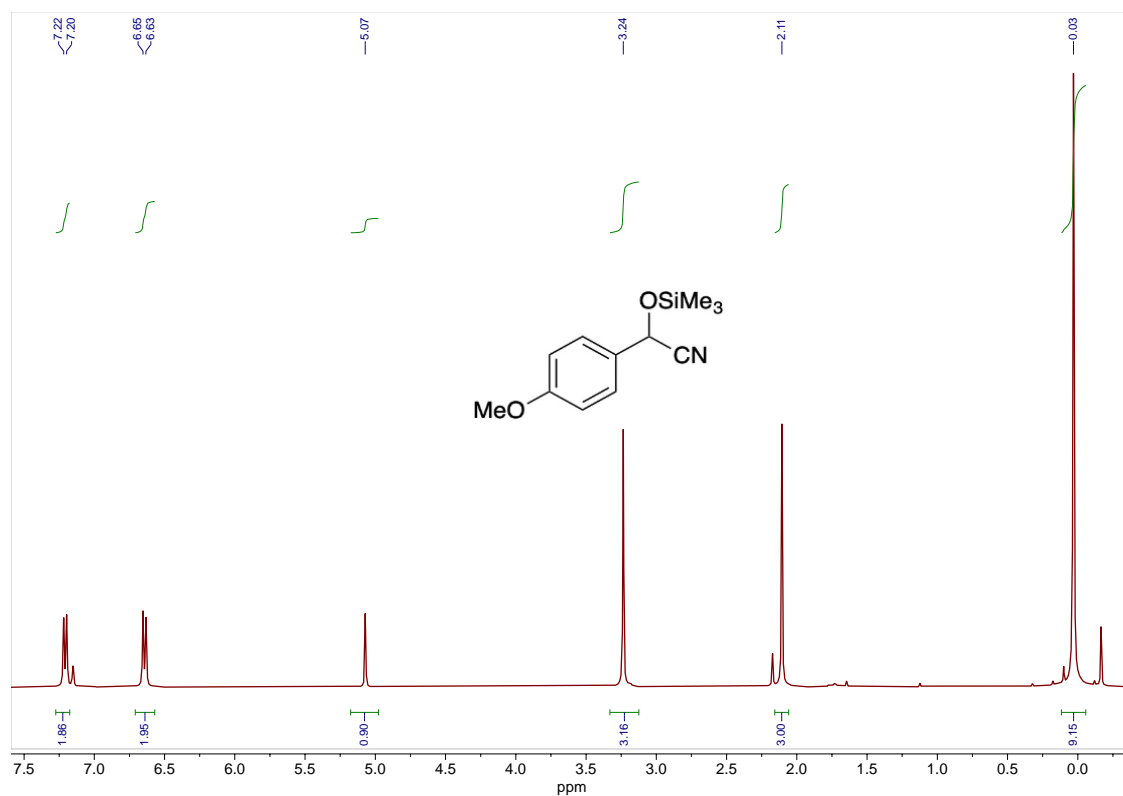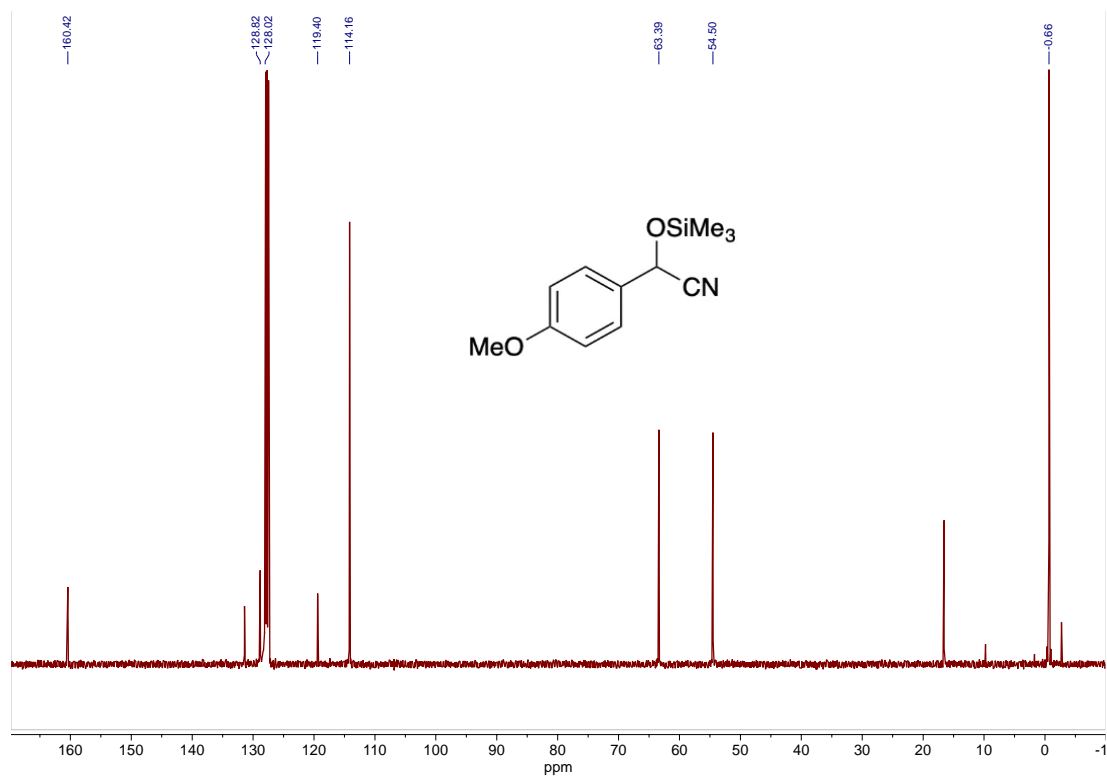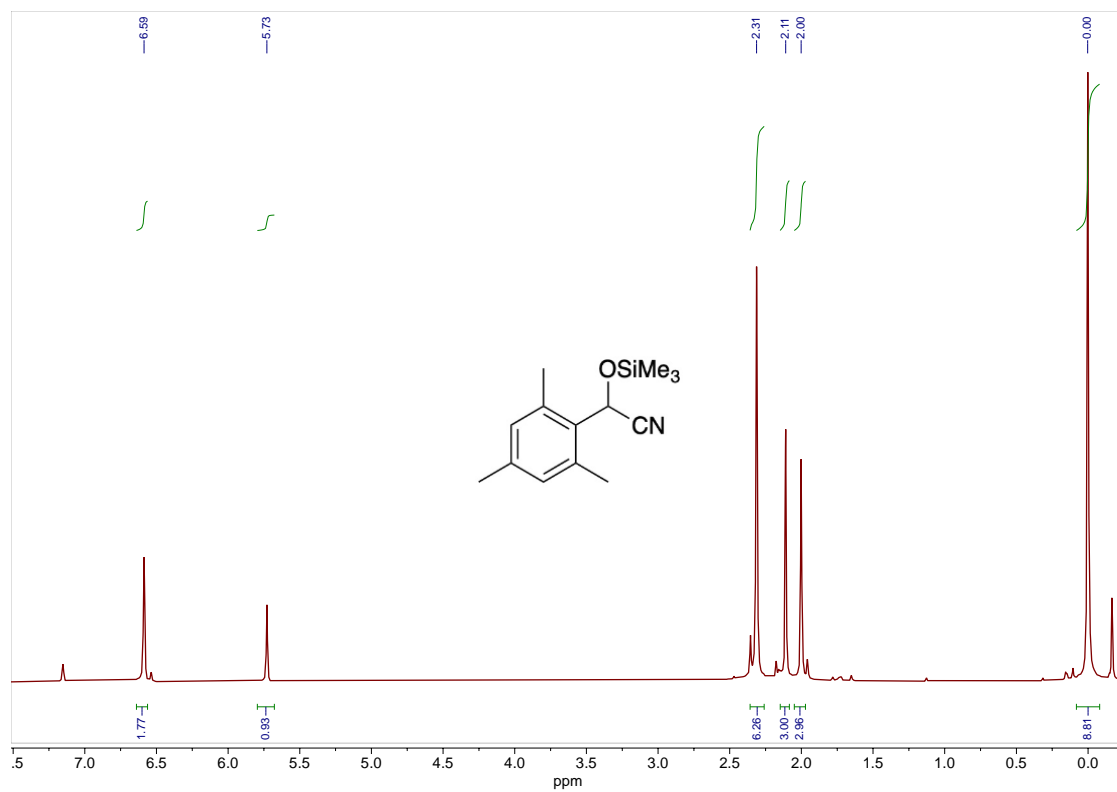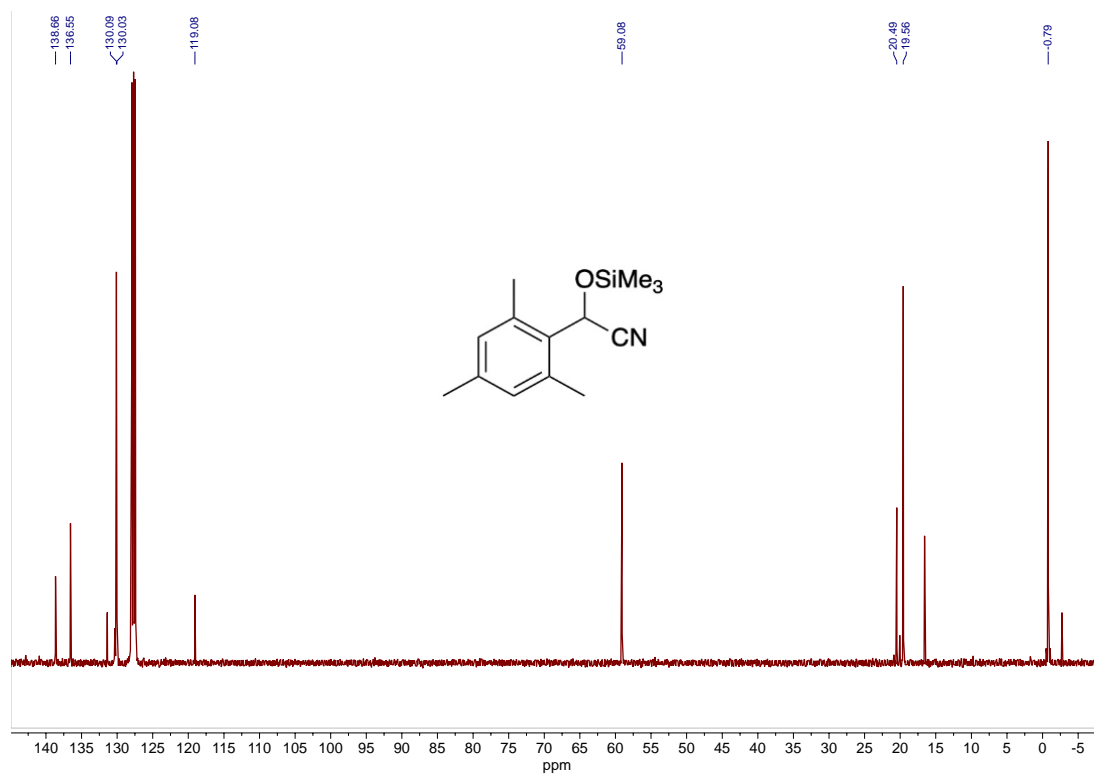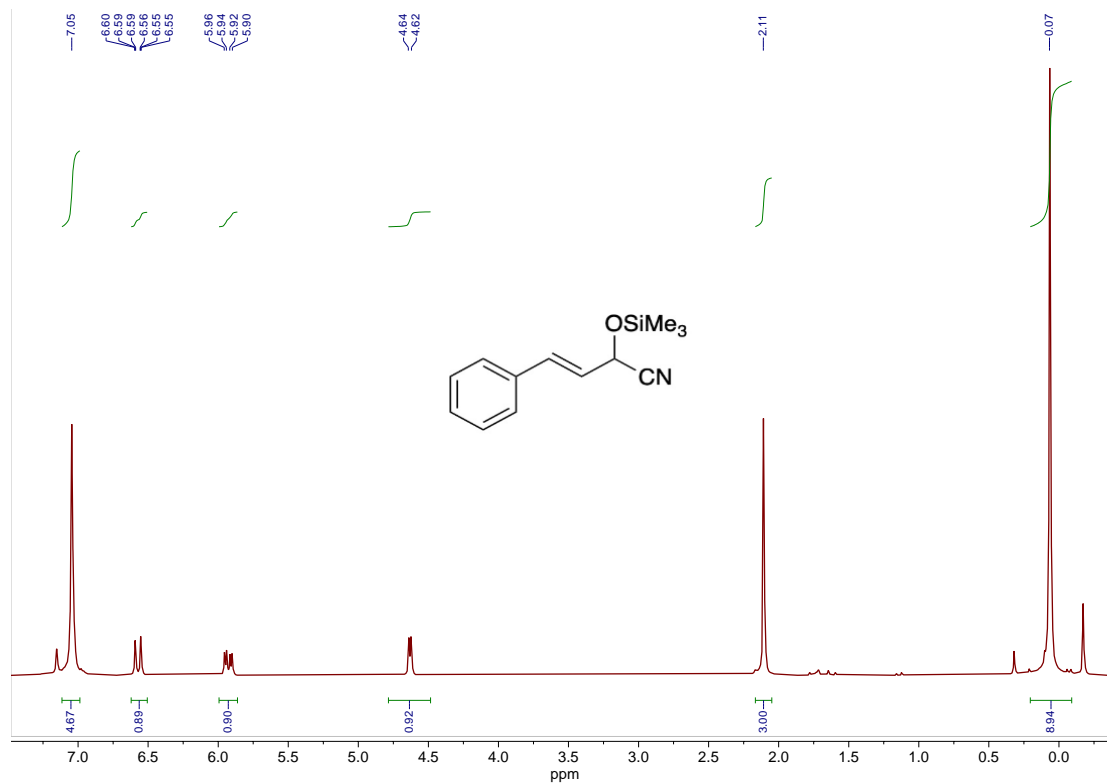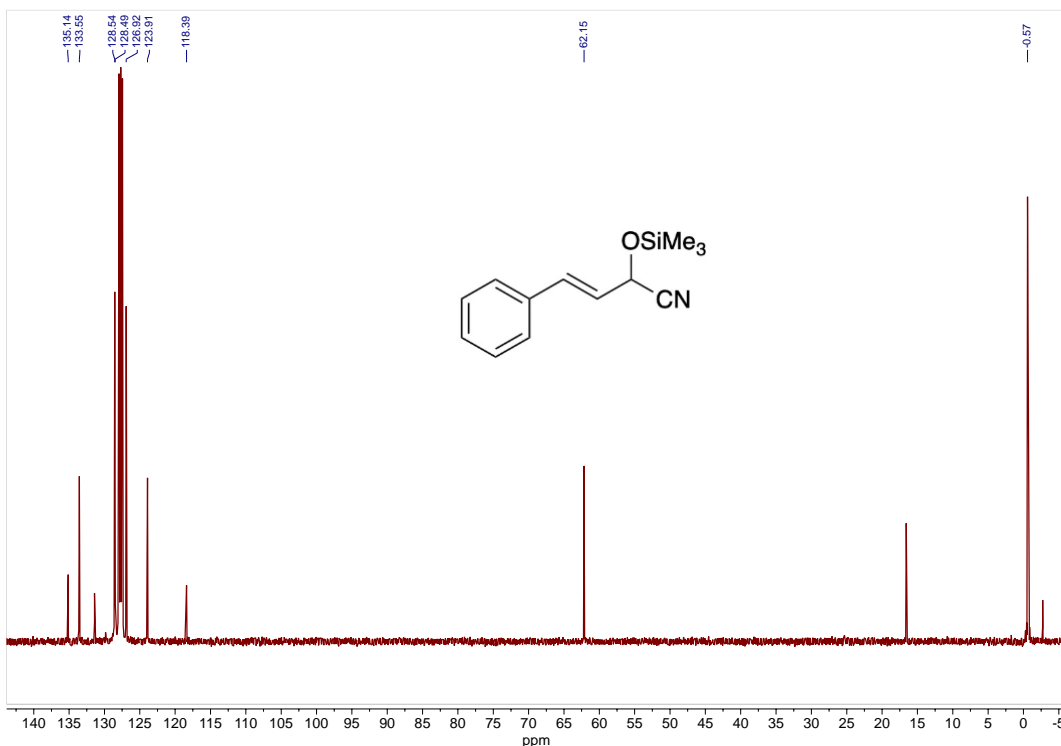
Figure S70. $^{13}C\{^1H\}$ NMR spectrum of **9f** in benzene-d_6. The signals at 16.7 and 131.4 ppm are the hexamethylbenzene internal standard.

References

[1]   L. Wirtz, M. Jourdain, V. Huch, M. Zimmer, A. Schäfer, Synthesis, Structure, and Reactivity of Disiloxa[3]tetrelocenophanes, ACS Omega. 4 (2019) 18355–18360. https://doi.org/10.1021/acsomega.9b02605.

[2]   A. Schöpper, W. Saak, M. Weidenbruch, Molecular structure of decamethylgermanocene in the solid state, J. Organomet. Chem. 691 (2006) 809–810. https://doi.org/10.1016/j.jorganchem.2005.10.024.

[3]   P. Jutzi, F. Kohl, P. Hofmann, C. Krüger, Y.-H. Tsay, Bis(pentamethylcyclopentadienyl)germanium und -zinn sowie (Pentamethylcyclopentadienyl)germanium- und -zinn-Kationen: Synthese, Struktur und Bindungsverhältnisse, Chem. Ber. 113 (1980) 757–769. https://doi.org/10.1002/cber.19801130233.

[4]   P. Jutzi, R. Dickbreder, H. Nöth, Blei(II)-Verbindungen mit π-gebundenen Pentamethylcyclopentadienylliganden – Synthesen, Strukturen und Bindungsverhältnisse, Chem. Ber. 122 (1989) 865–870. https://doi.org/10.1002/cber.19891220512.

[5]   U.K. Das, C.S. Higman, B. Gabidullin, J.E. Hein, R.T. Baker, Efficient and Selective Iron-Complex-Catalyzed Hydroboration of Aldehydes, ACS Catal. 8 (2018) 1076–1081. https://doi.org/10.1021/acscatal.7b03785.

[6] T. Ghatak, K. Makarov, N. Fridman, M.S. Eisen, Catalytic regeneration of a Th–H bond from a Th–O bond through a mild and chemoselective carbonyl hydroboration, Chem. Commun. 54 (2018) 11001–11004.
https://doi.org/10.1039/C8CC05030A.

[7] D.M.C. Ould, R.L. Melen, Arsenic Catalysis: Hydroboration of Aldehydes Using a Benzo-Fused Diaza-benzyloxy-arsole, Chem. - Eur. J. 24 (2018) 15201–15204.
https://doi.org/10.1002/chem.201803508.

[8] V.L. Weidner, C.J. Barger, M. Delferro, T.L. Lohr, T.J. Marks, Rapid, Mild, and Selective Ketone and Aldehyde Hydroboration/Reduction Mediated by a Simple Lanthanide Catalyst, ACS Catal. 7 (2017) 1244–1247.
https://doi.org/10.1021/acscatal.6b03332.

[9] X. Xu, D. Yan, Z. Zhu, Z. Kang, Y. Yao, Q. Shen, M. Xue, Catalyst-Free Approach for Hydroboration of Carboxylic Acids under Mild Conditions, ACS Omega. 4 (2019) 6775–6783.
https://doi.org/10.1021/acsomega.9b00406.

[10] S. Bagherzadeh, N.P. Mankad, Extremely efficient hydroboration of ketones and aldehydes by copper carbene catalysis, Chem. Commun. 52 (2016) 3844–3846.
https://doi.org/10.1039/C5CC09162D.

[11] R.K. Sahoo, M. Mahato, A. Jana, S. Nembenna, Zinc Hydride-Catalyzed Hydrofuntionalization of Ketones, J. Org. Chem. 85 (2020) 11200–11210.
https://doi.org/10.1021/acs.joc.0c01285.

[12] N. Eedugurala, Z. Wang, U. Chaudhary, N. Nelson, K. Kandel, T. Kobayashi, I.I. Slowing, M. Pruski, A.D. Sadow, Mesoporous Silica-Supported Amidozirconium-Catalyzed Carbonyl Hydroboration, ACS Catal. 5 (2015) 7399–7414.
https://doi.org/10.1021/acscatal.5b01671.

[13] M.W. Stanford, A. Bismuto, M.J. Cowley, Silyl Anion Initiated Hydroboration of Aldehydes and Ketones, Chem. – Eur. J. 26 (2020) 9855–9858.
https://doi.org/10.1002/chem.202000897.

[14] Z. Kang, X. Xu, Y. Wang, W. Zhang, S. Zhou, X. Zhu, M. Xue, *n*-Butyllithium as a highly efficient precatalyst for cyanosilylation of aldehydes and ketones, Org. Biomol. Chem. 19 (2021) 7432–7437.
https://doi.org/10.1039/D1OB01297E.

[15] Y. Kim, K.M. Lee, S.H. Kim, J.H. Moon, Y. Kim, Dimeric alumatranes as catalysts for trimethylsilylcyanation reaction, RSC Adv. 7 (2017) 48151–48160.
https://doi.org/10.1039/C7RA09851K.

[16] S. Rawat, M. Bhandari, B. Prashanth, S. Singh, Three Coordinated Organoaluminum Cation for Rapid and Selective Cyanosilylation of Carbonyls under Solvent-Free Conditions, ChemCatChem. 12 (2020) 2407–2411.
https://doi.org/10.1002/cctc.202000309.